



Faculty of Science and Technology

MASTER'S THESIS

Study program/Specialization: Petroleum Geosciences Engineering	Spring semester, 2016 Open
Author: Hans Østebø	<hr/> (signature author)
Main faculty supervisor: Alejandro Escalona Co-supervisor(s): Nestor Cardozo	
Title of thesis: 2D Flexural Deformation of the Barents Sea	
Credits (ECTS): 30	
Keywords: Barents Sea Sedimentary loads Tectonic loads Flexure	Pages: 92 + CD Stavanger, 15.06.2016

2D flexural deformation of the Barents Sea

Hans Østebø, Master in Petroleum Geosciences
The University of Stavanger, 2016

Supervisor: Alejandro Escalona
Co-Supervisor: Nestor Cardozo

Acknowledgements

First off, I want to express my gratitude to my supervisor Alejandro Escalona and Co-supervisor Nestor Cardozo for their guidance and constructive feedback. Their comments and input has been a key for the accomplishment of this study.

Special thanks to Andreas Habel for software guidance and support.

Thanks to my family for the support and encouragement and finally my classmates and friends in the Petroleum Geoscience class, which made the semester a lot more fun.

Abstract

2D flexural deformation of the Barents Sea

Hans Østebø, MSc

The University of Stavanger, 2016

Supervisor: Alejandro Escalona

The Barents Sea, located north of Norway and Russia, is a complex basin with several structures. The Barents Sea is characterized by a platform area to the north (e.g. Svalbard, Bjarmeland platform, Kong Karl platform); and area of rifted basins and highs to the southwest (e.g. Hammerfest, Tromsø basin, Loppa High), and an area of deep and large basins with gentle highs to the east. Several tectonic events have affected the basins since the Late Paleozoic, resulting in large areas of accommodation and erosion. However, many of these processes are poorly understood. Therefore, very little is known about the impact of tectonic and sedimentary loads on the basin geometry and evolution. In this study, three regional transects that cover large parts of the Barents Sea are constructed and analyzed to understand the flexural response that resulted from tectonic and sedimentary loads in order to provide insight into the possible processes that have accumulated in the current basin geometry. The results shows that there are a distinct change between the western and eastern Barents Sea and an increase of tectonic loads towards the southwest for the younger deposits. This study is important to understand the evolution of the Barents Sea in regards of tectonic and sedimentary loads.

Table of Contents

1. Introduction.....	1
2. Geological setting	6
2.1 Devonian – Base Tertiary (Sequence 1):	7
2.2 Base Tertiary – Base Cretaceous (Sequence 2):	9
2.3 Base Cretaceous - Top Cretaceous (Sequence 3):	11
2.4 Top Cretaceous - Quaternary (Sequence 4):	12
3. The Lithosphere and Flexure	13
3.1 Rheology	13
3.2 Isostasy.....	14
3.3 Flexure of the Lithosphere	14
3.4 Gravitational and magnetic maps.....	18
4. Data and Methodology.....	23
4.1 Profile and data	23
4.2 Depth Conversion	23
4.3 Well Correlation.....	28
4.4 Data and uncertainty analysis	30
4.5 Decompaction and 2D Restoration	32
4.6 Erosional and Flexural Modelling	35
5. Observation and Results	38
5.1 Horizon characteristics.....	38
5.2 Flexural behavior	43

Sequence 1	43
Sequence 2	48
Sequence 3	53
5.3 Flexural behavior due to change in elastic thickness.....	58
Discussion	60
Correlation between flexural model and flexural zone divisions	60
Sequence 1	62
Sequence 2	63
Sequence 3	63
Sequence 4	64
Summary and comparison.....	64
Eastern Barents Basin	66
Southwestern Barents Basin	67
Northern Barents Basin.....	68
The effect of erosional events on the flexural models	69
Uncertainty in the results	69
Conclusions.....	71
Further work.....	73
References.....	74
Appendix.....	77
A)	77

List of Figures

Figure 1: A map of the basins and highs in the Barents Sea. The red lines represent the transect lines that are used in this study. The dotted line is a regional line from Henriksen et al., (2011) used for the Russian part of the Barents Sea. Modified from (Henriksen et al., 2011).....	2
Figure 2: (A) Bouguer anomaly map (reference density = 2260 g/m ³), (B) magnetic map with magnetic trends and fault zones, (C) map of the structures in the Barents Sea and (D) Pseudogravity map divided into three different zones due to their flexural behavior and analysis of map A, B and C. Modified from (Marello et al., 2010; Henriksen et al., 2011; Marello, 2012)	3
Figure 3: Main lithological and tectonic events in the Barents Sea. The four main sequences described in this thesis are highlighted. Modified from (Henriksen et al., 2011)	5
Figure 4: Late Carboniferous carbonate build-ups and shallow shelf deposits. Modified from (Worsley, 2008).....	7
Figure 5: Upper Permian separating the eastern and western basins with a shallow shelf. Modified from (Worsley, 2008).....	8
Figure 6: Mid-Triassic with the start of alluvial fan deposits towards the larger basins. Modified from (Worsley, 2008).....	9
Figure 7: Late Triassic covers large parts of today's Barents Sea with alluvial fan deposits sourced from the mainland Norway in the south, Novaya Zemlya in the east and also some deposits from the north-east. Modified from (Worsley, 2008).	10
Figure 8: Early Cretaceous influenced by a low amount of deposits and erosional events in the highs. Modified from (Worsley, 2008).....	11
Figure 9: Late Paleogene influenced by glacier erosion and uplift. (Worsley, 2008) .	12
Figure 10: (A) Elastic thickness variation in a narrow rift basin and (B) elastic thickness variation in a wide rift basin. From Allen and Allen, 2013.	15
Figure 11: Example of how the load profile (A) and displacement profile (B) relates to tectonic and sedimentary loads and combines to form the relative topography profile (C) (Modified from Campos, 2011; Cardozo and Jordan, 2001).....	17

Figure 12: Example of a continuous (a) and broken (b) elastic plate with the vertical loads applied and deflection due to the tectonic and sedimentary loads. 18

Figure 13: Bouguer map, with a reduction density of 2200kg/m³ offshore and 2670kg/m³ onshore. Modified from Marelo (2012). 20

Figure 14: Magnetic maps with directional trends shown in blue and red and the grey lines are major faults. Modified from Marelo (2012). 21

Figure 15: Pseudogravity map with a distinct change in gravitational response from the western to the eastern and northern parts. Modified from Marelo (2012). 22

Figure 16: The yellow lines are 2D seismic lines used in this thesis. The Seismic was only available in the Norwegian sector. The white contours are the different structures found in the Barents Sea. The wells with time depth relationship is marked in orange and is mainly located south. 24

Figure 17: The western of the north-south trending transect lines, showing the seismic lines used in time (A), depth (B) and with interpretations (C). The vertical exaggeration is set to 15 for all figures. 25

Figure 18: The eastern of the north-south trending transect lines, showing the seismic lines used in time (A), depth (B) and with interpretations (C). The vertical exaggeration is set to 20 for both figures. 26

Figure 19: The east-west trending transect line, showing the seismic lines used in time (A), depth (B) and with interpretations (C). The vertical exaggeration is set to 12.5 for both figures. 27

Figure 20: Well 7229/11-2, with density log in orange and general trend in green. 29

Figure 21: Percentage error and standard deviation for the density (g/cm³) and velocity (m/s) analysis, based on the well analysis. 30

Figure 22: Velocities acquired from well logs. Trend lines showing how the velocity changes with depth and bars indicating the percentage error of the velocities. 31

Figure 23: Densities acquired from well logs. Trend lines showing how the density changes with depth and bars indicating the percentage error of the density. 31

Figure 24: The lithological properties used for the decompaction. Unit 1, 2, 3 and 4 was used for sequence 4, 3, 2 and 1 respectively. Generally the default values seen at

the top was applied, but the grain density (labeled 15:density) was calculated based on the amount of shale and sand for sequence 2,3 and 4, while sequence 1 used the standard limestone value.....32

Figure 25: (A) Before decompaction and (B) after decompaction. The sequences in figure B thickened due to the decompaction process and were used as an input for the restoration part. The vertical exaggeration is 15 times in both figures.....33

Figure 26: Flexural Slip unfolding principle. A shows the input beds and fault, B shows how the program uses bisectors and a given direction (pin) to restore the transects into C.....34

Figure 27: Simple shear (A) versus flexural shear (B) for a seismic line crossing the Hammerfest Basin.....34

Figure 28: Example showing the amount of minimum and maximum erosion that was calculated in Sentral Banken High for sequence two and three.....35

Figure 29: Example of the three transect lines (here restored at top cretaceous). To the right, between the red lines, are the same transects showing the variation in elastic thickness throughout the transect lines. The transect lines shown are (A) the east-west trending, (B) the western north-south trending and (C) the eastern north-south trending transects.37

Figure 31: The four different sequences defined at the Russian part of the Barents Sea. Orange=sequence 1, dark blue= sequence 2, green= sequence3, light blue=sequence 4 (Modified from Henriksen et al., (2011)).39

Figure 32: East-West transect line, illustrating the distribution of the different sequences. Red=Basement, orange=sequence 1, dark blue= sequence 2, green= sequence3, light blue=sequence 4.....40

Figure 33: Eastern north-south transect line, illustrating the distribution of the different sequences. Red=Basement, orange=sequence 1, dark blue= sequence 2, green= sequence3, light blue=sequence 4.....41

Figure 34: Western north-south Transect line, illustrating the distribution of the different sequences. Red=Basement, orange=sequence 1, dark blue= sequence 2, green= sequence3, light blue=sequence 4.....42

Figure 35: A section restored to base Triassic of the eastern of the north-south trending transect (B). The deflection due to sedimentary loads are shown to the right (D) with different amounts of erosion applied. Generally an elastic thickness of 30km is used, but the variable elastic thickness model uses the elastic thickness shown at the bottom left (E). These flexural models are combined in the bottom left figure (C) to describe the effect of the sedimentary loads. The difference could be due to either some of the input parameters (e.g. density, erosion etc.) or tectonic loads in the nearby area creating tectonic deflections. High tectonic deflection missing is indicated with a red circle and green indicates low. Figure A show the maximum and minimum erosion applied in the flexural models.45

Figure 36: A section restored to base Triassic of the western of the north-south trending transect (B). The deflection due to sedimentary loads are shown to the right (D) with different amounts of erosion applied. Generally an elastic thickness of 30km is used, but the variable elastic thickness model uses the elastic thickness shown at the bottom left (E). These flexural models are combined in the bottom left figure (C) to describe the effect of the sedimentary loads. The difference could be due to either some of the input parameters (e.g. density, erosion etc.) or tectonic loads in the nearby area creating tectonic deflections. High tectonic deflection missing is indicated with a red circle and green indicates low. Figure A show the maximum and minimum erosion applied in the flexural models.46

Figure 37: A section restored to base Triassic of the east-west trending transect (B). The deflection due to sedimentary loads are shown to the right (D) with different amounts of erosion applied. Generally an elastic thickness of 30km is used, but the variable elastic thickness model uses the elastic thickness shown at the bottom left (E). These flexural models are combined in the bottom left figure (C) to describe the effect of the sedimentary loads. The difference could be due to either some of the input parameters (e.g. density, erosion etc.) or tectonic loads in the nearby area creating tectonic deflections. High tectonic deflection missing is indicated with a red circle and green indicates low. Figure A show the maximum and minimum erosion applied in the flexural models.47

Figure 38: A section restored to base Cretaceous of the eastern of the north-south trending transect (B). The deflection due to sedimentary loads are shown to the right (D) with different amounts of erosion applied. Generally an elastic thickness of 30km is used, but the variable elastic thickness model uses the elastic thickness shown at the bottom left (E). These flexural models are combined in the bottom left figure (C) to describe the effect of the sedimentary loads. The difference could be due to either some of the input parameters (e.g. density, erosion etc.) or tectonic loads in the nearby area creating tectonic deflections. High tectonic deflection missing is indicated with a red circle and green indicates low. Figure A show the maximum and minimum erosion applied in the flexural models.50

Figure 39: A section restored to base Cretaceous of the western of the north-south trending transect (B). The deflection due to sedimentary loads are shown to the right (D) with different amounts of erosion applied. Generally an elastic thickness of 30km is used, but the variable elastic thickness model uses the elastic thickness shown at the bottom left (E). These flexural models are combined in the bottom left figure (C) to describe the effect of the sedimentary loads. The difference could be due to either some of the input parameters (e.g. density, erosion etc.) or tectonic loads in the nearby area creating tectonic deflections. High tectonic deflection missing is indicated with a red circle and green indicates low. Figure A show the maximum and minimum erosion applied in the flexural models.51

Figure 40: A section restored to base Cretaceous of the east-west trending transect (B). The deflection due to sedimentary loads are shown to the right (D) with different amounts of erosion applied. Generally an elastic thickness of 30km is used, but the variable elastic thickness model uses the elastic thickness shown at the bottom left (E). These flexural models are combined in the bottom left figure (C) to describe the effect of the sedimentary loads. The difference could be due to either some of the input parameters (e.g. density, erosion etc.) or tectonic loads in the nearby area creating tectonic deflections. High tectonic deflection missing is indicated with a red circle and green indicates low. Figure A show the maximum and minimum erosion applied in the flexural models.52

Figure 41: A section restored to top Cretaceous of the eastern of the north-south trending transect (B). The deflection due to sedimentary loads are shown to the right (D) with different amounts of erosion applied. Generally an elastic thickness of 30km is used, but the variable elastic thickness model uses the elastic thickness shown at the bottom left (E). These flexural models are combined in the bottom left figure (C) to describe the effect of the sedimentary loads. The difference could be due to either some of the input parameters (e.g. density, erosion etc.) or tectonic loads in the nearby area creating tectonic deflections. High tectonic deflection missing is indicated with a red circle and green indicates low. Figure A show the maximum and minimum erosion applied in the flexural models.55

Figure 42: A section restored to top Cretaceous of the western of the north-south trending transect (B). The deflection due to sedimentary loads are shown to the right (D) with different amounts of erosion applied. Generally an elastic thickness of 30km is used, but the variable elastic thickness model uses the elastic thickness shown at the bottom left (E). These flexural models are combined in the bottom left figure (C) to describe the effect of the sedimentary loads. The difference could be due to either some of the input parameters (e.g. density, erosion etc.) or tectonic loads in the nearby area creating tectonic deflections. High tectonic deflection missing is indicated with a red circle and green indicates low. Figure A show the maximum and minimum erosion applied in the flexural models.56

Figure 43: A section restored to top Cretaceous of the east-west trending transect (B). The deflection due to sedimentary loads are shown to the right (D) with different amounts of erosion applied. Generally an elastic thickness of 30km is used, but the variable elastic thickness model uses the elastic thickness shown at the bottom left (E). These flexural models are combined in the bottom left figure (C) to describe the effect of the sedimentary loads. The difference could be due to either some of the input parameters (e.g. density, erosion etc.) or tectonic loads in the nearby area creating tectonic deflections. High tectonic deflection missing is indicated with a red circle and green indicates low. Figure A show the maximum and minimum erosion applied in the flexural models.57

Figure 44: Example of a case where the flexural models does not follow the local changes, but rather the general thickness of the region. A is from the top Cretaceous restored section and B is the flexural models on top of the topography..... 58

Figure 45: Example of the Southern Barents Basin, where the basin is wide enough to respond to the flexural effect of the sedimentary loads. A is from the top Cretaceous restored section and B is the flexural models on top of the topography..... 59

Figure 46: Comparison of the elastic thickness applied to “the best fit” model (A) and the proposed flexural behavior in the Barents Sea (B). 61

Figure 47: A model showing the increase of tectonic deflections for the three first sequences. Structural map from Henriksen et. al. (2012). 65

Figure 48: The Eastern Barents Sea evolution for each sequence. 66

Figure 49: The south western Barents Sea evolution for each sequence. 67

Figure 50: The Eastern Barents Sea evolution for each sequence. 68

Figure 51: Erosion at the different structures in meters /percentage of total thickness. The green sections are the platform areas, yellow are the highs and blue is the basin areas. (Nyland et al., 1992; Riis and Fjeldskaar, 1992; Gustavsen et al., 1996; Torsvik and Buitter, 2007; Worsley, 2008; Nazarova, 2009; Hassan, 2012)..... 77

Figure 52: Example of how the different thicknesses in the different seismic lines were calculated. The white areas are the inputs of thickness (z) and location (x), the yellow parts are calculations for the densities (ρ_1 =sequence 1, ρ_2 =sequence 2 and ρ_3 =sequence 3) and the green parts are the calculation needed for the flexural modelling. The normalized section is used for the calculation of densities to weight the densities of the thickest sequences correctly. The maximum and minimum erosion was added in different files to calculate the response..... 78

List of Equations

Equation 1.....	15
Equation 2.....	16
Equation 3.....	16
Equation 4.....	30

1. INTRODUCTION

The Barents Sea is located north of Norway within the Norwegian and Russian continental shelves. It is bounded to the west by the Norwegian-Greenland Sea, to the north by the Arctic Sea, to the east by Novaya Zemlya and to the south by the Norwegian and Russian mainland (figure 1). From Late Devonian, the Barents Sea has been influenced by several tectonic and depositional events, resulting in complex structures described and modeled by several authors (Faleide et al., 1993; Worsley, 2008; Faleide et al., 2009; Henriksen et al., 2011; Gabrielsen, 2013; Gac et al., 2013).

In the western Barents Sea, extensional tectonics starting in the Devonian has been the dominant process, with a prominent peak during the breakup between Greenland and Norway in the Paleocene period (Henriksen et al., 2011). These tectonic events led to large Cenozoic sediment deposits in the southwestern Barents Sea, while the northern Barents Sea has mainly Devonian to Jurassic deposits, due to a more stable tectonic regime and erosion of younger deposits due to uplift during the Cretaceous. The Russian side of the Barents is mainly affected by a large subsiding event that started in the Devonian, with an acceleration in the Triassic and finishing in the Cretaceous (Ramberg et al., 2008). Since then, the eastern Barents Sea has been stable with some uplift in the Cenozoic (Gac et al., 2012) and recent glacier events causing regional erosion.

In the Barents Sea structural highs are often found next to deeper basins. How these structures are affected by sedimentary and tectonic loads is still poorly understood. Magnetic, structural and gravitational maps show a distinct change between the northern, eastern and southwestern parts of the Barents Sea, which could indicate a change in elastic thickness (figure 2D).

The sedimentary and tectonic loads are related to the thickness of the elastic part of the lithosphere called the elastic plate. The thickness of this plate relates to tectonism and is increasing with time due to isostatic effects. High amount of tectonism have a tendency to decrease the elastic thickness, resulting in a thinner or broken elastic plate. This results in a shorter wavelength of flexural deformation, resulting in a higher amount of deflection. The crust behaves in regards of different elastic parameters. When these parameters are set, it is possible to calculate the flexural response in the crust. The Flexural response is calculated by some standard elastic parameters and due to the density and amount of sediments applied. By calculating a distribution of loads, with the related densities, a model showing the uplift created due to sedimentary loads is created. By comparing the resulting flexural models related to sedimentary loads with the topography, the difference between them is the missing tectonic deflections necessary to create the structures.

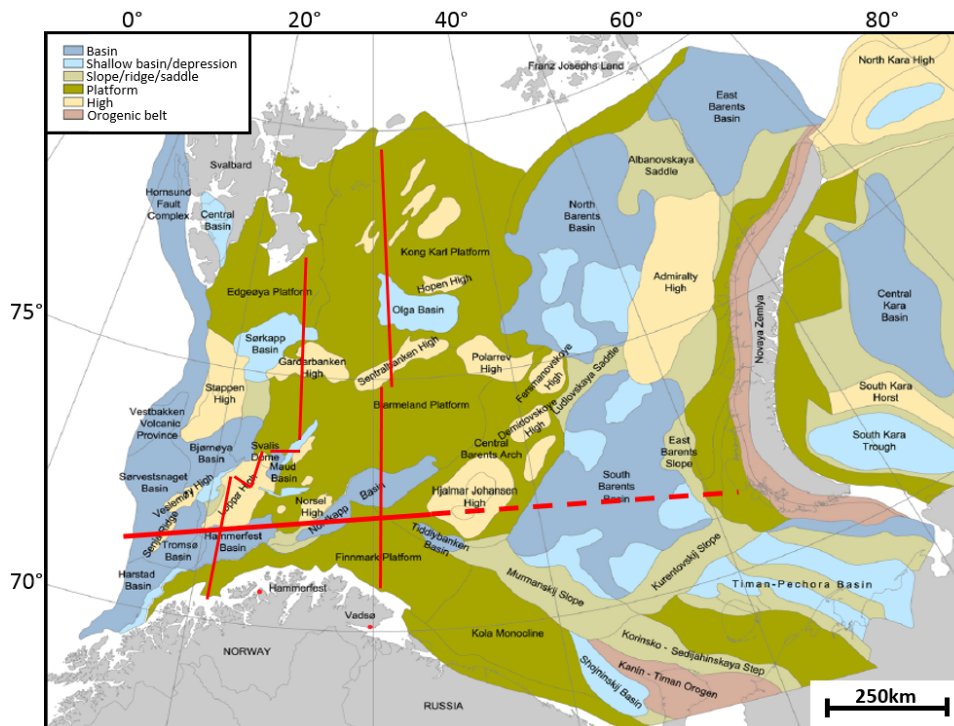


Figure 1: A map of the basins and highs in the Barents Sea. The red lines represent the transect lines that are used in this study. The dotted line is a regional line from Henriksen et al., (2011) used for the Russian part of the Barents Sea. Modified from (Henriksen et al., 2011)

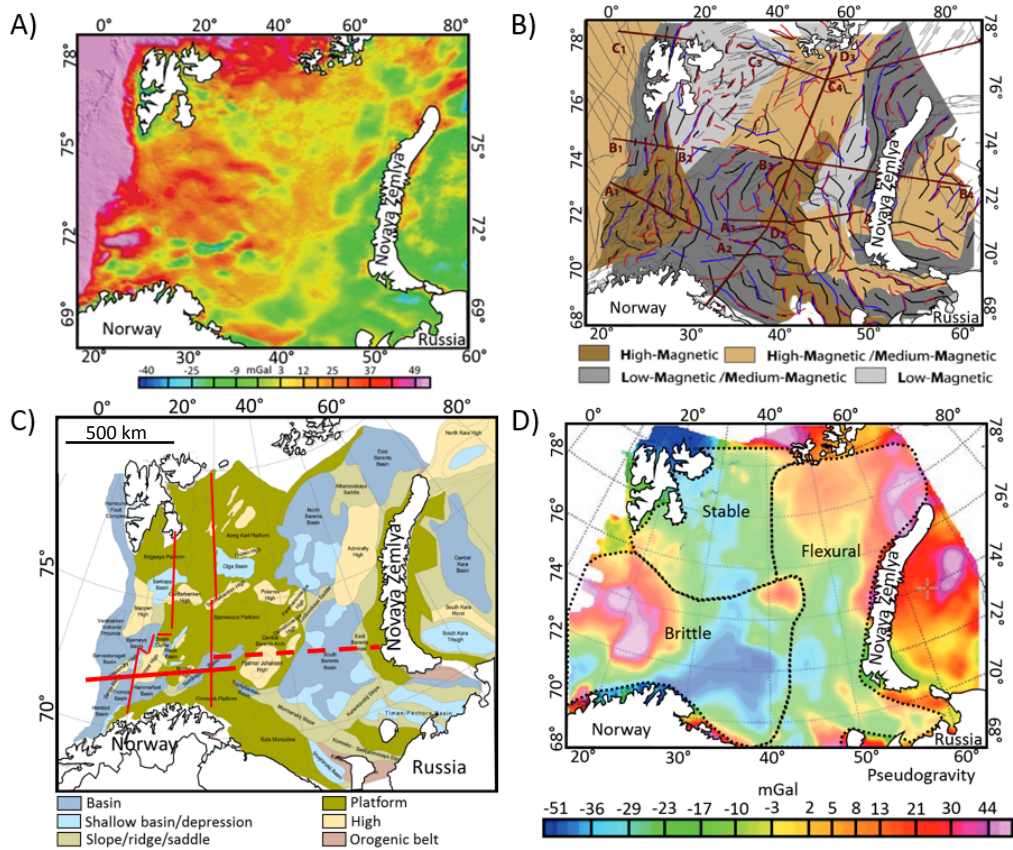


Figure 2: (A) Bouguer anomaly map (reference density = 2260 g/m³), (B) magnetic map with magnetic trends and fault zones, (C) map of the structures in the Barents Sea and (D) Pseudogravity map divided into three different zones due to their flexural behavior and analysis of map A, B and C. Modified from (Marello et al., 2010; Henriksen et al., 2011; Marello, 2012)

The goal of this thesis is to explain the flexural effect from sedimentary and tectonic loads on structures in the Barents Sea by building 2D flexural models of the four defined sequences, and focus on the the major structures.

This will result in a flexural model for each of the sequences in each transect line, that will describe the impact of the sedimentary load on the structures in the Barents Sea through time.

To be able to make these flexural models, a restoration of each sequence using a flexural slip method, which maintain the length and thickness of the different sequences, was conducted. Understanding the tectonic and sedimentary loads in the Barents Sea result in a better understanding of how the structures are today, the structures evolution and describes the effect of sediments versus the tectonic loads for the different parts of the Barents Sea.

Figure 1 show the transect lines, resulting in a approximate length of 2200 kilometers. Due to the extent of this study, the lithology have been divided into four sequences defined in figure 3, related to different lithologies and erosional events.

Different scenarios of erosion and elastic thickness and a flexural model of each sequence were constructed. The amount of erosion are widely described in articles (Riis and Fjeldskaar, 1992; Richardsen et al., 1993; Gustavsen et al., 1996; Torsvik and Buiter, 2007; Nazarova, 2009; Høy and Lundschie, 2011; Hassan, 2012; Sobolev, 2012), but since some areas are poorly described, the amount of erosion will be estimated for each sequence, based on seismic interpretation (see chapter 4).

The variation of the erosional phases and lithology have implications for this study. The amount of erosion, elastic thickness, and thickness of the sediments are uncertain, and the key to this study is too minimise these uncertainty and create different scenarios varying the most uncertain factors.

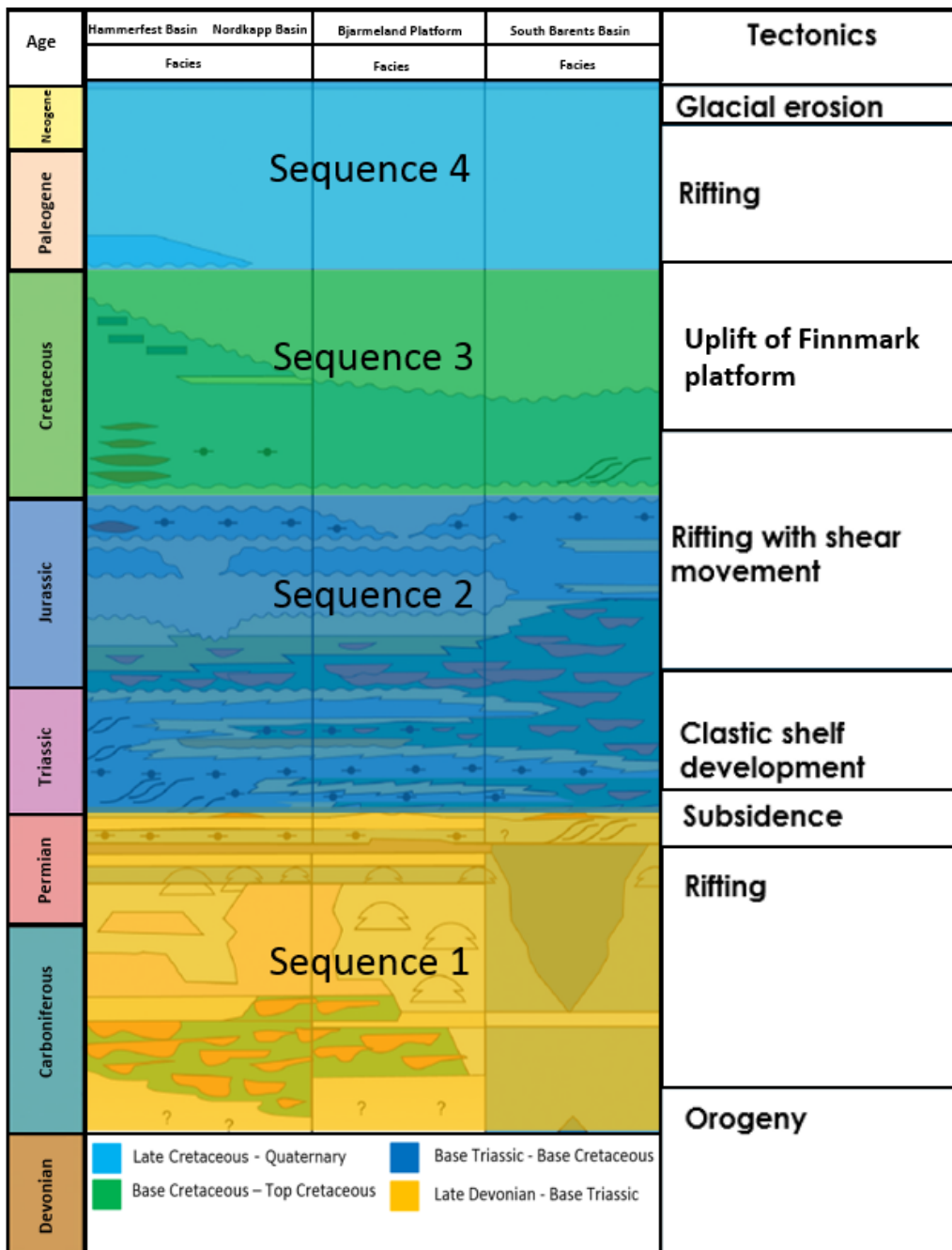


Figure 3: Main lithological and tectonic events in the Barents Sea. The four main sequences described in this thesis are highlighted. Modified from (Henriksen et al., 2011)

2. GEOLOGICAL SETTING

The Barents Sea is subdivided into several basins, highs and platforms as seen in figure 1. From the east, there are large basins to the west of Novaya Zemlya arc including the Timan – Pechora Basin and the Northern and Southern Barents Basin, which consists mainly of Devonian to Cretaceous sediments. West of these basins, a large platform area (Bjarmeland Platform) is located, which is partly separated to the eastern basins by structural highs like the Hjalmar Johansen, Demidovskoye and Fermanovskoye Highs. The northern platform area consists mainly of thick Devonian to Lower Cretaceous sediments. In the southwestern Barents Sea, there are basins with some younger Cenozoic sedimentary rocks on top, like the Nordkapp Basin. This basin is known for its 16 salt domes from Late Paleozoic (Nilsen et al., 1995). The most southwestern parts of the Barents Sea has many recent deposits due to major rifting events. The following sub chapters will describe the major events for the four major sequences used in this thesis.

2.1 Devonian – Base Tertiary (Sequence 1):

Tectonic development in the Devonian resulted in north-west trending highs in the eastern Barents Sea, while in the western Barents Sea, the crustal movement created rift basins close to the Barents shelf edge close to the fractured zones in the west (see figure 4). The fault zones from this time were controlled by older structures formed during the Caledonian Orogeny. The basins formed in the Early Carboniferous in the rift zones was large and affected by subsidence, resulting in deeper basins. In the Middle Carboniferous, these basins became smaller and ended with a stable platform in the Late Carboniferous due to large changes in plate tectonic (causing uplift) and sea level changes (Figure 4) (Ramberg et al., 2008; Worsley, 2008; Henriksen et al., 2011).

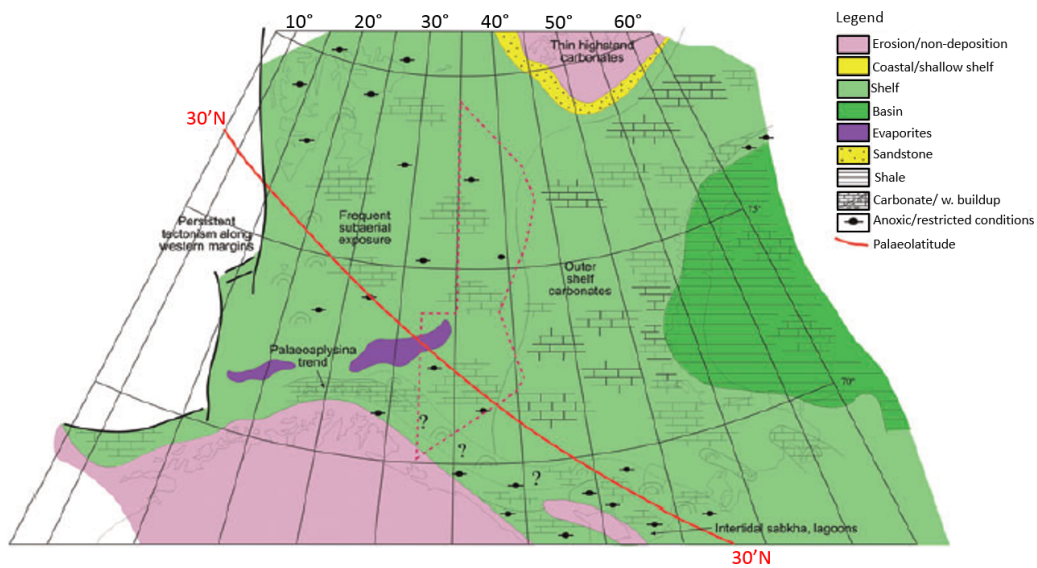


Figure 4: Late Carboniferous carbonate build-ups and shallow shelf deposits. Modified from (Worsley, 2008).

The late Carboniferous to Early Permian was affected by hot and dry climate, which resulted in carbonate build-ups in an extensive shelf sea (Ramberg et al., 2008). These deposits were characterized by warm salt-water conditions.

In the Upper Permian, the Barents Sea drifted into the northern temperate zone and mudstones, sandstones and some carbonates in a lot cooler and deeper sea than before were deposited (figure 5) (Ramberg et al., 2008). The Nordkapp Basin had especially cool water carbonates deposited in the subsiding parts, with some siliceous shales in the deeper parts (Worsley, 2008).

The sediments deposited were mainly alluvial/fluvial channels in a coastal/deltaic plain in the western basin and a large carbonate platform to the east (figure 4) (Henriksen et al., 2011).

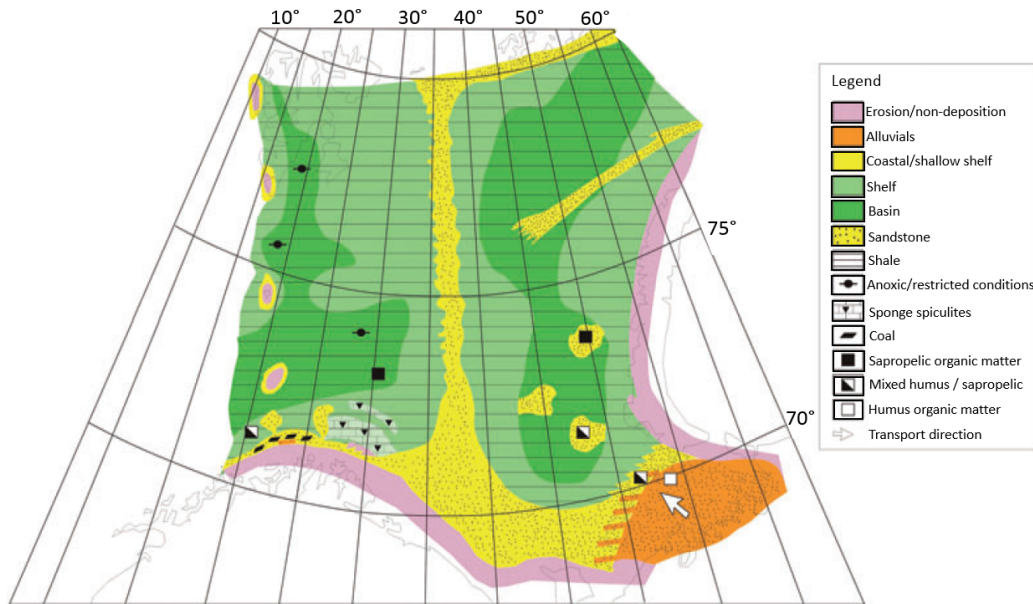


Figure 5: Upper Permian separating the eastern and western basins with a shallow shelf. Modified from (Worsley, 2008)

2.2 Base Tertiary – Base Cretaceous (Sequence 2):

The Permian is characterized by carbonate build-ups in the early to middle stages and clastic sedimentation in the late stage, while the Triassic deposits have alternating mud and sand. This transition from clastic sedimentation to fine muds is a well-defined boundary throughout the Barents Sea. The sedimentation rate in the western basins was lower than in the eastern basins due to the formation of Novaya Zemlya. In the large eastern basins, up to 8000-meter thick successions of clastic sediments from this sequence are found (Ramberg et al., 2008).

A large early Triassic subsidence event in the areas that would become the Nordkapp, Hammerfest, Bjørnøya and Tromsø Basins created accommodation space for clastic sediments, keeping the basins filled throughout this period. In addition, many alluvial fans started to build out in the Middle Jurassic as seen in figure 6, sourced mainly by the eroded sediments of Novaya Zemlya.

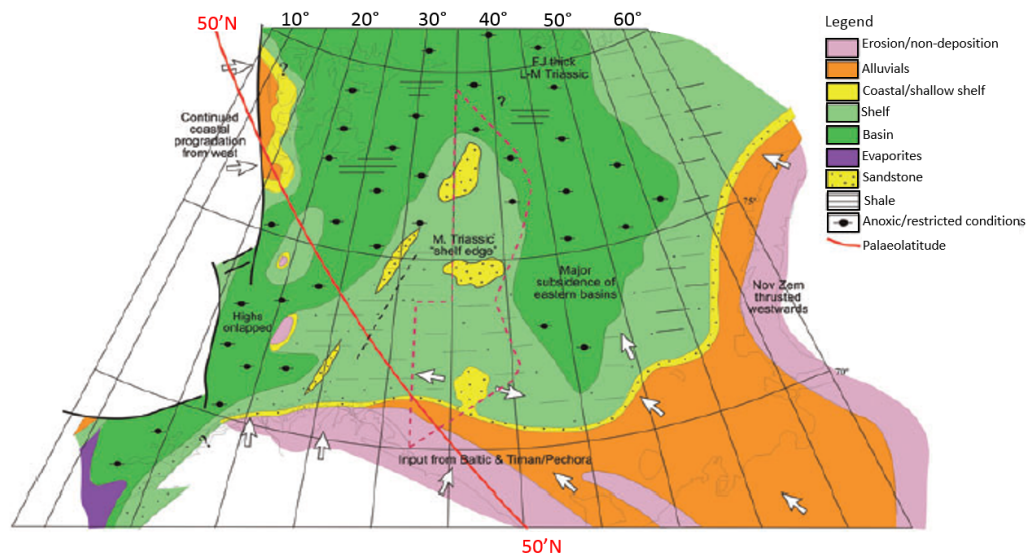


Figure 6: Mid-Triassic with the start of alluvial fan deposits towards the larger basins. Modified from (Worsley, 2008).

The late stages of Triassic was affected by the sediment supply from Novaya Zemlya and a continuous subsidence of the eastern basins (figure 7) (Ramberg et al., 2008; Worsley, 2008).

In the Early Jurassic, the Barents Sea was a stable platform, but had increasing tectonic movements towards the Late Jurassic. In the Early Jurassic stages, there were some deposits of coastal sands, but the real change in depositional system and tectonism initiated in the Middle Jurassic, where the tectonic movement separated the southern and northern sub basins and also resulting in alluvial fans from Novaya Zemlya, Russia and Norway. The end of Jurassic had an increase of tectonism, leading to erosion in certain areas, while other places build up accommodation space (Ramberg et al., 2008; Worsley, 2008).

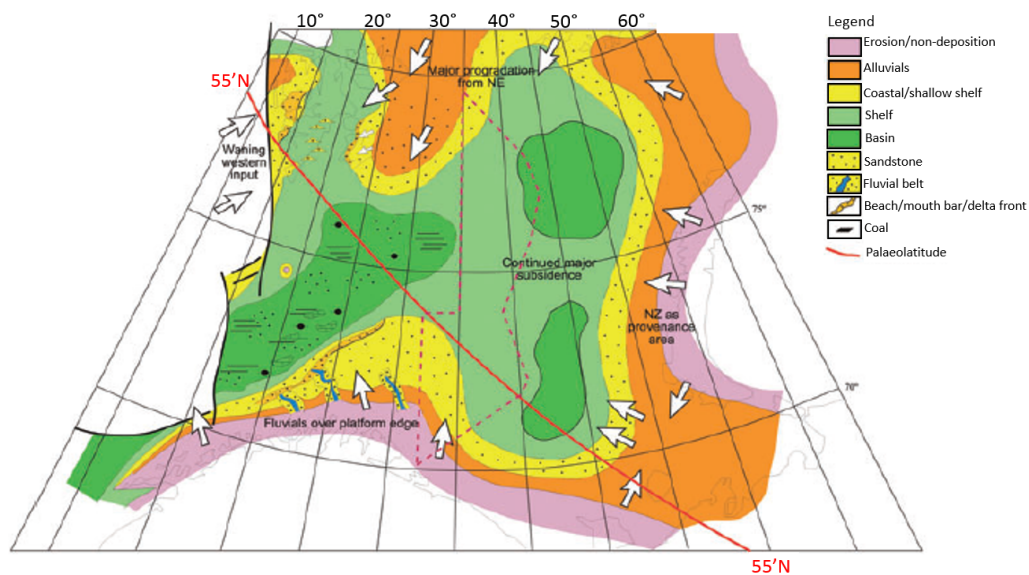


Figure 7: Late Triassic covers large parts of today's Barents Sea with alluvial fan deposits sourced from the mainland Norway in the south, Novaya Zemlya in the east and also some deposits from the north-east. Modified from (Worsley, 2008).

2.3 Base Cretaceous - Top Cretaceous (Sequence 3):

In the Early Cretaceous the tectonism from Jurassic terminated, which led to the main structures that are found in the Barents Sea today. At this time the Bjørnøya and Hammerfest basin was fully formed and the rifting that previously was here shifted to the continental slope, west of Svalbard (Ramberg et al., 2008). The stable platform areas had a decrease of deposits compared to the southwestern basins, where several clinoform deposits are found. The highs had several episodes of erosion and uplift, making it difficult to get a regional view of the distribution to this sequence.

(Ramberg et al., 2008; Worsley, 2008; Henriksen et al., 2011). In addition, some igneous intrusions have been found in the northern Barents Sea (Vestbakken Volcanic Province). These intrusions are related to the opening of the Atlantic Ocean during Mesozoic and Cenozoic time. This phenomenon is defined as the High Arctic Large Igneous Province (HALIP) and has influenced certain parts of the arctic with uplift, resulting in erosion of sediments from Mesozoic to base Cretaceous with an unknown extent (Corfu et al., 2013).

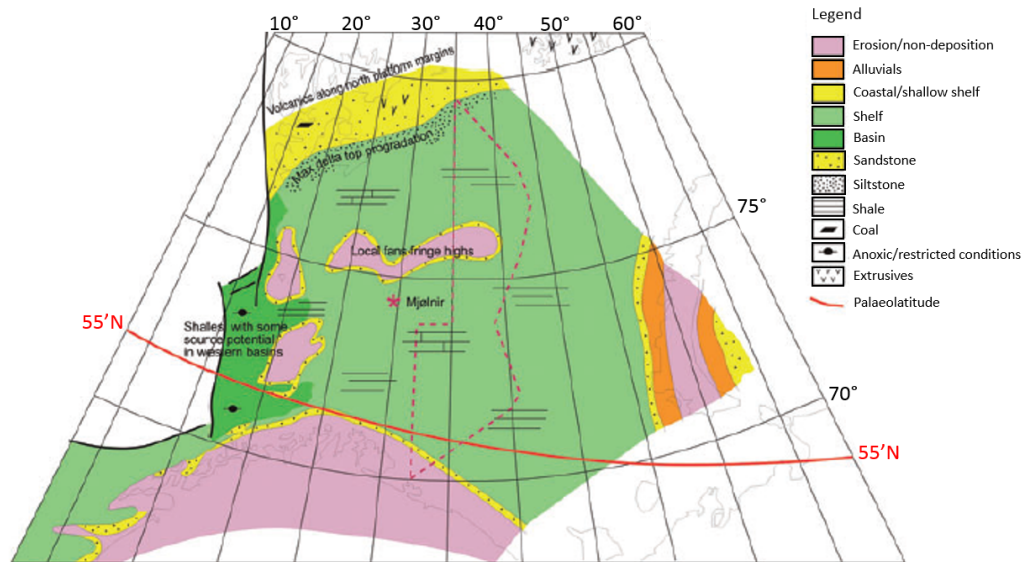


Figure 8: Early Cretaceous influenced by a low amount of deposits and erosional events in the highs. Modified from (Worsley, 2008).

2.4 Top Cretaceous - Quaternary (Sequence 4):

The Cretaceous – Quaternary succession is mainly related to the opening of the Norwegian – Greenland Sea. There are found minor amounts of deposits in the eastern basins, but the major amount of deposits are found along the fractured zones in the southwestern Barents Sea. The other parts were affected by erosional events, both from glacier events in the Neogene and uplift in the later stages.

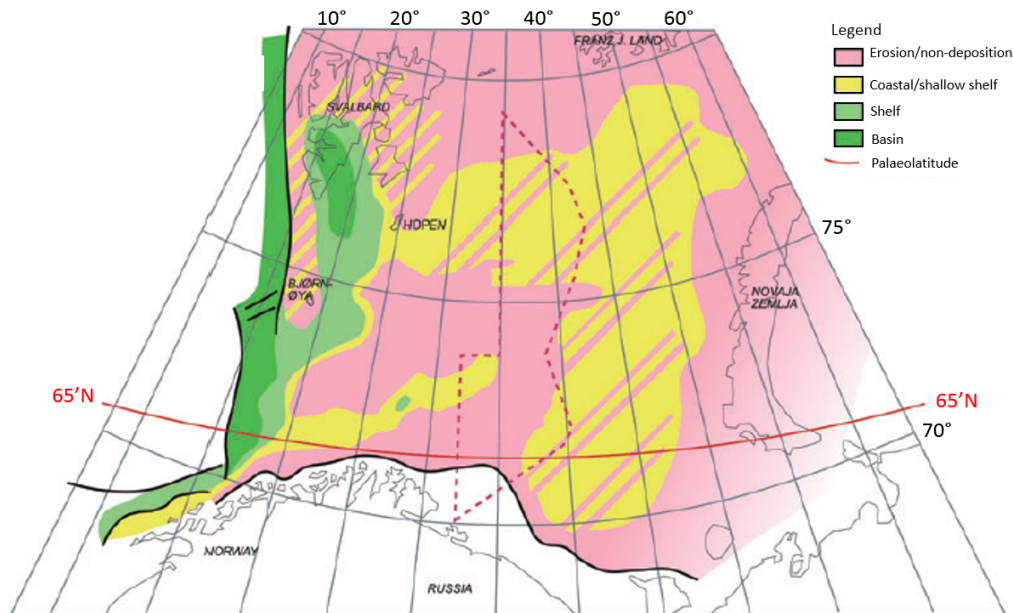


Figure 9: Late Paleogene influenced by glacier erosion and uplift. (Worsley, 2008)

3. THE LITHOSPHERE AND FLEXURE

This chapter will describe the theory about lithospheric behavior and the flexural response due to tectonic and sedimentary loads. Flexure and lithospheric stretching is a widely discussed topic, which means that this chapter will emphasis on the topics that are related to the Barents Sea and will be a reference to the terminology used in the next chapters.

3.1 Rheology

Rheology is described by Allen and Allen (2013) as “The linkage between the forces on the lithosphere and its deformation is the rheology of lithospheric materials” (p. 92). The rheology does therefore control the deformation of the lithosphere and is dependent on a correct strength envelope to be treated correctly. In a basin model, it is essential to define a strength envelope for both the brittle and ductile deformational mechanism. Brittle rocks are rocks that break into pieces under deformation, while ductile rocks will flow or bend under deformation. Since these mechanisms relay on strain rate, temperature and pressure, the data is often based on experiments following the power law creep, which relates to the strain rate, temperature, pressure and some stress factors (Allen and Allen, 2013).

Gravitational maps and data related to faulted and fractured zones could give a general idea of how rocks in a certain area behave. High gravity could indicate to a higher amount of faults and fractures (brittle zone), while low gravity could respond to a low fractured zone (ductile zone).

3.2 Isostasy

Watts (2001) explain that isostasy is “the temporal and spatial scales over which the earth’s crust and upper mantle adjust to geological loads” (p. 176). This is the basics behind the flexural behavior of sedimentary and tectonic loads. Multiple concepts of isostasy exists, e.g. Pratt, Airy and the flexure model, which relates to the different densities and thicknesses applied.

The most used theories are the Airy and flexural models. The concept behind these models are basically the same, but the flexural model calculates the isostasy in a regional area, whereas the Airy model calculates the isostasy in a local area. By using these models, it is assumed that (1) the crust has the same density as the load, (2) the material that infills the flexure is the same density as the crust and (3) the crust is of uniform density. These assumptions are often wrong due to the change in density from the infill sediments to the loads (Watts, 2001).

For the flexural program used in this thesis called Flex2D (Nestor Cardozo), a flexural isostasy model is applied as long as the elastic thickness is more than zero. When zero elastic thickness is applied, it is assumed that the loads and their compensation are local.

3.3 Flexure of the Lithosphere

The flexural rigidity characterizes the apparent strength of the lithosphere, which is a parameter expressed through the effective elastic thickness of the lithosphere.

Watts (2001) explains the elastic thickness as a filter, which suppresses the largest amplitudes and short wavelength deformation by the use of local models of isostasy. He also says that this “filter” allows for passage of small amplitudes that has a long wavelength deformation and is associated with flexure.

A high elastic thickness tends to make the crust more rigid and previous work of flexure results in oceanic crusts shows that the elastic thickness increases with age and therefore gets more rigid (Watts, 1994). Figure 10A shows how the elastic thickness in

a narrow rift basin is more or less continuous, while in a wide rift basin (figure 10B), the elastic thickness thins out towards the mid ocean ridge.

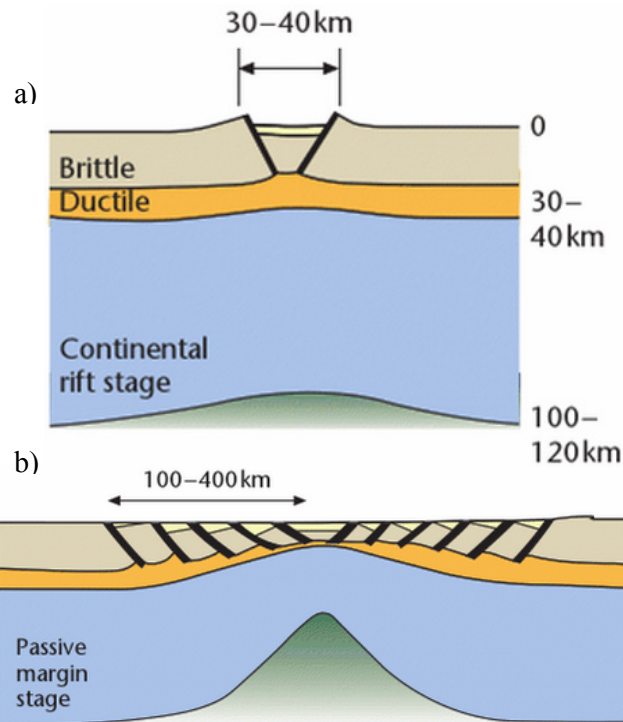


Figure 10: (A) Elastic thickness variation in a narrow rift basin and (B) elastic thickness variation in a wide rift basin. From Allen and Allen, 2013.

Flexure is caused by external forces and is a deflection of the lithosphere. The main factor for flexure is the flexural rigidity, D , calculated at a location x as:

$$x = \frac{E \cdot T^3 e}{12 \cdot (1 - \nu^2)} \quad \text{Equation 1}$$

Where E is the Young's modulus, T_e is the elastic plate thickness and ν is Poisson's ratio (Audet and Mareschal, 2004).

The Flexural rigidity corresponds to how much the plate is affected by loads and forces. Figure 11 shows how the sedimentary and tectonic loads deflect the continental lithosphere, creating a deflection of the continental lithosphere next to the sedimentary basin. The load profile illustrates the direction and parameters that causes the vertical loads, while the displacement profile shows how these loads affect the flexural response of the crust. The combined load profile and displacement profile illustrates the relative topography profile in 11b

For a distribution of loads (as used in this thesis), the deflection, y is calculated over an area x as:

$$y = D * \frac{Pb\lambda}{2 * (\rho m - \rho infill) * g} * e^{-\lambda x} * (\cos \lambda x + \sin \lambda x) \text{ Equation 2}$$

Where D is the flexural rigidity, g the gravitation, Pb the line load, ρm the density of the mantel, $\rho infill$ is the density of the sediments and λ is related to the elastic properties of the beam. In terms of elastic thickness, the parameter λ is divided from the formula:

$$\lambda = 3g * (\rho m - \rho infill) * (1 - \nu^2) * g / Te^3 \text{ Equation 3}$$

Here ν is the Poisson ratio and Te is the effective elastic thickness.

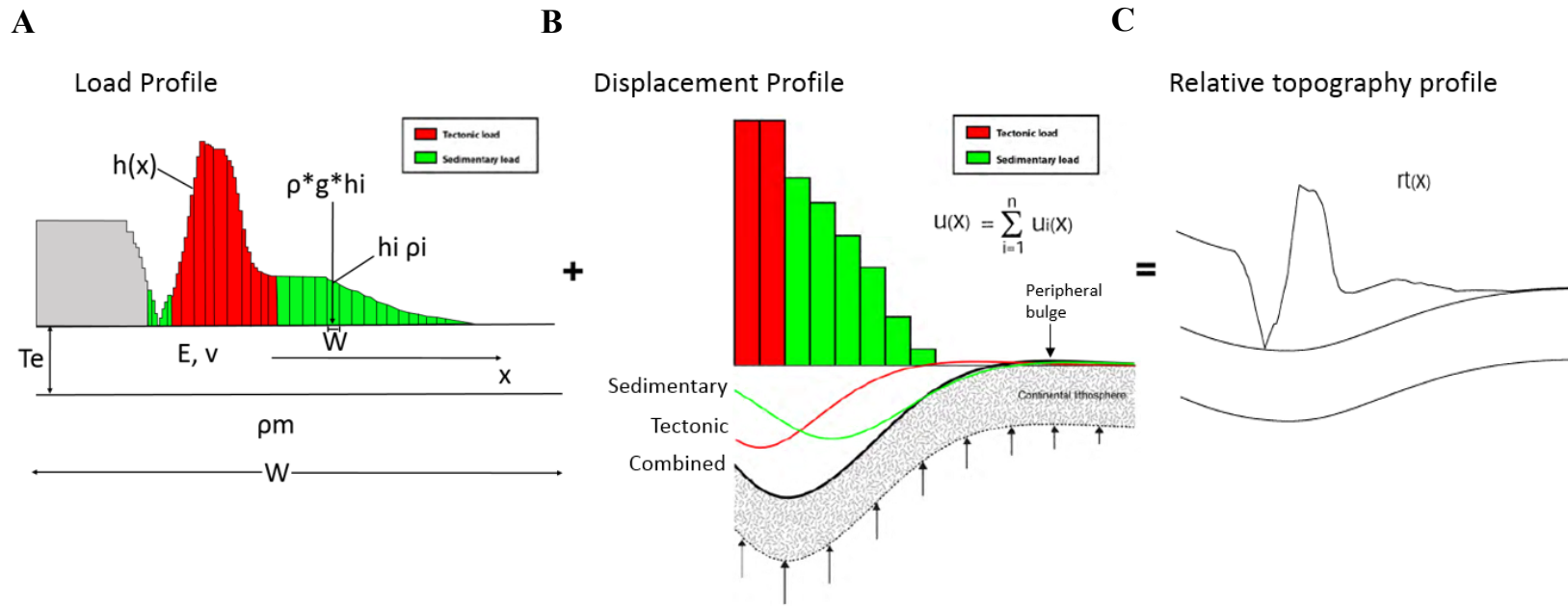


Figure 11: Example of how the load profile (A) and displacement profile (B) relates to tectonic and sedimentary loads and combines to form the relative topography profile (C) (Modified from Campos, 2011; Cardozo and Jordan, 2001).

Under loads, a continuous elastic plate bends and deflects in regards of the equation 3.2 given above, but if the plate is broken (figure 12b), the maximum deflection is twice of that of an unbroken plate, with same flexural rigidity and same vertical loads (Turcotte and Schubert, 2002). A broken elastic plate is in reality not possible, but implies that the effect of equal loads on the lithosphere could vary a lot.

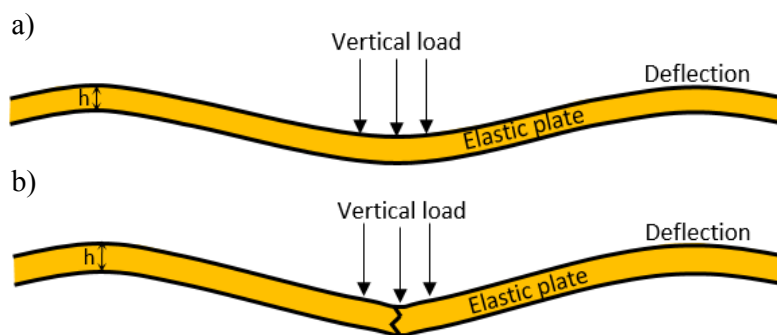


Figure 12: Example of a continuous (a) and broken (b) elastic plate with the vertical loads applied and deflection due to the tectonic and sedimentary loads.

3.4 Gravitational and magnetic maps

The Barents Sea was divided into three zones based on structural, magnetic, gravitational and Bouguer maps to get a general overview of the changes in flexural response.

The Bouguer map (figure 13) is created from a gravity anomaly map, which is corrected for the height of where it is measured and then corrected for the density of the layers. The first correction was a free air correction, which corrected the gravity anomalies for elevation from where the measurement is made (Watts, 2001). The Bouguer anomaly map is created by subtracting the Bouguer correction from the free-air anomaly.

$\text{Bouguer anomaly} = \text{Free-air anomaly} - \text{Bouguer correction}$, where the Bouguer correction is calculated by summing the gravitational contribution of masses in different locations above a datum (Watts, 2001). Since Bouguer maps usually are created in regional areas, there is used a regional density for the Bouguer correction. This could often be conflicting, if the density of the rocks are of variable density in the horizontal direction. A Bouguer map is then used to give a general description of the mass beneath the area of investigation. A strong low anomaly usually means that there is “a significant deficit of mass beneath the surface” (Watts, 2001). This could also indicate a low elastic thickness, but knowledge about the compression of sediments is crucial to be confident, since the Bouguer anomaly is calculated from a constant density. The Bouguer correction also assumes that the elevation around the area of measurement are flat, which is rarely the case. The Barents Sea is one example where the rocks in the eastern part is very compacted in the deep basins (Gac et al., 2013) compared to the western, which makes a much lower anomaly in the eastern Barents Sea (figure 13).

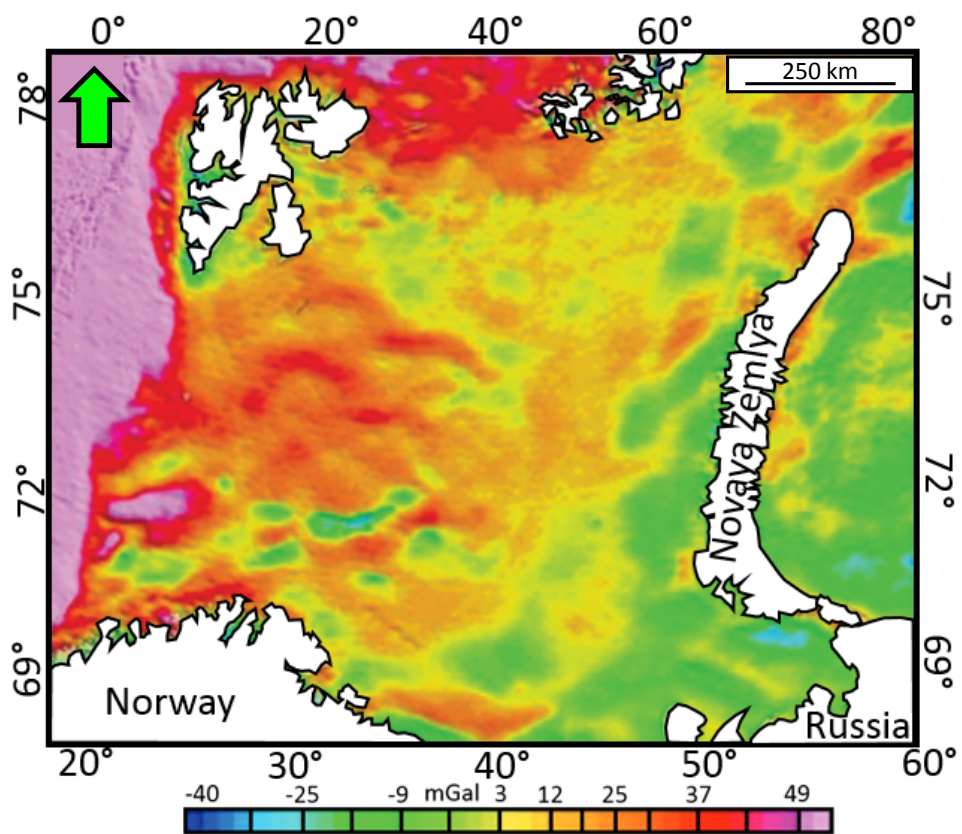


Figure 13: Bouguer map, with a reduction density of 2200kg/m^3 offshore and 2670kg/m^3 onshore. Modified from Marelllo (2012).

Magnetic maps (figure 14) measures the magnetic response of the crust. This often creates a high value in tectonically active areas. Tectonically active areas could have a high magnetic response due to faulting in the basement. (Kearey et al., 2013)

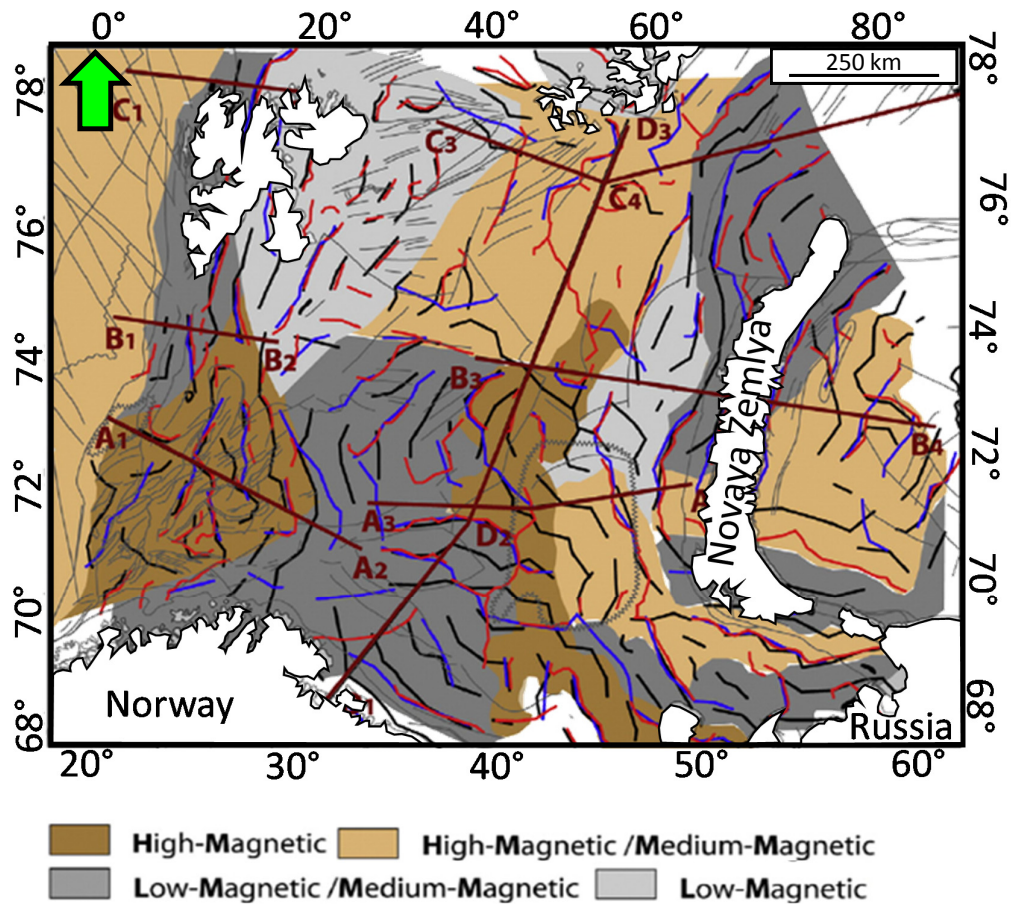


Figure 14: Magnetic maps with directional trends shown in blue and red and the grey lines are major faults. Modified from Marengo (2012).

Gravity maps (figure 15) are used to distinguish between large changes in geological structures. “Gravity anomalies have also shown that most of these major relief features are in isostatic equilibrium, suggesting that the lithosphere is not capable of sustaining significant loads and yields isostatically to any change in surface loading” (Kearey et al., 2013).

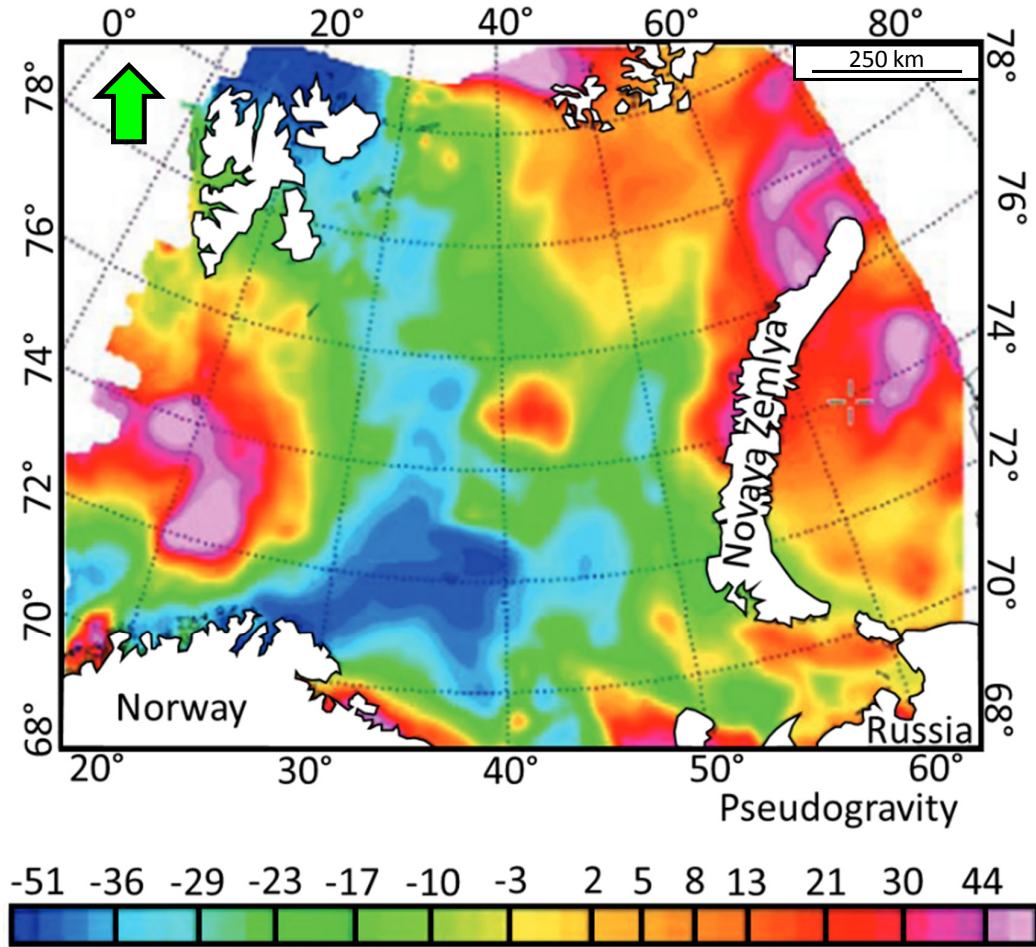


Figure 15: Pseudogravity map with a distinct change in gravitational response from the western to the eastern and northern parts. Modified from Marelllo (2012).

4. DATA AND METHODOLOGY

The Seismic interpretation done in this thesis is used as input for the basin modeling, which will be the base of flexural calculations. Four sequences has been defined by five horizons and faults are interpreted and depth converted as an input for the decompaction and restoration process in a software called Move by Midland Valley.

4.1 Profile and data

The surveys and wells available were provided by NPD and covers the entire Norwegian sector of the Barents Sea. The data used was 18 seismic lines creating three transect lines, two in the NS direction and one in the EW direction. The seismic resolution of these lines varies due to the regional extent of this study, but generally has a range of 23 to 53m, where the first and second sequence has a distinctly lower resolution than the third and fourth sequence. These transect lines were created to cover the largest and most interesting parts (Hammerfest Basin, Loppa High, Bjarmeland Platform, Nordkapp Basin etc., see figure 16). Wells throughout the Barents Sea have provided formation tops for correlation and time depth curves for depth conversion. This has been used as a reference for the horizon tops created. Since there was no data available for the Russian sector, a seismic line published from Henriksen et. al. (2011) to describe the Russian part of the Barents Sea was used (yellow dashed line in figure 16). The seismic-well tie was created as part of the LoCrA project (<http://locra.uv.uio.no>) and the wells are therefore tied regionally to the seismic.

4.2 Depth Conversion

The program used for the interpretation of the sequences is called DecisionSpace, from Landmark. The interpretations and data were then imported to petrel to create a velocity model. The velocity model was based on the surfaces of each horizon, which was tied to the wells with time-depth curves and well tops from the LoCrA project (LoCrA –

<http://locra.uis.no>). The challenge creating the Velocity model was that the wells with time-depth curve were located in the southern parts of the Barents Sea. Due to this, an interval velocity for the northern parts that was tied to the surfaces and well tops from wells located further south was used. The time-depth curves had a better coverage for the youngest deposits due to the well depths, which makes the oldest deposits more uncertain. Figure 17, 18 and 19 illustrates the seismic lines used, compared with the depth conversion and interpretation of the sequences.

The depth converted seismic and horizons was then imported to Move for further processing.

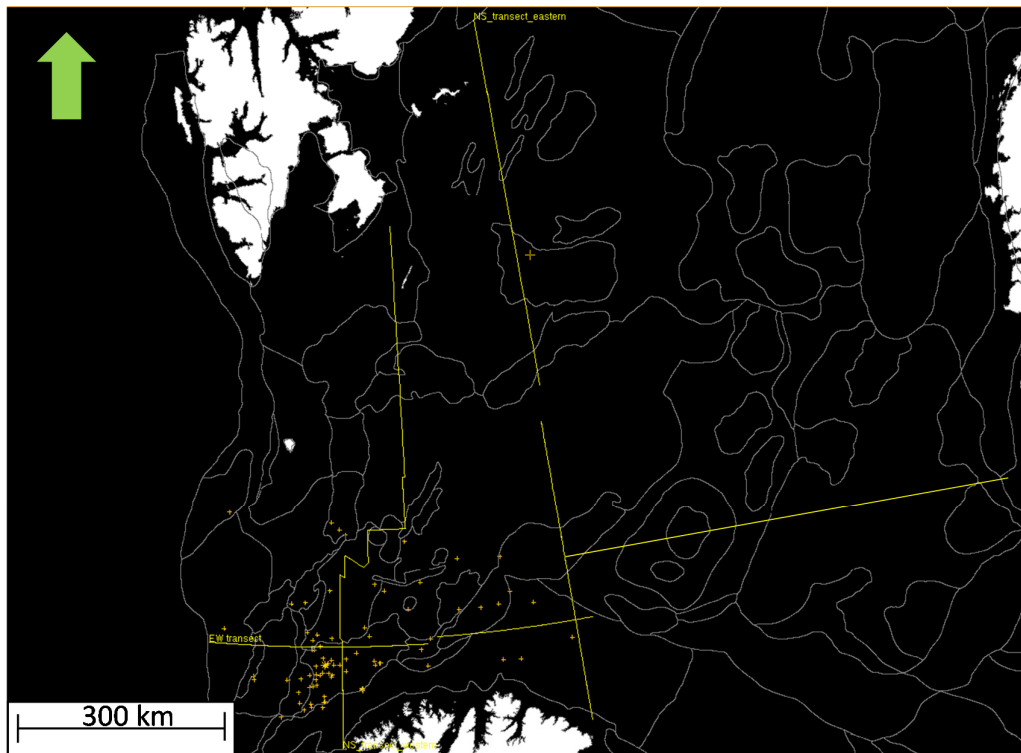


Figure 16: The yellow lines are 2D seismic lines used in this thesis. The Seismic was only available in the Norwegian sector. The white contours are the different structures found in the Barents Sea. The wells with time depth relationship is marked in orange and is mainly located south.

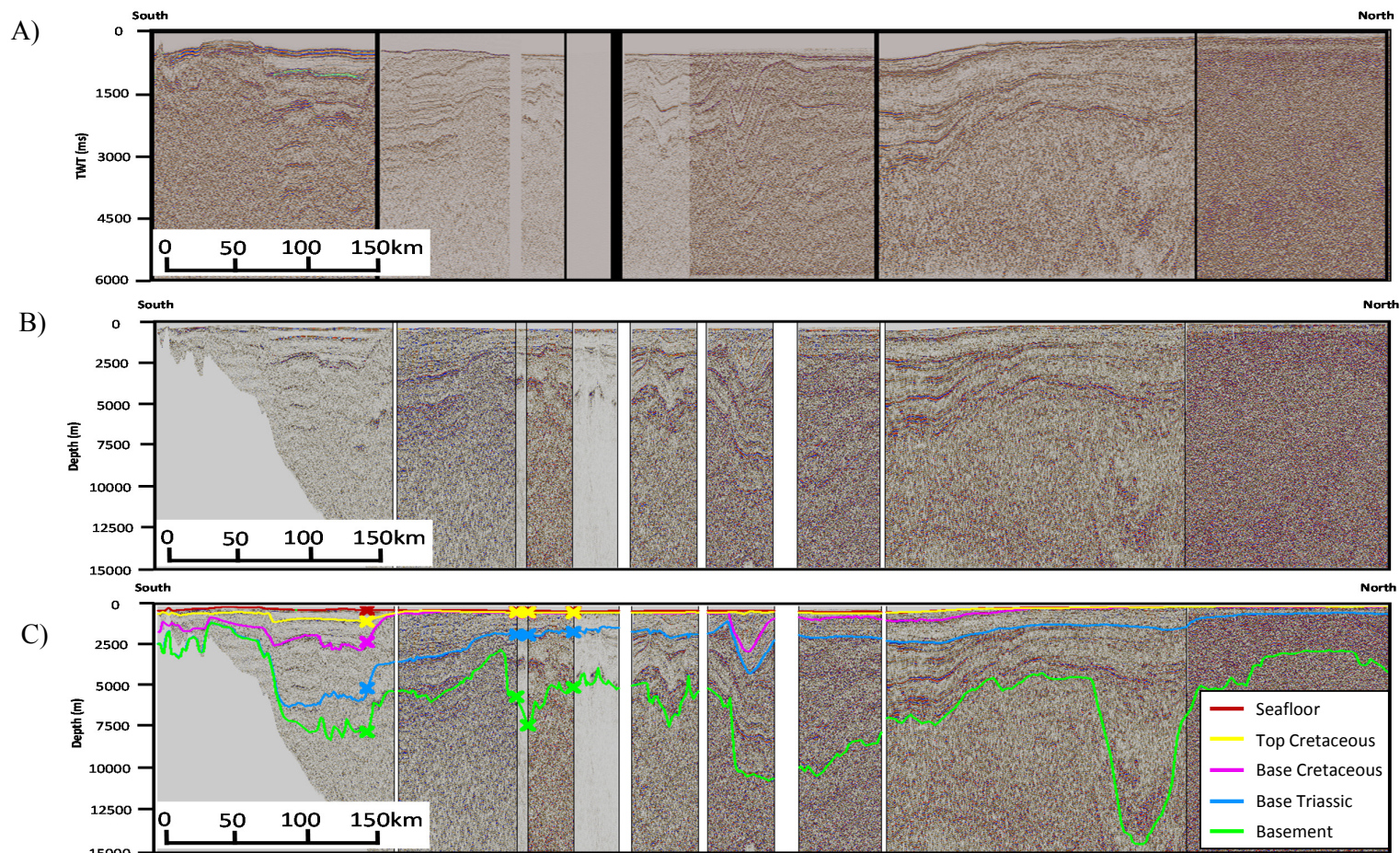


Figure 17: The western of the north-south trending transect lines, showing the seismic lines used in time (A), depth (B) and with interpretations (C). The vertical exaggeration is set to 15 for all figures.

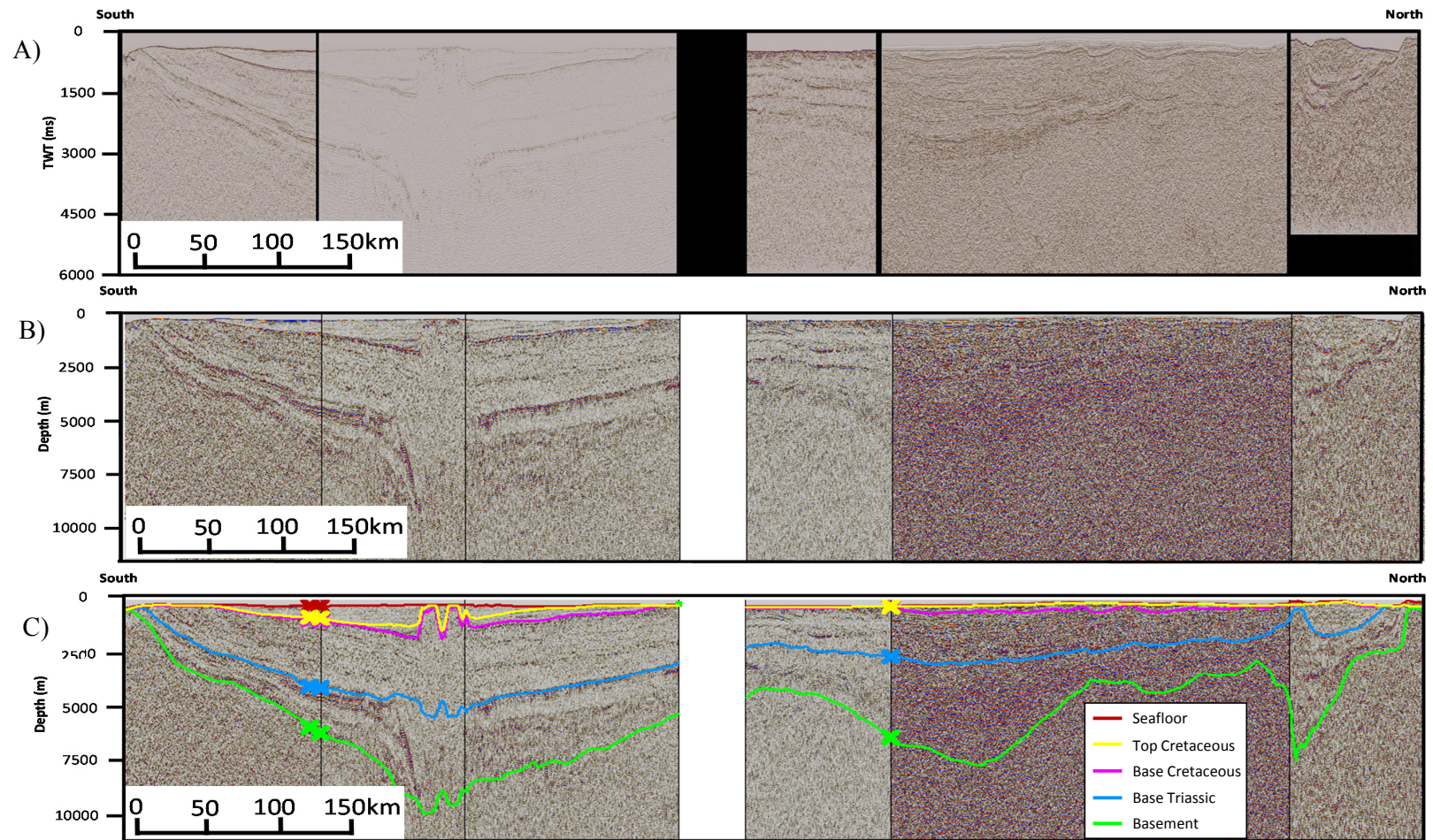


Figure 18: The eastern of the north-south trending transect lines, showing the seismic lines used in time (A), depth (B) and with interpretations (C). The vertical 26
exaggeration is set to 20 for both figures.

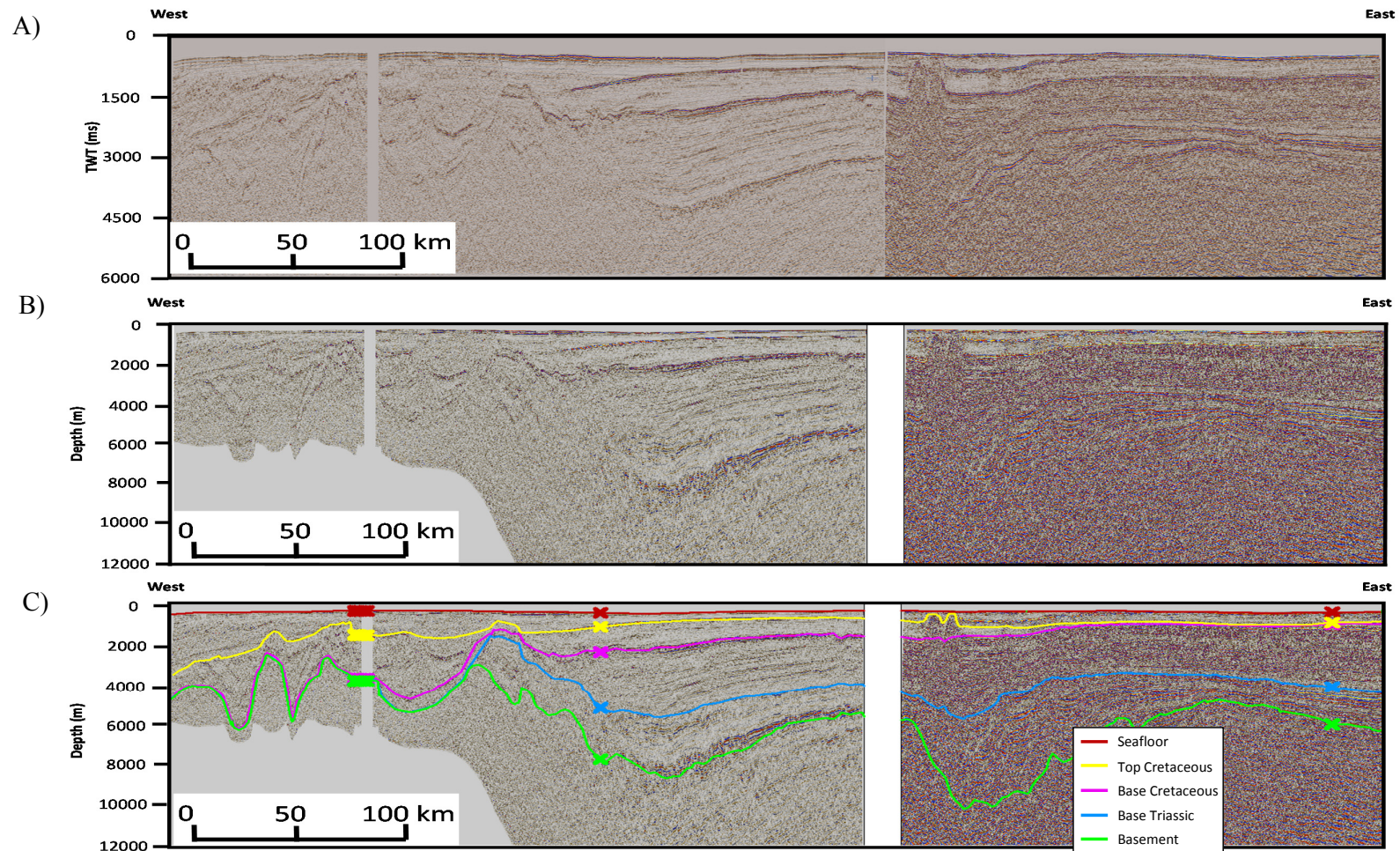


Figure 19: The east-west trending transect line, showing the seismic lines used in time (A), depth (B) and with interpretations (C). The vertical exaggeration is set to 12.5 for both figures.

4.3 Well Correlation

The Well correlation was carried out as a necessity due to the high uncertainty of the density and velocity picks throughout the Barents Sea. A spatial distribution of wells has been picked along the transect lines to best represent the horizontal and vertical variation of density and velocity's in the logs. Well tops provided from The Norwegian Petroleum Directorate (NPD) was used as input for the definition of sequences.

The wells picked seemed to have similar density and velocity trends in most wells, and due to the large time gap between sequences, the logs has to have a wide range of values, but generally a defined trend in each sequence. Figure 20 shows an example of a density log for well 7229/11-2, where the green line represent the general density trend in each sequence and the orange line represent the density values. Generally low densities and a low spread of the data characterized sequence four (~ 1800 to $\sim 2000\text{kg/m}^3$). Sequence 3 has a very distinct trend, with a high change in density with depth (~ 2200 to $\sim 2500\text{kg/m}^3$), sequence 2 has a low change in density with depth, but a high amount of variation in the data (~ 2500 to $\sim 2700\text{kg/m}^3$). Sequence 1 has two distinct density trends (~ 2500 to $\sim 2800\text{kg/m}^3$), indicating a sudden change in lithology from carbonates to shales as described in chapter 2. The large changes seen between the sequences represent erosional zones often also with lithological changes, while the rapid changes of densities as for example seen in sequence two represent change of lithological deposition (for example sand and shale intervals).

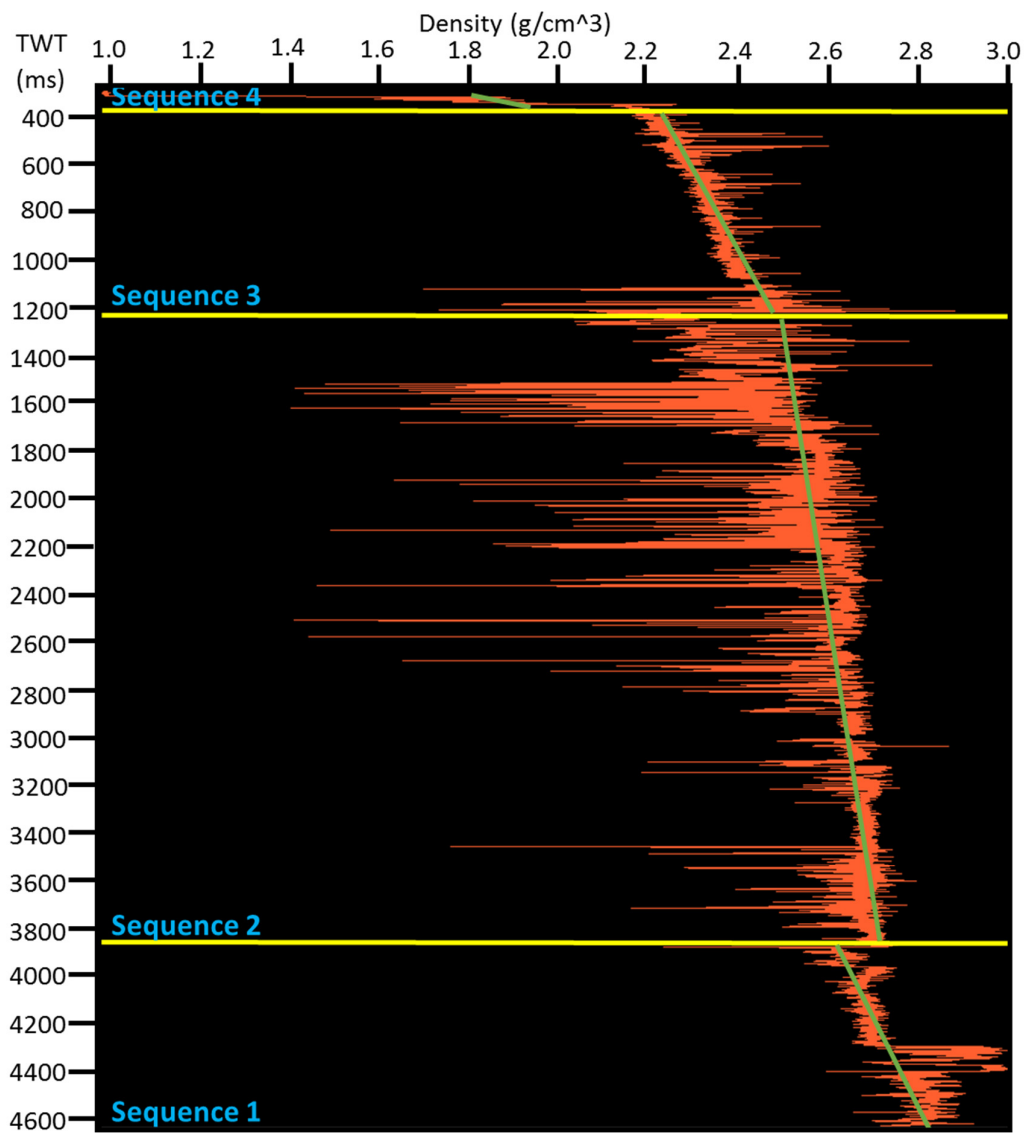


Figure 20: Well 7229/11-2, with density log in orange and general trend in green.

4.4 Data and uncertainty analysis

The three factors that were necessary to estimate for the flexural analysis was the length of sections, depth and densities of the four sequences. The length of the section is based on maps and therefore has a very low uncertainty, while the depth of the sequences and the densities are calculated based on well analysis.

From the well log analysis, the graphs in figure 22 and 23 were created to represent how the values vary with depth. The uncertainty are represented with bars, showing the largest percentage uncertainty for the four different sequences. These values are presented in figure 21 and represent how much the sequences vary both in a vertical and horizontal direction within the depths of where these deposits are located in the wells. This means that sequence 3 is varying with approximately seven percentages in density from the given trend lines, while sequence 4 is more stable and does not vary a lot from the trend line.

The spread of data is represented by the standard deviation (Ostanin et al., 2012) in figure 21, calculated by the simple formula;

$$SD = \sqrt{\frac{1}{N} * \sum_{i=1}^N (xi - \mu)^2} \quad \text{Equation 4}$$

Where N is the amount of data, xi the individual points and μ is the average of the points. For both the percentage error and the standard deviation (SD), show a general increase of uncertainty with depth. The exception is sequence 3, which as previously mentioned changes a lot vertically and horizontally throughout the Barents Sea.

Sequence	Density % error	SD	Sequence	Velocity % error	SD
4	4,5	0,059279	4	1,2	242,1859
3	7	0,140287	3	2,6	405,0026
2	4	0,060828	2	2,6	375,3588
1	2,1	0,088972	1	3,1	514,4199

Figure 21: Percentage error and standard deviation for the density (g/cm^3) and velocity (m/s) analysis, based on the well analysis.

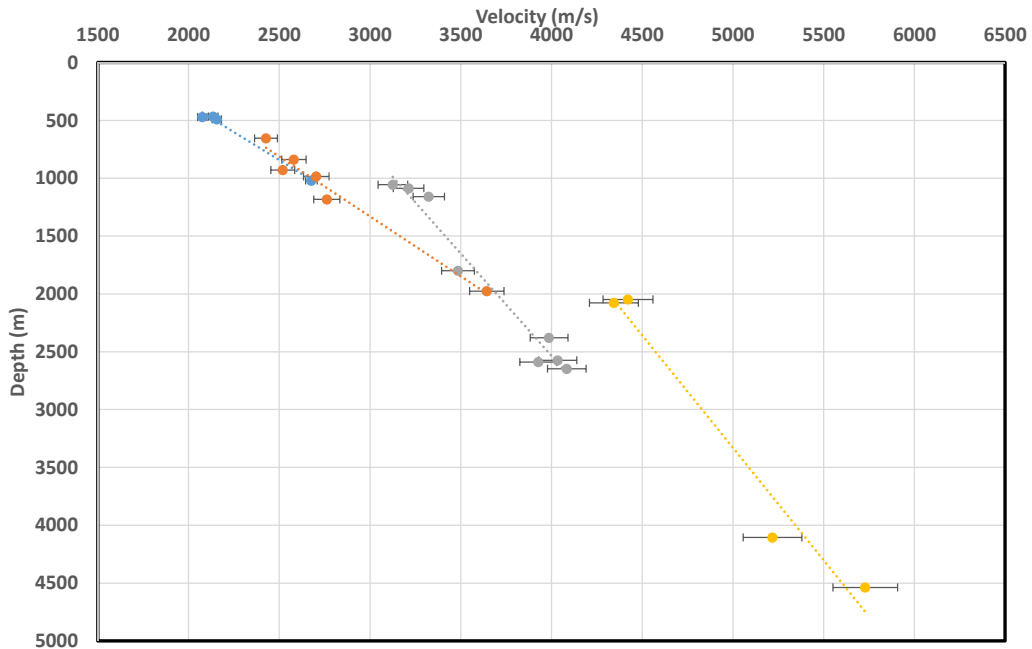


Figure 22: Velocities acquired from well logs. Trend lines showing how the velocity changes with depth and bars indicating the percentage error of the velocities.

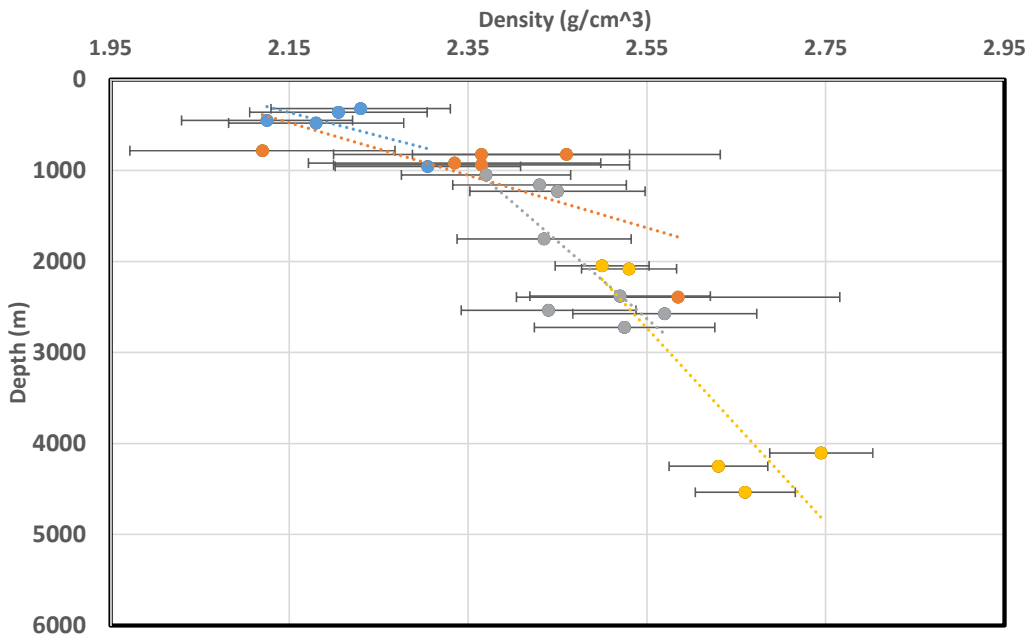


Figure 23: Densities acquired from well logs. Trend lines showing how the density changes with depth and bars indicating the percentage error of the density.

4.5 Decompaction and 2D Restoration

In order to restore the sequences, a decompaction and a restoration process was applied to the horizons. For both these operations, the program Move, from Midland Valley was used. The decompaction is mainly affected by the lithology, which includes parameters about the density, depth coefficient, and initial porosity. In order to get a reasonable estimate of these values, a stratigraphic chart including the rock properties was transferred into the database in Move and used as input for the decompaction process. The values in this model are based on the values from the density and velocity analysis described in chapter 4.4.

The decompaction process is based on an equation from Sclater and Christie (1980): $f = f_0 * (e^{-cy})$, where f is the present day porosity, f_0 the porosity at the surface, c porosity-depth coefficient and y the depth in meters. This formula assumes a decrease of porosity with depth (compaction). This means that a decrease of depth (to present day) will decompact the sequences applied in this model and thicken the sequences.

The decompaction result is based on the lithological databased created (figure 24). A shaley interval like sequence 3 and 4 is therefore more affected than the sand intervals in sequence 2. Figure 25 illustrates the three sequences (Sequence 1, 2, and 3) before (25A) and after (25B) decompaction, where the thickening of each sequence is related to depth and thickness. The top sequence 4 in red is removed in the decompacted part, since this layer already is located at the present day.

1: Rock Type	2: Rock Group	3: Background_colour	4: pattern	5: Sandstone(%)	6: Shale(%)	7: Limestone(%)	8: Porosity	9: DepthCoefficient	10: Compaction Curve	11: v0	12: k	13: Vshale	14: Grain Size	15: Density	16: Young Modulus	17: Poisson Ratio
Sandstone	Sand	Yellow	Diagonal lines	100.0000	0.0000	0.0000	0.4900	0.27	Default	3500	0.50	0.0000	0.0375	2650	15000.0	0.2550
Shale	Shale	Brown	Horizontal lines	0.0000	100.0000	0.0000	0.6300	0.51	Default	2500	0.50	1.0000	0.0047	2720	32500.0	0.3000
Limestone	Limestone	Blue	Vertical lines	0.0000	0.0000	100.0000	0.4100	0.40	Default	2600	0.50	0.0000	0.0005	2710	45000.0	0.2150
Unit				%	%	%		km ⁻²		m/s	Hz		cm	kg/m ³	MPa	
1	Cenozoic	Shale	Black						Default					2700		
2	Cretaceous	Shale	Black						Default					2700		
3	Jurassic-Triassic	Sand	Black						Default					2670		
4	Permian-Devonian	Limestone	Black						Default					2710		

Figure 24: The lithological properties used for the decompaction. Unit 1, 2, 3 and 4 was used for sequence 4, 3, 2 and 1 respectively. Generally the default values seen at the top was applied, but the grain density (labeled 15: density) was calculated based on the amount of shale and sand for sequence 2,3 and 4, while sequence 1 used the standard limestone value.

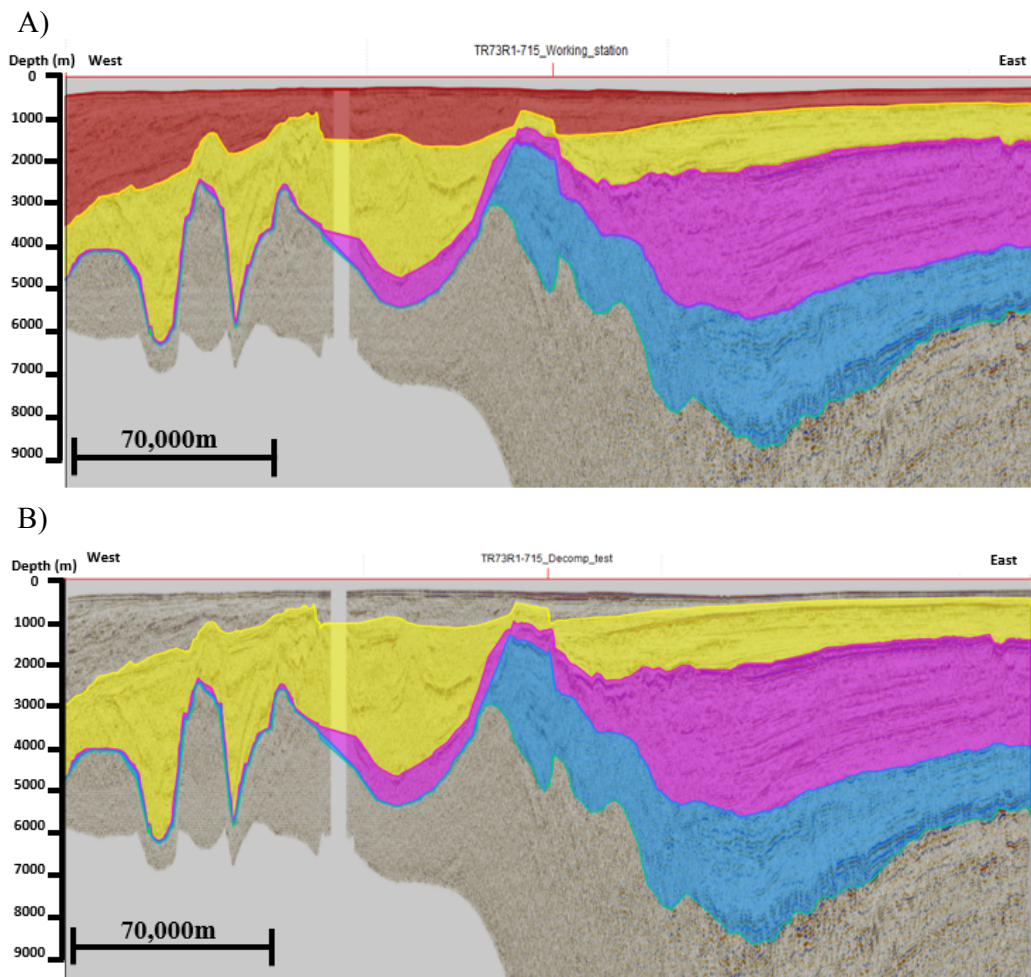


Figure 25: (A) Before decompaction and (B) after decompaction. The sequences in figure B thickened due to the decompaction process and were used as an input for the restoration part. The vertical exaggeration is 15 times in both figures.

After the decompaction, the three sequences below datum were restored to top Cretaceous, base Cretaceous and base Triassic with a 2D restoration module in Move. A flexural slip method as seen in figure 26 was used for the unfolding. This method assumes parallel layering and needs a pin as seen in figure 26B to indicate the direction of unfolding. This results in a section as seen in figure 26C.

As a comparison, the simple shear method unfolds the layers like unfolding a deck of cards in the vertical direction, while the flexural slip method unfolds the beds like in a deck of cards being unfolded in the horizontal direction. The advantages of the flexural slip method in comparison to other methods like simple shear, is that this method maintains the line length of the horizon in the direction of the pin (usually 90°). It also maintains the thickness of the decompacted beds and other horizons will also be maintained underneath the template horizon. Figure 27 illustrates the difference in a simple shear restoration and a flexural slip restoration. This clearly indicates that the horizons are stretched out in the flexural slip method whereas the simple shear method uses vertical vectors to recreate the original line length.

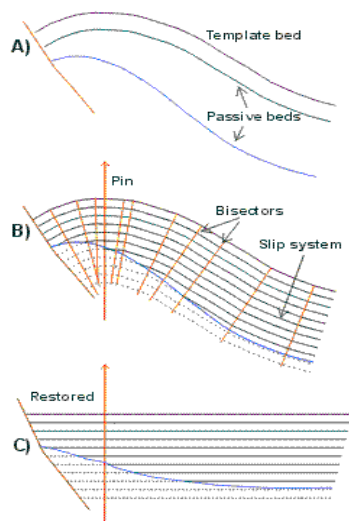


Figure 26: Flexural Slip unfolding principle. A shows the input beds and fault, B shows how the program uses bisectors and a given direction (pin) to restore the transects into C.

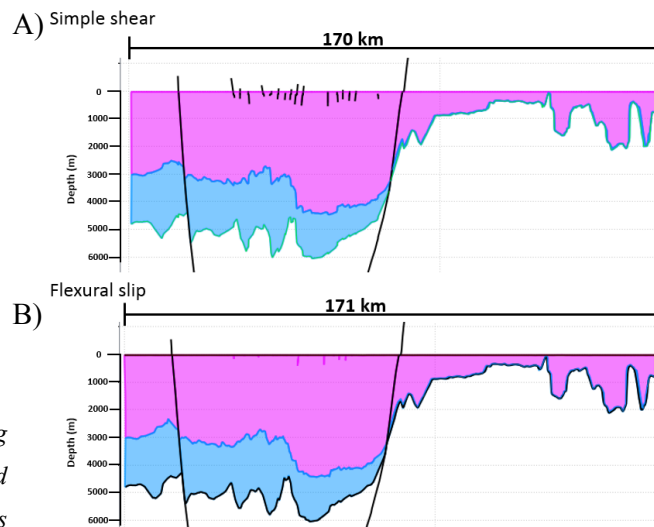


Figure 27: Simple shear (A) versus flexural shear (B) for a seismic line crossing the Hammerfest Basin.

4.6 Erosional and Flexural Modelling

The final step before creating the flexural models was to add the minimum and maximum erosion to each transect and sequence. The erosion rates were based on seismic analysis and previous work describing the amount of erosion (Nyland et al., 1992; Riis and Fjeldskaar, 1992; Gustavsen et al., 1996; Torsvik and Buitter, 2007; Worsley, 2008; Nazarova, 2009; Hassan, 2012), which can be found in Appendix A. Here the different amounts of erosion are listed by sequences and structures in the Barents Sea. Figure 23 shows how the thickest and thinnest continuous sequences were extrapolated and contribute to the maximum and minimum erosion in this area.

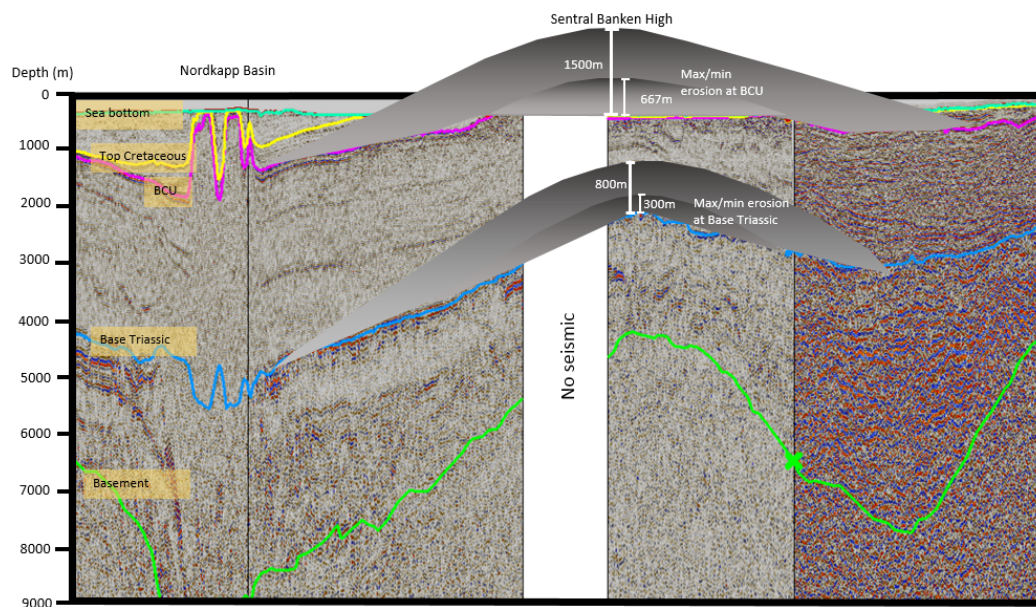


Figure 28: Example showing the amount of minimum and maximum erosion that was calculated in Sentral Banken High for sequence two and three.

To convert the three different decompacted and restored transect lines, each of the sequences for each seismic line was converted to Excel (from Microsoft) for the calculation of densities and thicknesses. Each sequence was then separately imported to calculate the average density of the total thickness and then put together with the other seismic lines covering the same sequence (see appendix B for example of calculations in excel). Since some of these seismic lines were a few kilometers separated from the others, an average density and thickness was added with the correct length between them.

The minimum and maximum erosion was then added separately to each sequence on each transect line as an input for the flexural model. The density was then calculated based on the thickness and depth of each sequence and exported to a program called Flex2D (Nestor Cardozo), which calculated the flexural effect for each of the transect inputs. The flexural modelling tool uses the 2D flexural calculation described in chapter 3 (equation 3.2). For the calculations some standard parameters for the Poisson modulus equal to 0.25 GPa, Young modulus equal to 70 000 GPa, density of the mantle equal to 3300 kg/m³ and an interval of 5 km for computing the flexural response are used.

When creating the flexural model, the elastic thickness was set as both variable elastic thickness (between 10-50km) and to a constant elastic thickness of 30 kilometers to compare the effects. The variable elastic thickness was created based on the assumption that the brittle southwestern parts had a lower elastic thickness in the faulted regions, whereas the more stable and flexural parts had a higher elastic thickness (see figure 29). Figure 29 only represent the variable elastic thickness applied for sequence 2. The other sequences have similar variable elastic thicknesses

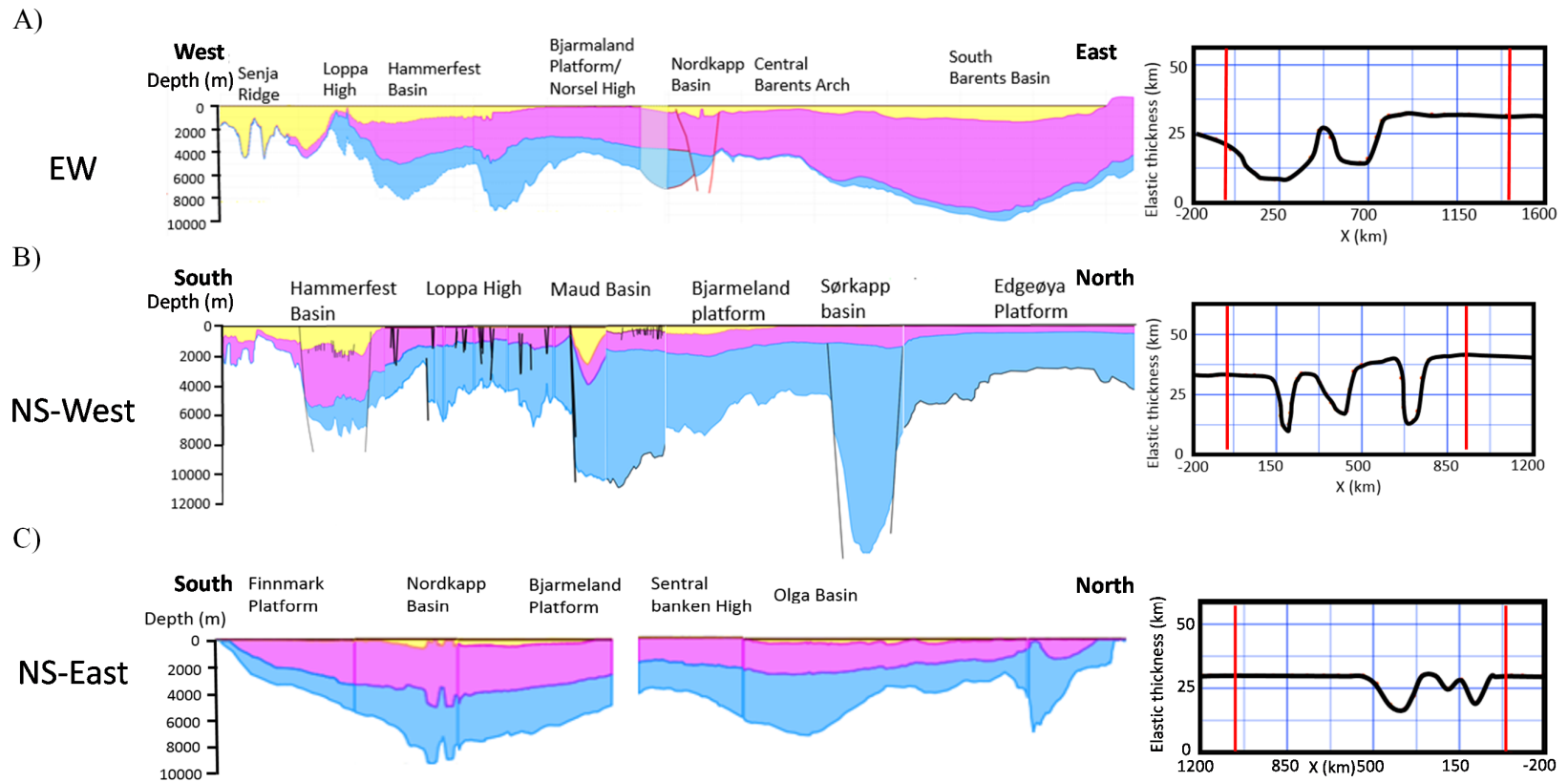


Figure 29: Example of the three transect lines (here restored at top cretaceous). To the right, between the red lines, are the same transects showing the variation in elastic thickness throughout the transect lines. The transect lines shown are (A) the east-west trending, (B) the western north-south trending and (C) the eastern north-south trending transects.

5. OBSERVATION AND RESULTS

5.1 Horizon characteristics

The interpretation made for the flexural models, were based on the seismic lines represented in figure (32, 33 and 34). These interpretations of the different sequences are based on major changes in depositional systems and/or erosional events, which relates to strong seismic reflections. To complete the east-west going transect line, the seismic line from Henriksen et. al. (2011) in figure 32 was interpreted. The observations seen in these transect lines are described in this chapter based on the deposition of the four different sequences and covers a total length of ~2400km.

The deposition of the first sequence is related to the sedimentation of Novaya Zemlya, created during the Caledonian orogeny. The large amount of sediments filled the large eastern basins creating subsidence, while the Nordkapp Basin and Hammerfest Basin started to form structurally by faulting in fractures created during the Caledonian orogeny. It was mainly the eastern basins that started forming, while the northern and western parts had a low amount of deposits. Some smaller basins like the Sørkapp Basin in the north had large amount of Triassic deposits, due to rifting events Devonian, mid-Carboniferous.

The western basins really started to form in Sequence 2, like the Hammerfest and Nordkapp Basins, both structurally and by sandy alluvial deposits all the way from the eastern basins to the Tromsø basin in the west. It was mainly the areas close to Novaya Zemlya that had these deposits, but extended all the way north and to the Tromsø Basin in the west.

Sequence 3 had mainly shaley deposits, with some sand deposits in between. This sequence is related to uplift and major erosion of Cretaceous to Jurassic deposits. The rifting events that previously had a northeast direction, change to a north trending

direction, away from the Nordkapp and Hammerfest Basin towards the west of Svalbard, creating basins further west than previously. The sediment supply from Novaya Zemlya was reduced and due to the erosional events, there are mainly deposits in the west and in the deeper basins north and east. The high arctic large igneous province in the north created major uplifts in the northern parts, which led to erosion of the entire sequence in the platform and high areas in the northern parts. Loppa High, the Bjarmeland Platform, Edgøya Platform, Sørkappe Basin, Kong Karl Platform and the Sentralbanken High is some of the areas that has the entire sequence 3 eroded.

Sequence 4 from top Cretaceous to Quaternary were related to the opening of the Norwegian-Greenland Sea and therefore has the largest accumulation of shaley sediments in the western basins, but still with some sediments in the Nordkapp and eastern basins. Erosional events due the glacial events have removed large amounts of sediments from this sequence.

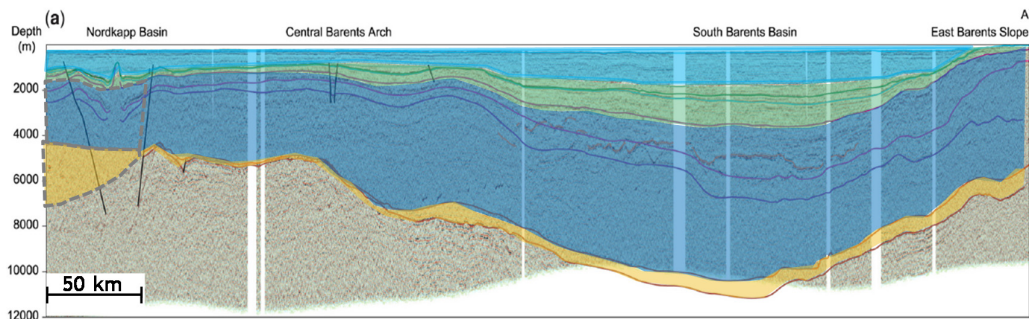


Figure 30: The four different sequences defined at the Russian part of the Barents Sea. Orange=sequence 1, dark blue= sequence 2, green= sequence3, light blue=sequence 4 (Modified from Henriksen et al., (2011)).

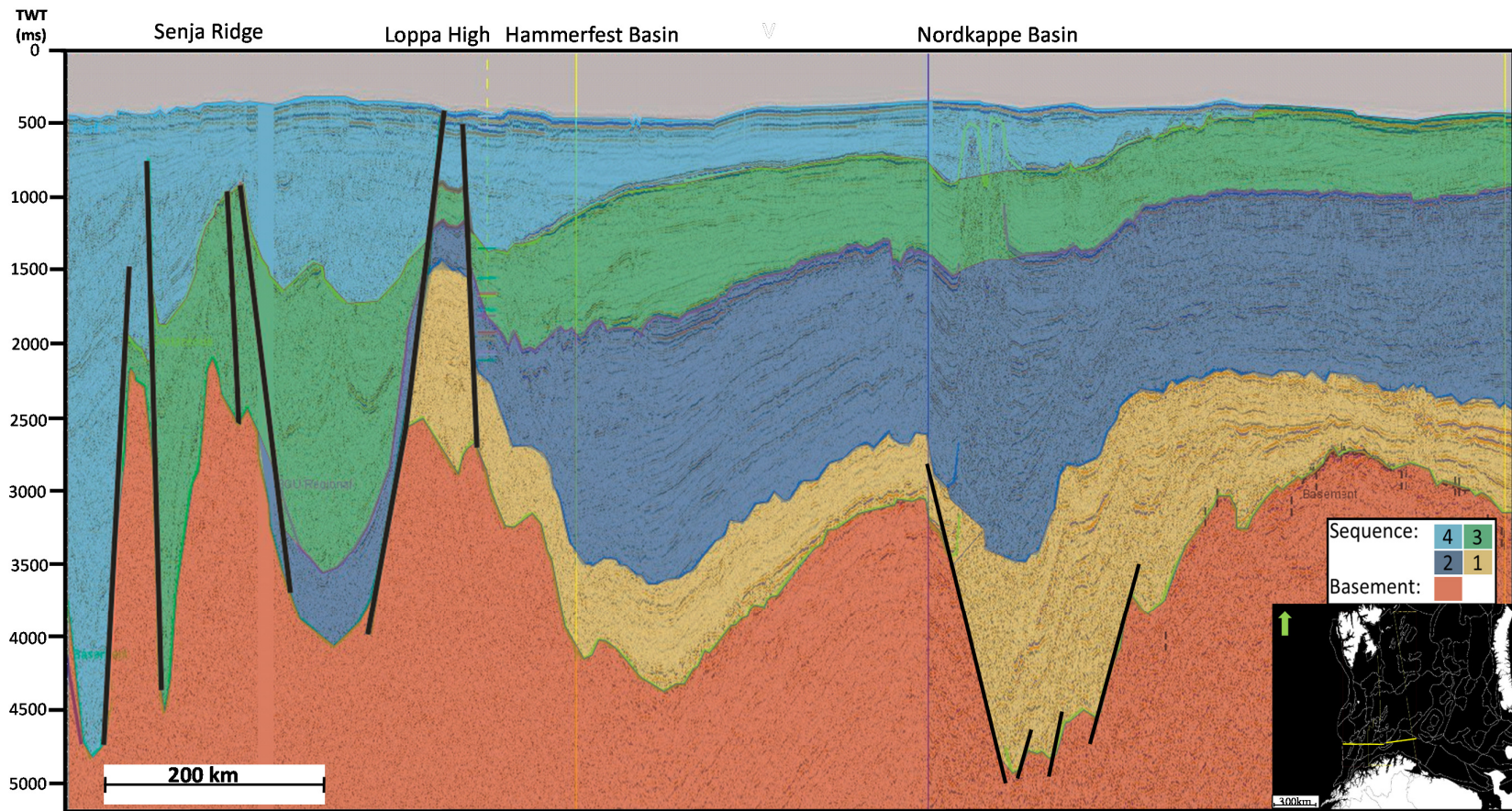


Figure 31: East-West transect line, illustrating the distribution of the different sequences. Red=Basement, orange=sequence 1, dark blue=sequence 2, green= sequence3, light blue=sequence 4.

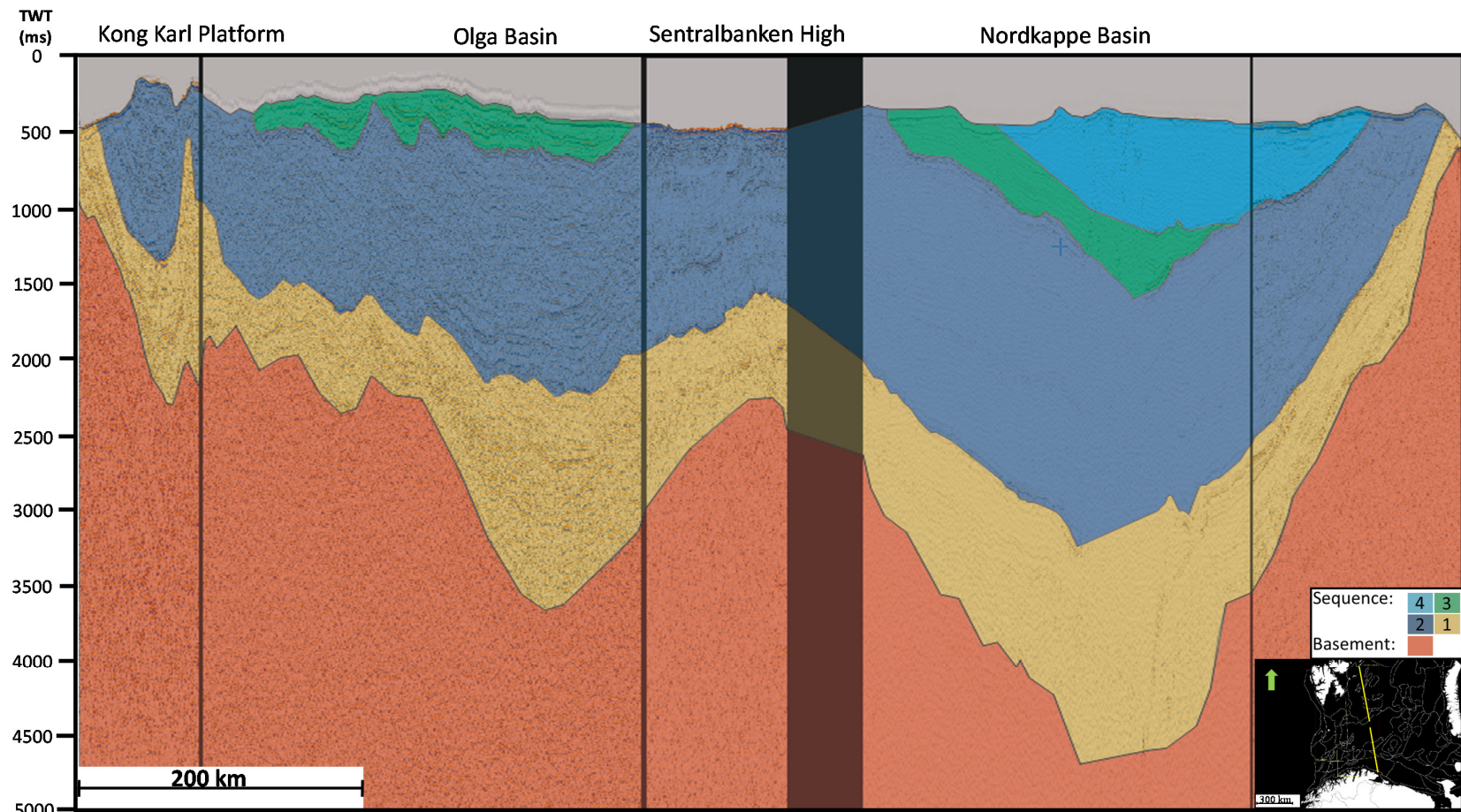


Figure 32: Eastern north-south transect line, illustrating the distribution of the different sequences. Red=Basement, orange=sequence 1, dark blue= sequence 2, green= sequence3, light blue=sequence 4.

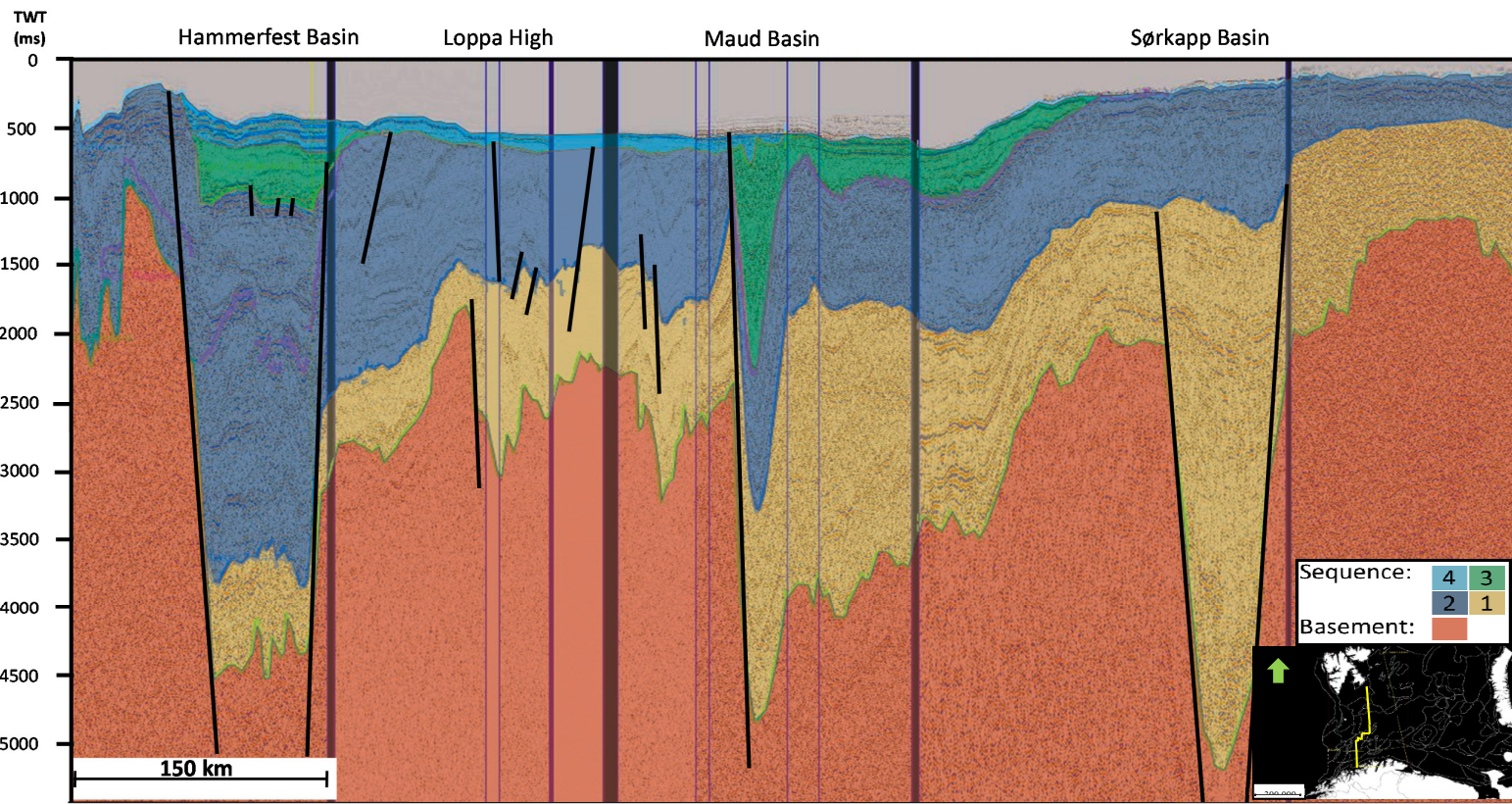


Figure 33: Western north-south Transect line, illustrating the distribution of the different sequences. Red=Basement, orange=sequence 1, dark blue=sequence 2, green= sequence3, light blue=sequence 4.

5.2 Flexural behavior

The next sections (figure 35-43) will describe the flexural effect of loads due to the sedimentary loads, and how the elastic thickness, erosion and tectonic loads have affected the structural geometry. There are nine figures of each of the restored sections, for the different transects. These figures are divided into six parts (from top left in the figures); (A) the minimum and maximum erosion applied into the model, (B) the restored section, (C) a combination of the three flexural models created from this transect in regards to the topography and the three last ones (D, E and F) are separate flexural models of the maximum, minimum and variable elastic thickness. For the maximum and minimum erosional models, an elastic thickness of 30 kilometers was used as a reference to the “best fit” variable elastic thickness, which is shown in the bottom left of the combined flexural models. The red lines in the variable elastic indicates were the restored transect line starts and ends.

Sequence1

Short description of the sequence

Sequence 1 was related to a carbonate platform in the entire Barents Sea. A tectonic event in the Devonian time resulted in north-west trending highs in the eastern Barents Sea, while in the western Barents Sea, the crustal movement created rift basins close to the Barents shelf edge close to the fractured zones in the west (see figure 4). The fault zones from this time was bounded by older fractures that formed during the Caledonian Orogeny.

Restored sections

The restored sections (figure 35, 36 and 37) from this sequence shows that in the northern parts had created a large basin in form of the Sørkapp Basin, with a large amount of sediments accumulated in the basin. Calculated results shows a minimum of 10% extension in the Sørkapp Basin related to these events. Additional extension before this sequence and subsidence due to the sedimentary loads seen in figure 36 are factors that is essential for constructing the geometry seen

in this basin. The basins and highs seen in the southwestern Barents Sea today was not developed at this time. The amount of sediments is decreasing towards the eastern Barents Sea, which had a low amount of carbonate build-ups, while the western parts created a thicker carbonate platform area from the Nordkapp Basin to Loppa High.

Flexural behavior

The flexural response shows that sedimentary loads are not sufficient to reproduce the topography found in the Barents Sea at this sequence. For the eastern north-south trending transects (figure 35) the Sedimentary loads creates deflections in the undeveloped Nordkapp and Olga Basin and a low deflection in the north.

The same trends can be seen in the western north-south trending transect (figure 36), where there is a deflection in the Maud Basin and a large deflection north in the Sørkapp Basin. The Hammerfest Basin, Tromsø Basin and Loppa High have no deflections created in this sequence seen from this transect.

From the east-west trending transect in figure 37, it is possible to see a different deflection in the Hammerfest Basin, than in the western north-south trending transect. Both the Hammerfest Basin and the Nordkapp Basin have a large sedimentary deflection, but with some missing loads underneath as seen in green circles on figure 37. The eastern Barents Sea has a much lower sedimentary deflection and the tectonic deflections missing are low and local as seen in the green circle (figure 37).

Interpretation

As seen from the missing deflections underneath the sedimentary flexural response, there is a generally low amount of missing loads in the southwest and east, and local and large deflections missing in the northern basins. Previous work believes that these northern tectonic events are related to far-field stress related to the Uralide indentation (Anell et al., 2013). The platforms in the northern area (seen in red circles and the green circles shown in figure 35 and 36) indicates a significantly lower tectonic activity than in the basins. This sequence had a low amount of erosion and a generally higher tectonic deflection in the east-west direction, as seen in figure 36 and 37.

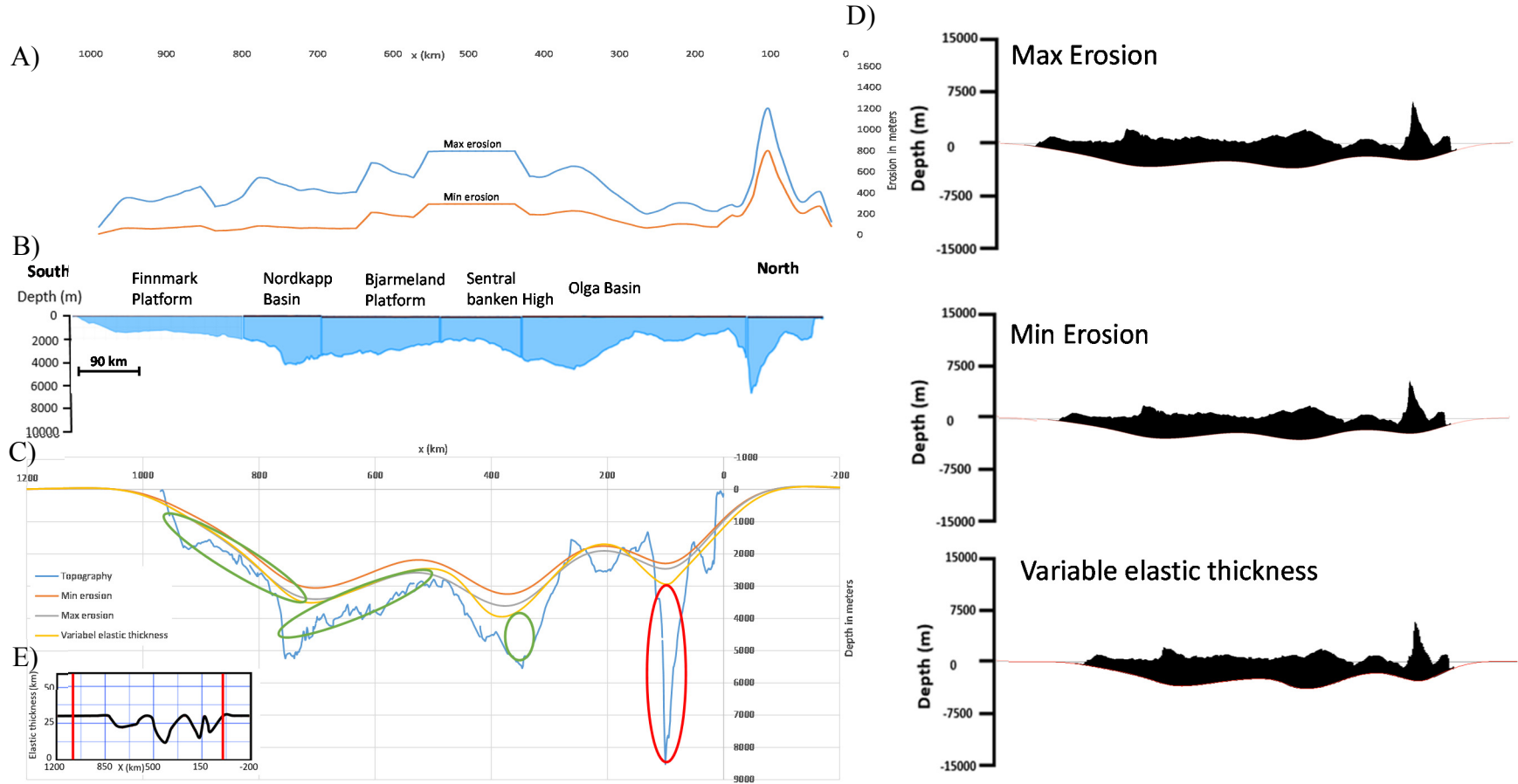


Figure 34: A section restored to base Triassic of the eastern of the north-south trending transect (B). The deflection due to sedimentary loads are shown to the right (D) with different amounts of erosion applied. Generally an elastic thickness of 30km is used, but the variable elastic thickness model uses the elastic thickness shown at the bottom left (E). These flexural models are combined in the bottom left figure (C) to describe the effect of the sedimentary loads. The difference could be due to either some of the input parameters (e.g. density, erosion etc.) or tectonic loads in the nearby area creating tectonic deflections. High tectonic deflection missing is indicated with a red circle and green indicates low. Figure A show the maximum and minimum erosion applied in the flexural models.

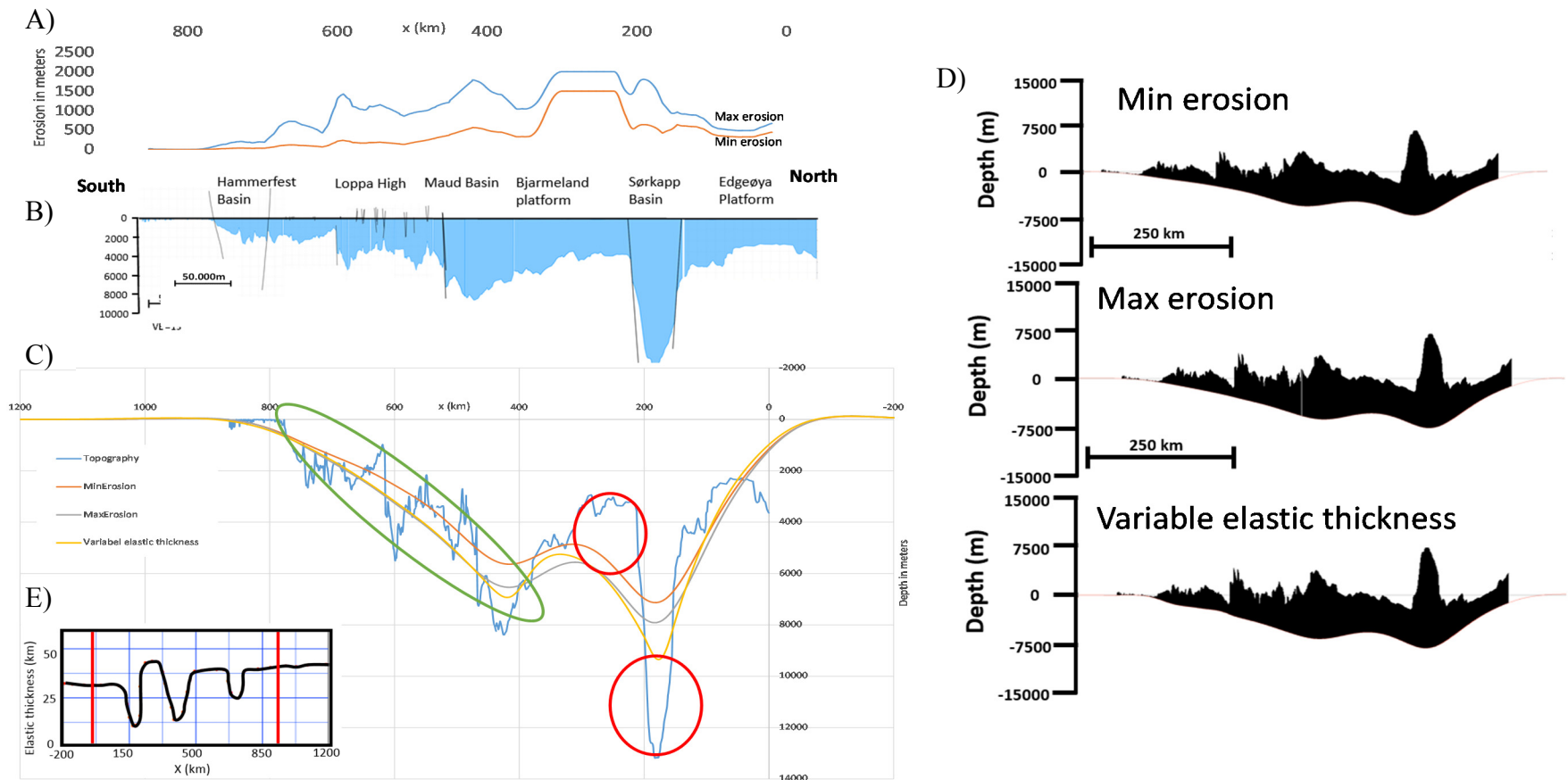


Figure 35: A section restored to base Triassic of the western of the north-south trending transect (B). The deflection due to sedimentary loads are shown to the right (D) with different amounts of erosion applied. Generally an elastic thickness of 30km is used, but the variable elastic thickness model uses the elastic thickness shown at the bottom left (E). These flexural models are combined in the bottom left figure (C) to describe the effect of the sedimentary loads. The difference could be due to either some of the input parameters (e.g. density, erosion etc.) or tectonic loads in the nearby area creating tectonic deflections. High tectonic deflection missing is indicated with a red circle and green indicates low. Figure A show the maximum and minimum erosion applied in the flexural models.

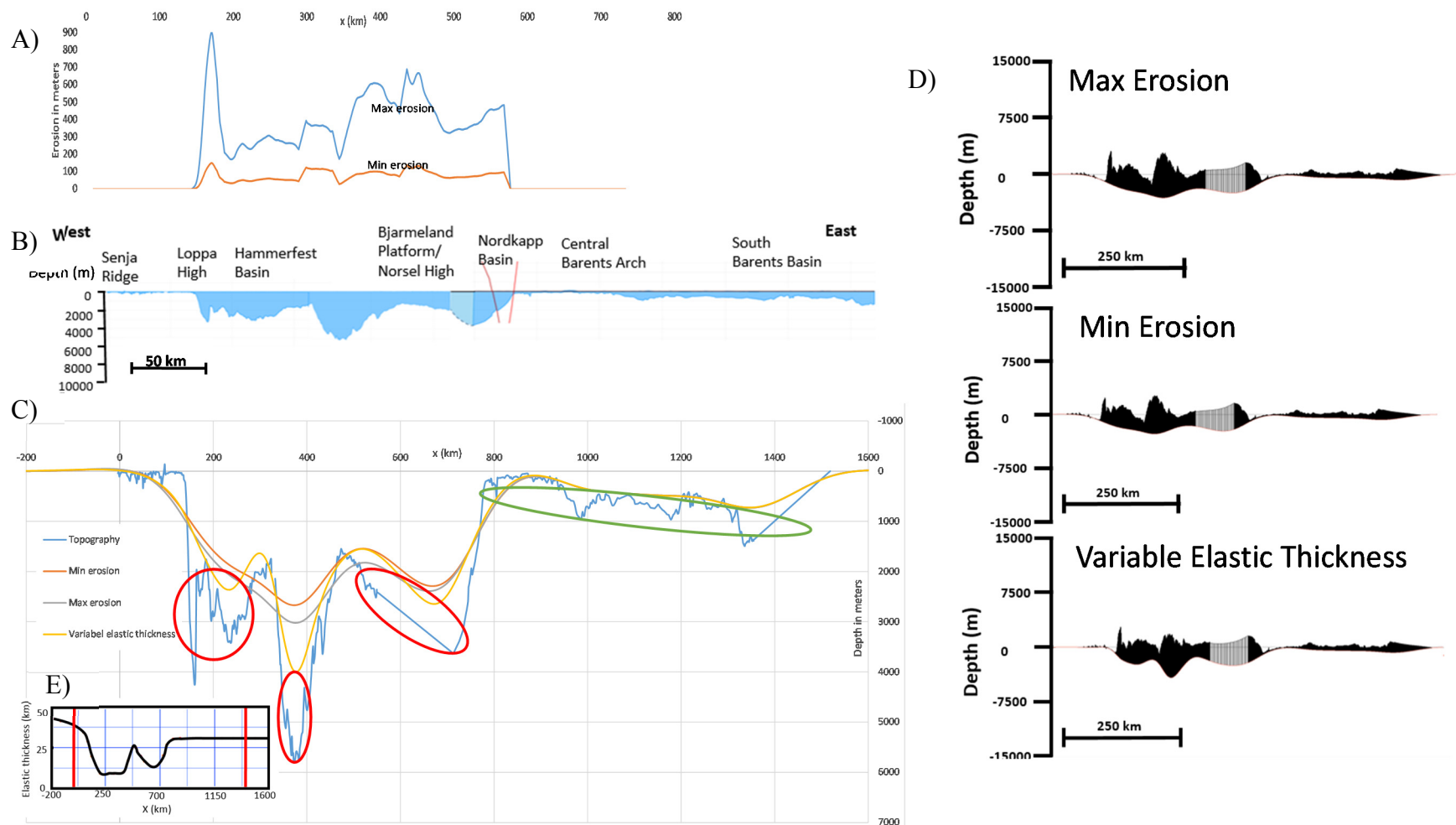


Figure 36: A section restored to base Triassic of the east-west trending transect (B). The deflection due to sedimentary loads are shown to the right (D) with different amounts of erosion applied. Generally an elastic thickness of 30km is used, but the variable elastic thickness model uses the elastic thickness shown at the bottom left (E). These flexural models are combined in the bottom left figure (C) to describe the effect of the sedimentary loads. The difference could be due to either some of the input parameters (e.g. density, erosion etc.) or tectonic loads in the nearby area creating tectonic deflections. High tectonic deflection missing is indicated with a red circle and green indicates low. Figure A show the maximum and minimum erosion applied in the flexural models.

Sequence 2

Short description of Sequence

Alternating sand and shale deposits characterize sequence 2. The sequence was mainly a stable platform, but the latest stages had an increase of tectonism in the west. Novaya Zemlya was an active source of sediment supply throughout this sequence.

Restored sections

The restored sequences seen in figure 38, 39 and 40 shows a high amount of sediments from the South Barents Basin in the east to the Loppa High in the west. Further north there is a decrease of sediments. Structurally it is possible to see that the Nordkapp and Hammerfest Basin really started to form in the west and the Southern Barents Basin seemingly subsiding due to the high amount of sediments accumulated here.

Flexural behavior

In the southwestern Barents Sea, the sedimentary deflections are increasing from sequence 1 due to the sedimentary infill, while the tectonic deflections are low, as seen by the green circles in figure 38, 39 and 40.

The eastern north-south trending transect (figure 38) shows a continuous low difference between the flexural response due to the sediments and the topography in the Nordkapp Basin. Similar features can be seen in the Olga Basin, which has the same magnitude as sequence 1, indicating that these deflections were created in the first sequence. Similarly, the northern parts have the same deflections as the previous sequence, indicating a low amount of tectonic activity.

From the western north-south trending transect (figure 39), it is possible to see similar features in Loppa High as seen in the Nordkapp Basin, where there is a generally low difference between the topography and the sedimentary load profile. Further north in the Sørkapp Basin, there are found approximately the same amount of tectonic deflection missing from the topography, similarly to the eastern transect line.

From the east west trending transect (figure 40), there is an increased deflection missing in the Bjarmeland Platform next to the Nordkapp Basin, which has a decrease of tectonic deflections.

Similarly, the Hammerfest Basin has a decrease of tectonic deflections missing. The eastern parts has approximately the same amount of tectonic deflections missing indicated by the long green circles in figure 40.

Interpretation

Generally, the Eastern Barents Sea has close to no tectonic activity in the flexural model of sequence 2, while the southwestern parts has a small increase of tectonic deflection. In contrast to sequence 1, this sequence does not seem to have any increase of tectonic deflections in the northern structures.

Summary

Figure 38, 39 and 40 shows a high amount of erosion and a low increase of tectonic loads throughout the Barents Sea. The few main tectonic features can be seen in the southwestern Barents Sea, while the northern and eastern Barents Sea are tectonically not active.

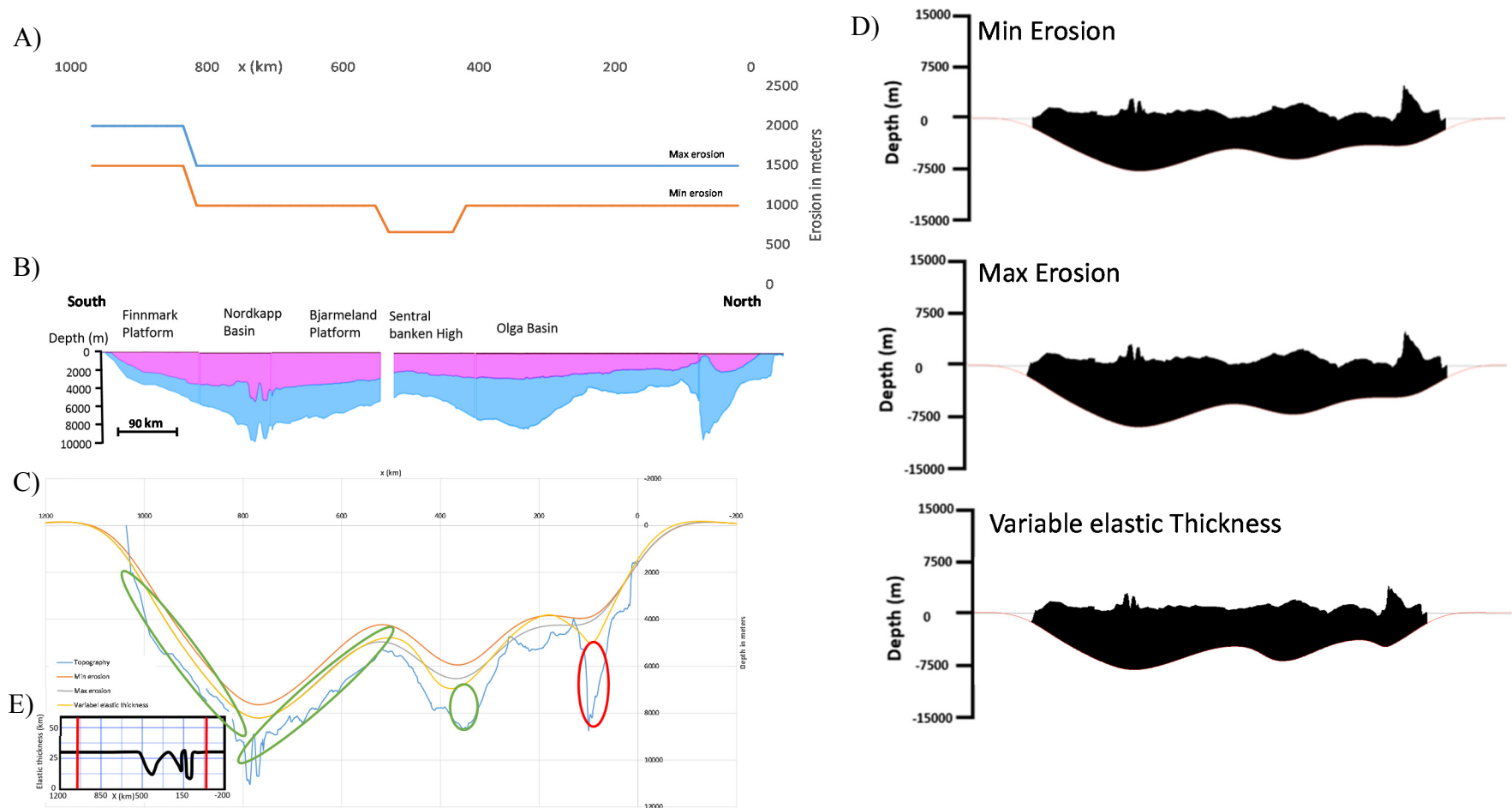


Figure 37: A section restored to base Cretaceous of the eastern of the north-south trending transect (B). The deflection due to sedimentary loads are shown to the right (D) with different amounts of erosion applied. Generally an elastic thickness of 30km is used, but the variable elastic thickness model uses the elastic thickness shown at the bottom left (E). These flexural models are combined in the bottom left figure (C) to describe the effect of the sedimentary loads. The difference could be due to either some of the input parameters (e.g. density, erosion etc.) or tectonic loads in the nearby area creating tectonic deflections. High tectonic deflection missing is indicated with a red circle and green indicates low. Figure A show the maximum and minimum erosion applied in the flexural models.

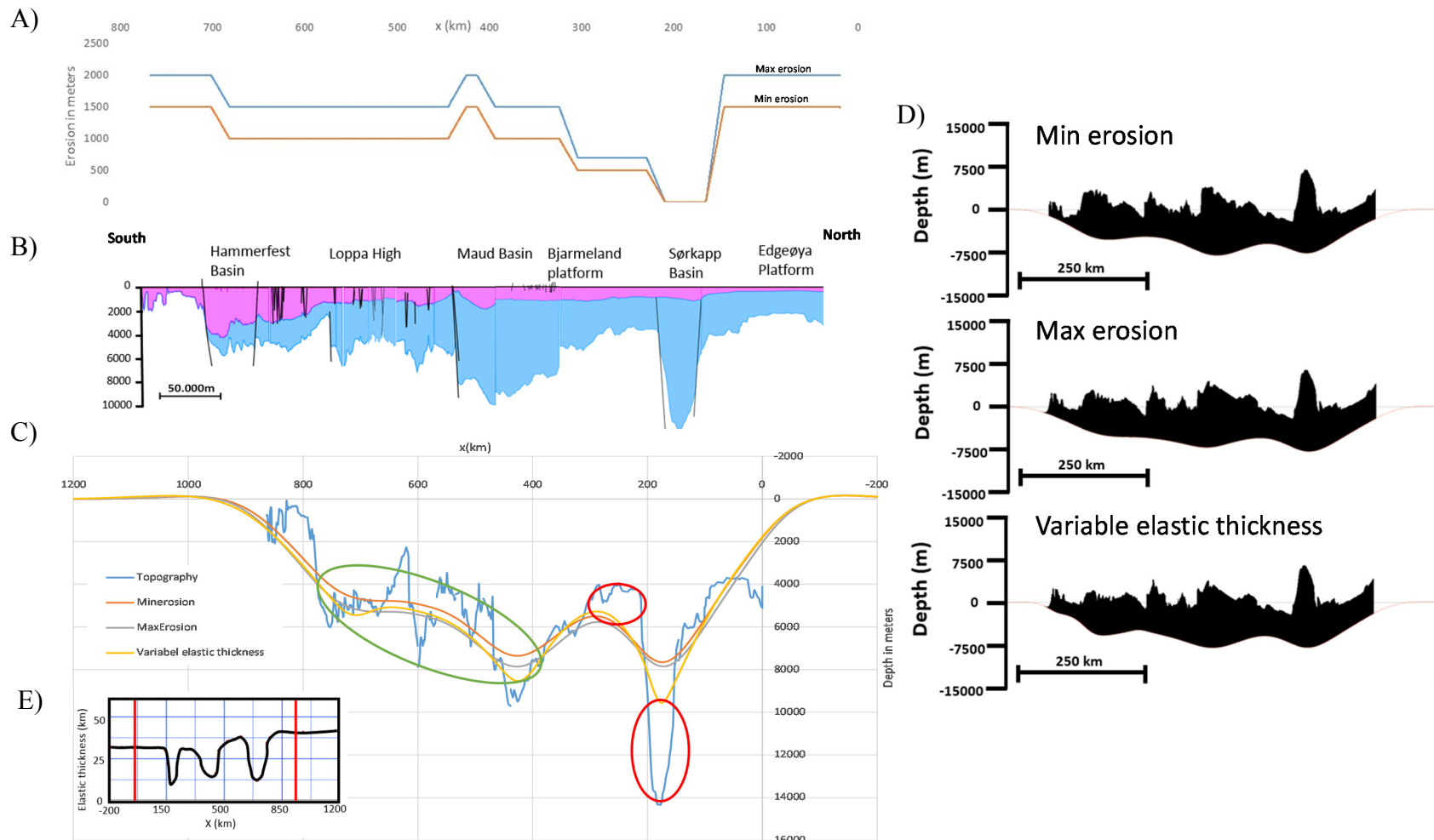


Figure 38: A section restored to base Cretaceous of the western of the north-south trending transect (B). The deflection due to sedimentary loads are shown to the right (D) with different amounts of erosion applied. Generally an elastic thickness of 30km is used, but the variable elastic thickness model uses the elastic thickness shown at the bottom left (E). These flexural models are combined in the bottom left figure (C) to describe the effect of the sedimentary loads. The difference could be due to either some of the input parameters (e.g. density, erosion etc.) or tectonic loads in the nearby area creating tectonic deflections. High tectonic deflection missing is indicated with a red circle and green indicates low. Figure A show the maximum and minimum erosion applied in the flexural models.

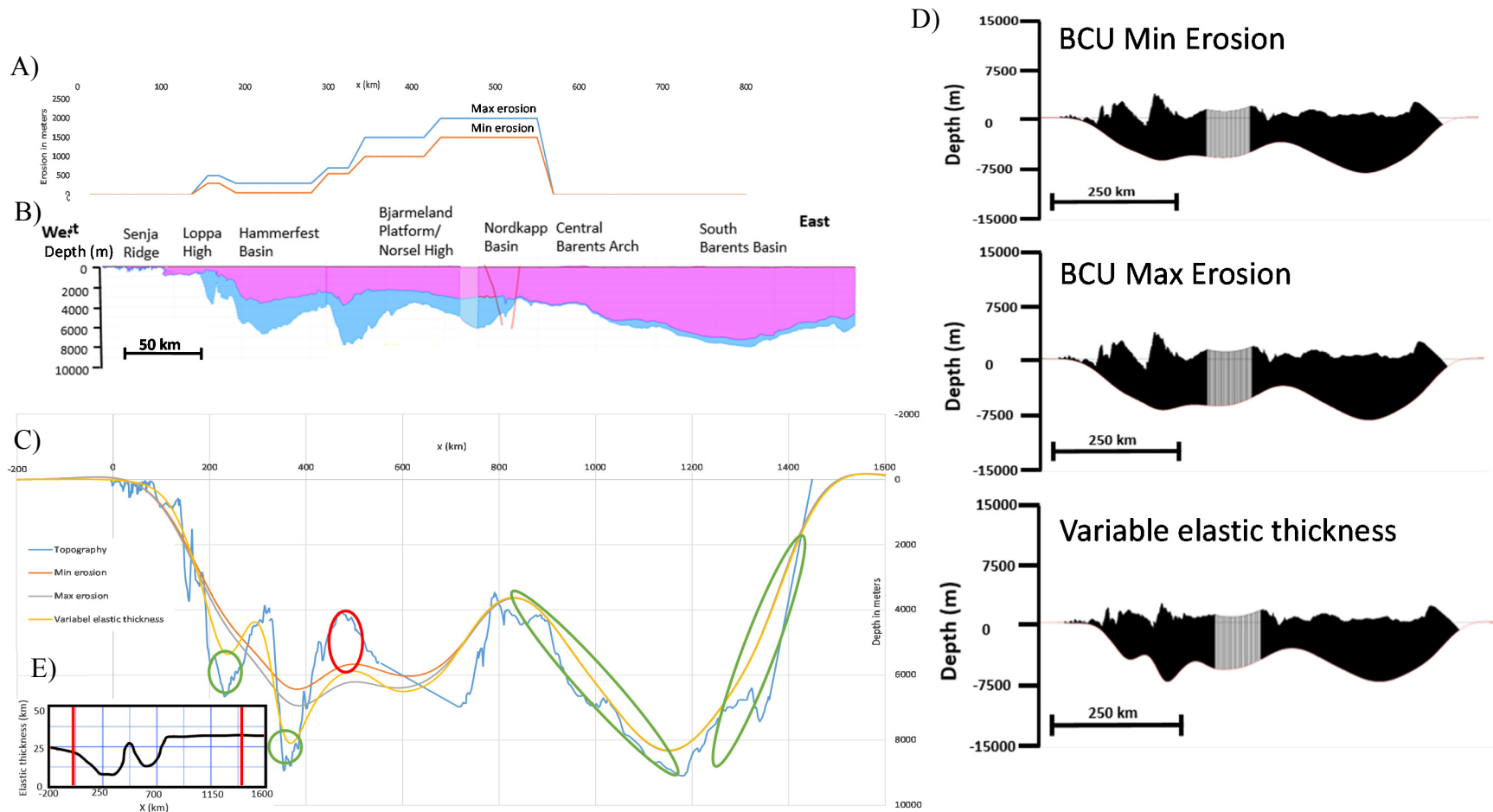


Figure 39: A section restored to base Cretaceous of the east-west trending transect (B). The deflection due to sedimentary loads are shown to the right (D) with different amounts of erosion applied. Generally an elastic thickness of 30km is used, but the variable elastic thickness model uses the elastic thickness shown at the bottom left (E). These flexural models are combined in the bottom left figure (C) to describe the effect of the sedimentary loads. The difference could be due to either some of the input parameters (e.g. density, erosion etc.) or tectonic loads in the nearby area creating tectonic deflections. High tectonic deflection missing is indicated with a red circle and green indicates low. Figure A show the maximum and minimum erosion applied in the flexural models.

Sequence 3

Short description of the sequence

This sequence is mainly affected by the change of a northeast trending rifting to a north trending rifting, which means that the rifting changed from the Nordkapp and Hammerfest Basin towards the west of Svalbard (Tromsø Basin, Sørvestsnaget Basin etc.). Uplift due to the high arctic large ingenious province (HALIP) caused erosion in certain areas. The remanence of this sequence is mainly shales deposited in the south west due to the rifting event related to the opening of the Greenland – Norwegian Sea.

Restored sections

Restored sections from this sequence (figure 41, 42 and 43) shows a high accumulation towards the south-west in the large basins, while the platform and high areas has no deposition or are eroded. The Eastern Barents Sea shows some deposits in the large South Barents Basin, but generally less than in the west.

Flexural behavior

The eastern of the north-south trending transect (figure 41) shows almost identical flexural responses as sequence 2. The Nordkapp Basin has the same low difference from the deflection profile to the topography, while the Olga Basin also has the same tectonic deflections from sequence 2 and 1.

The western north-south trending transect shows an increased sedimentary deflection in the Hammerfest Basin and Maud Basin as seen in figure 42. For the Sørkapp Basin, there were no major tectonism in this sequence, creating the same amount of deflections as sequence 1 and 2, seen in the red circles on figure 42.

A major change in tectonic events can be seen in the east-west trending transect. The red circles in figure 43 indicates that the all the basins has an increase of tectonic deflections in the west, while the eastern Barents Sea has no change in tectonic deflections (green circles in figure 43)

Interpretation

Since the increase of tectonic loads are mainly located in the east-west direction, it could be related to the rifting event in the west, creating the highest magnitude of extension in the east-west direction. The northern and eastern Barents Sea has a low amount of tectonic deflections and is therefore not related to the event in the southwestern Barents Sea.

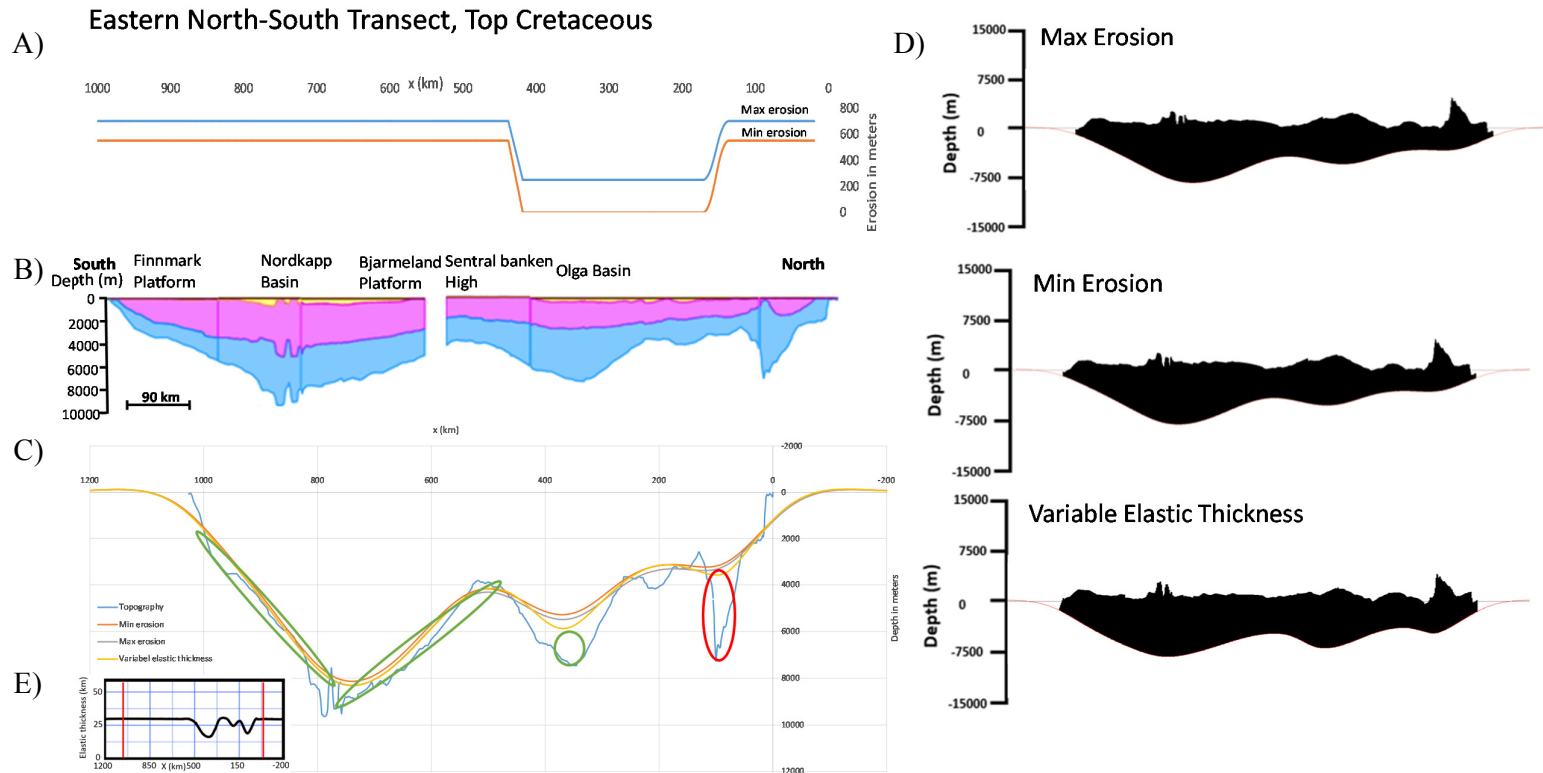


Figure 40: A section restored to top Cretaceous of the eastern of the north-south trending transect (B). The deflection due to sedimentary loads are shown to the right (D) with different amounts of erosion applied. Generally an elastic thickness of 30km is used, but the variable elastic thickness model uses the elastic thickness shown at the bottom left (E). These flexural models are combined in the bottom left figure (C) to describe the effect of the sedimentary loads. The difference could be due to either some of the input parameters (e.g. density, erosion etc.) or tectonic loads in the nearby area creating tectonic deflections. High tectonic deflection missing is indicated with a red circle and green indicates low. Figure A show the maximum and minimum erosion applied in the flexural models.

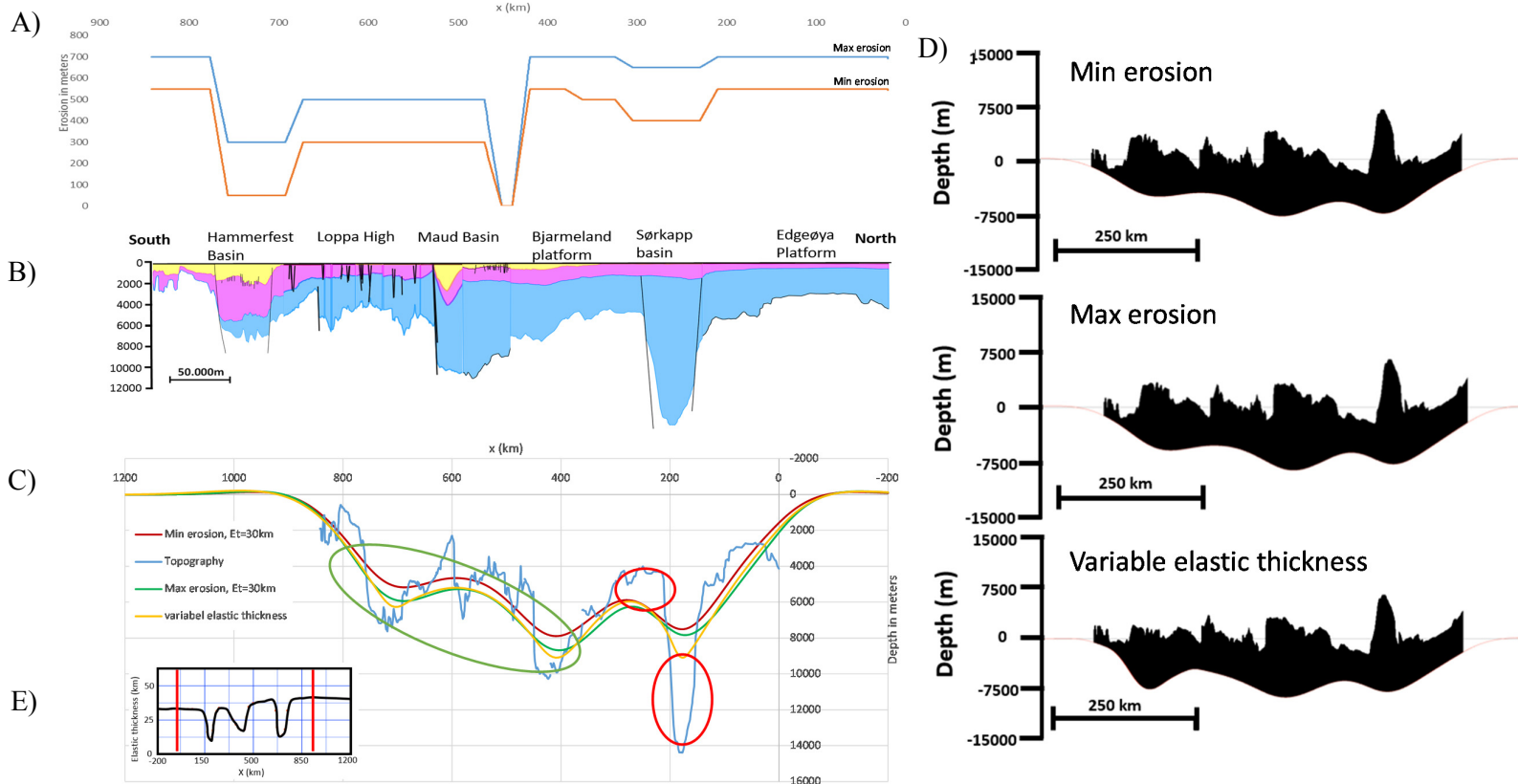


Figure 41: A section restored to top Cretaceous of the western of the north-south trending transect (B). The deflection due to sedimentary loads are shown to the right (D) with different amounts of erosion applied. Generally an elastic thickness of 30km is used, but the variable elastic thickness model uses the elastic thickness shown at the bottom left (E). These flexural models are combined in the bottom left figure (C) to describe the effect of the sedimentary loads. The difference could be due to either some of the input parameters (e.g. density, erosion etc.) or tectonic loads in the nearby area creating tectonic deflections. High tectonic deflection is indicated with a red circle and green indicates low. Figure A show the maximum and minimum erosion applied in the flexural models.

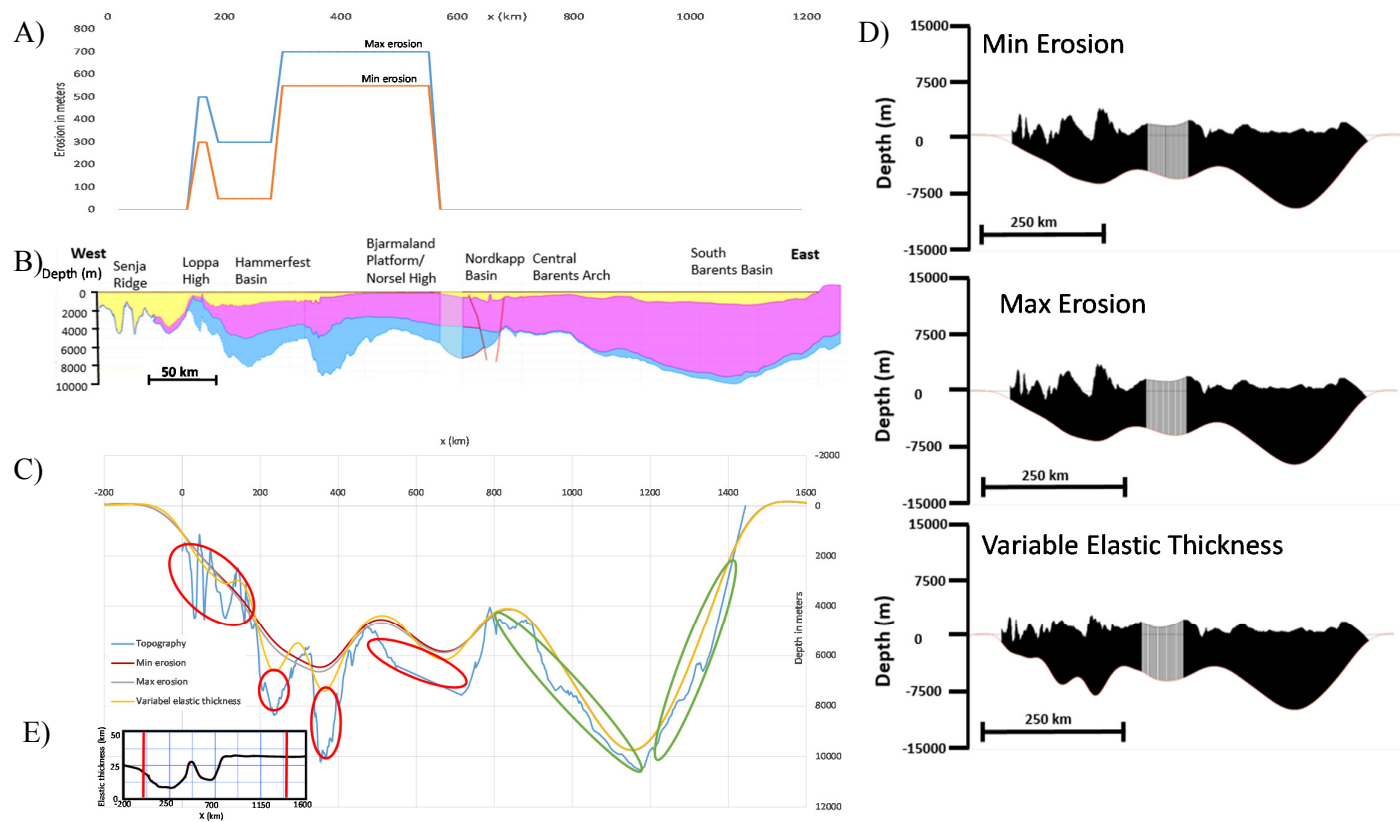


Figure 42: A section restored to top Cretaceous of the east-west trending transect (B). The deflection due to sedimentary loads are shown to the right (D) with different amounts of erosion applied. Generally an elastic thickness of 30km is used, but the variable elastic thickness model uses the elastic thickness shown at the bottom left (E). These flexural models are combined in the bottom left figure (C) to describe the effect of the sedimentary loads. The difference could be due to either some of the input parameters (e.g. density, erosion etc.) or tectonic loads in the nearby area creating tectonic deflections. High tectonic deflection missing is indicated with a red circle and green indicates low. Figure A show the maximum and minimum erosion applied in the flexural models.

5.3 Flexural behavior due to change in elastic thickness

A series of variable elastic thickness models were tested to find the “best-fit” model in regards to the restored topography. The variable elastic thickness for the transects is shown between the red lines in the variable elastic thickness box. As explained in chapter three, an increase in elastic thickness creates longer wavelength with lower amplitude. From the flexural model results, it is possible to see that the eastern Barents Sea basins and the Nordkapp Basin has a topography that is very similar to the deflection profile of the sedimentary loads. The same features is seen in the northern part with some few exceptions like the Sørkapp Basin. The southwestern part has as expected a very different setting than the other zones, even though the sedimentary displacement profile seems to fit with the structures (low in basins, high in highs), there is missing some loads to fit with the topography.

Due to how the flexural response is calculated in a regional scale, the topographic variation for small basins and highs does not seem to represent the local topography, but rather a general trend of the whole region. For example the Loppa High structure in the western of the north-south trending transects (figure 44) has these features.

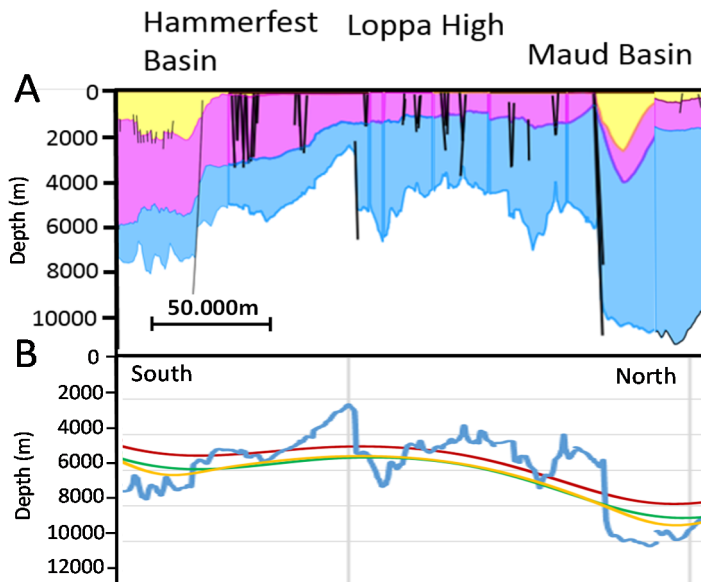


Figure 43: Example of a case where the flexural models does not follow the local changes, but rather the general thickness of the region. A is from the top Cretaceous restored section and B is the flexural models on top of the topography.

Larger areas like the Southern Barents Basin, which mainly is affected by sedimentary loads, have a close relationship between the sedimentary load profile and the topography (figure 45).

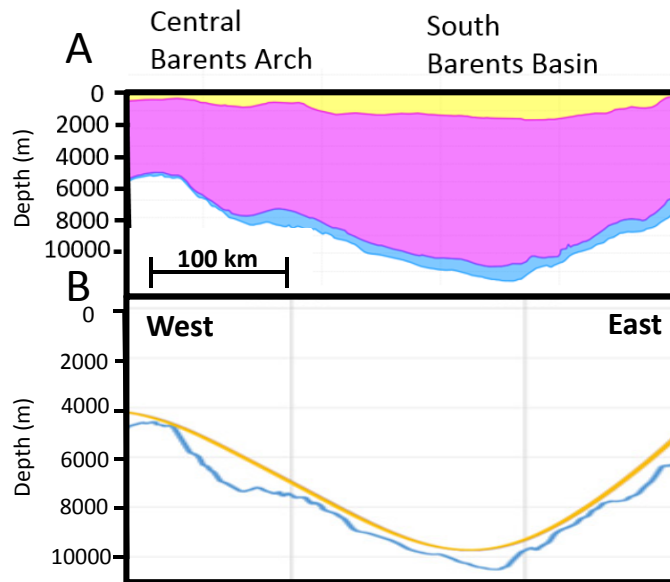


Figure 44: Example of the Southern Barents Basin, where the basin is wide enough to respond to the flexural effect of the sedimentary loads. A is from the top Cretaceous restored section and B is the flexural models on top of the topography.

DISCUSSION

Correlation between flexural model and flexural zone divisions

From the proposed division of three flexural zones in the Barents Sea (figure 46B), there is a close relationship to the elastic thickness used to create the “best fit” flexural models. Figure 46A shows that the elastic thickness is varying a lot in the southwestern Barents Sea, whereas the northern and eastern Barents Sea has a low variation of elastic thickness. From figure 46A, it is challenging to say where the transition from the brittle southwestern Barents Sea to the flexural Eastern Barents Sea but by looking at the change of elastic thickness through the Nordkapp Basin, it seems like the transition is somewhere between the Southern Barents Basin and the Nordkapp Basin. This fits with the proposed flexural zone division seen in figure 46B.

The Eastern Barents Sea has a long wavelength of the sedimentary load profile and a low contrast between the topography and load profile, indicating a crust deflecting mainly due to large accumulation of sedimentary loads. The high elastic thickness indicates a ductile crust and low amounts of tectonic activity.

The southwestern Barents Sea has in contrast to the eastern Barents Sea a very short wavelength of the sedimentary load profile, but with high amplitudes. These loads have the same deflection trends as the topography, but they are missing some tectonic loads to compensate for the deflections seen in the basins and highs. The tectonic loads in nearby areas are most likely caused by the extensive rifting events from the west. These missing deflections are increasing from a maximum of 500 meters in the east to a maximum of 1900 meters in the southwestern parts of the Barents Sea (figure 35) indicating a higher amount of tectonic loads to the west and a thinner elastic plate. These observations are similar to the theory represented in Braitenberg and Ebbing (2007) explaining how the eastern Barents Sea has a totally different flexural response to the western Barents Sea. The western Barents Sea acts in response to the major rifting events in the west, creating a higher mantle level and therefore a weak crust acting brittle compared to the thick package of sediments and deep mantle level seen in the eastern basins.

The northern part of the Barents Sea has a longer wavelength of the sedimentary load profile than the southwestern Barents Sea, but shorter than the eastern Barents Sea. The amplitude of these deflections are relatively small (maximum 1000 meters, figure 32), suggesting a stable platform area. This area is not affected with the same magnitude of sedimentary and tectonic loads (creating large amplitudes in the load profiles) as the Southwestern and Eastern Barents Sea. The exceptions are the Sørkapp Basin, which could have been created as a response to the late stages of the Uralide indentation.

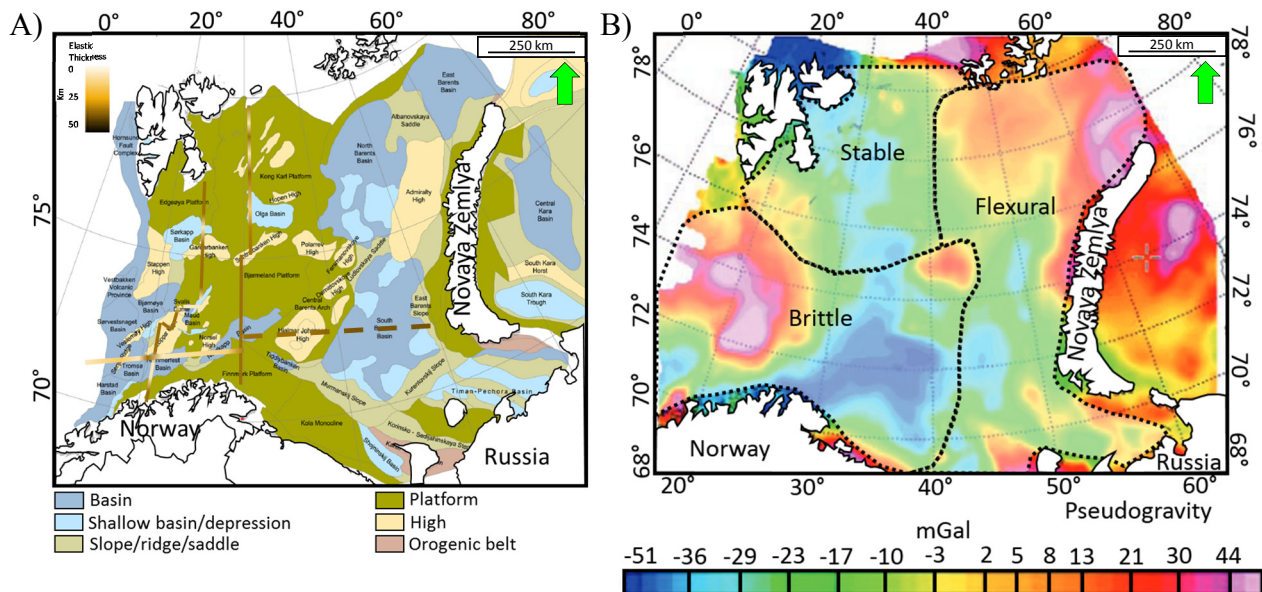


Figure 45: Comparison of the elastic thickness applied to “the best fit” model (A) and the proposed flexural behavior in the Barents Sea (B).

Sequence 1

During the Devonian to base Triassic time, there were deposited a low amount of sediments in to the Southern Barents Basin (figure 35). The flexural deflection of these sediments is not sufficient to recreate the basin geometry, which most likely is related to rifting events that caused faulting in the preexisting fractures from the Caledonian Orogeny.

The southwestern basins seen in the flexural models from sequence 1, relates to rifting events creating half graben structures from Devonian to early Permian. The flexural response shows a deflection in the Hammerfest and Nordkapp Basin for the East-west trending transect line, while the north-south trending transect line shows a gentle slope in the flexural response, indicating that the geometry and thickness of the sediments were small and undeveloped from compared to present. The flexural response of the east-west trending transect line also indicates that the structures had up to 1500 meters (figure 35) of deflection difference to the topography in the Nordkapp Basin, which could be related to tectonic deflections from loads created in the nearby areas. These tectonic deflections were most likely caused by tectonic loads created from rifting events such as footwall uplift or creation of half graben structures.

Since the deep northern basins with an age older than Base Triassic seems to create large tectonic deflection. The magnitude of these loads are higher than expected, which could partly be due to the velocity model, but also due to some kind of local rifting event. In the Eastern north south trending transects, there are not high amount of flexural response in the areas north of the Olga Basin. With the exception of the Basins, there are a maximum of ~1000 meters difference from the flexural profile to the topography in the first sequence indicating a large variation of tectonic activity in the platform areas. From this sequence, two main events could have caused such rifting events in the northern Barents Sea. The Scandian phase of the Caledonian orogeny, which created regional extension in Devonian, and a major rifting event that caused the formation of 1-3 km deep rift basins around mid-Carboniferous (Anell et al., 2014).

Sequence 2

A large accumulation of sediments is the major feature in the Barents Sea from the second sequence. This large accumulation of sediments created subsidence in the larger basins (e.g. Hammerfest, Nordkapp and Southern Barents Basin). The Thickness of this sequence is up to 8000 meters in the South Barents Basin.

The flexural response in the eastern Barents Sea seems to be related to these deposits sourced mainly from the erosion of Novaya Zemlya. The deflection profile indicates a high amplitude wavelength next to the basin causing uplift of the highs next to the basins. These features are similar to what you can find in a forbulge and fordeep area, but is in this case mainly related to deflection of the crust by sedimentary loads.

The east-west trending transect indicates that the flexural response is ~1900 meters under the topography in the Norsel High and ~300 meters above the topography in the Nordkapp Basin (figure 36), indicating a small increase in tectonic deflection from ~1500 meters in sequence 1. The western north-south trending transect shows a new deflection in the Hammerfest basin due to increase of sediments and possibly tectonic loads. The sedimentary deflection is not very dominant due to the undeveloped structures in the Hammerfest Basin, indicating that the Hammerfest Basin developed partly by the increase of tectonic, but also sedimentary loads.

Sequence 3

Major rifting events related to the opening of the Norwegian – Greenland Sea caused an increase of tectonism and sedimentation towards the southwest. The southwestern structures as the Tromsø Basin, Senja Ridge and Sørvestsnaget Basin were created due to these rifting events. Especially from the east-west trending transect, there is a large increase of tectonic deflections (red circles in figure 43). There is finally a dominant peak in the north-south trending flexural model for the Hammerfest Basin and Loppa High. The Hammerfest Basin is now at the same structural stage as seen today. These deflections are not as prominent in the north-south trending transect most likely because of the east-west oriented rifting event. For the east-west trending transects, there are also developed a small deflection in the Tromsø Basin. The deflections from this sequence has increased tectonic deflection from a maximum of ~1900 meters in sequence 2 to ~2400 meters in

sequence 3 (figure 43) related to creation of half graben and graben structures causing tectonic loads.

A relatively low amount of sediments to the Southern Barents Basin, created a small increase of sedimentary deflection, while the tectonic loads that could be seen in the west, did not seem to impact these eastern structures.

Most of the northern parts are non-deposited or eroded. Due to the low increase of sediments and tectonic loads, the sedimentary load profile created the same flexural response as for the second sequence.

Sequence 4

The deposition of sequence 4 and the continuous rifting in the southwestern Barents Sea created a similar flexural response as the one seen from sequence 2 too sequence 3. This means an increase of sedimentary and tectonic loads for the most southwestern basins. The Hammerfest Basin has an increase in sedimentary loads, but the structures were already developed in the areas east of the Hammerfest Basin, indicating a low increase of tectonic loads.

Summary and comparison

Figure 47 shows the increase of tectonic deflections for the three first sequences. These maps are created by calculating the increase of missing loads underneath the sedimentary load profile since the last sequence. The map clearly shows that the tectonic events drifted from the east in the first sequence, to the structures around the Hammerfest and Nordkapp Basin in the second sequence and finally to the southwestern Barents Sea in the third and fourth sequence.

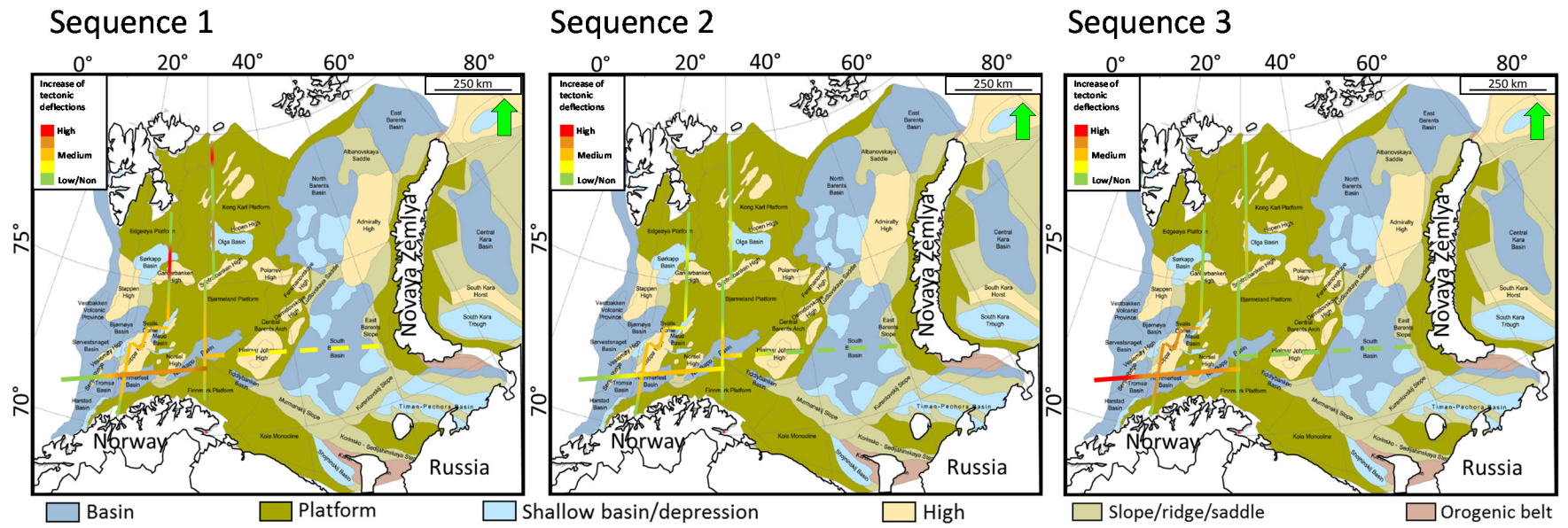


Figure 46: A model showing the increase of tectonic deflections for the three first sequences. Structural map from Henriksen et. al. (2012).

Eastern Barents Basin

Since the first sequence, there are no evidence of any increase in tectonic loads at the Southern Barents Basin in the flexural model, indicating that the Southern Barents Basin is mainly created due to the flexural response of sedimentary loads deposited after the first sequence. This could be seen from figure 48, which shows the increase of sedimentary and tectonic deflections for sequence 1 to 3. The missing deflections are approximately the same throughout the different sequences.

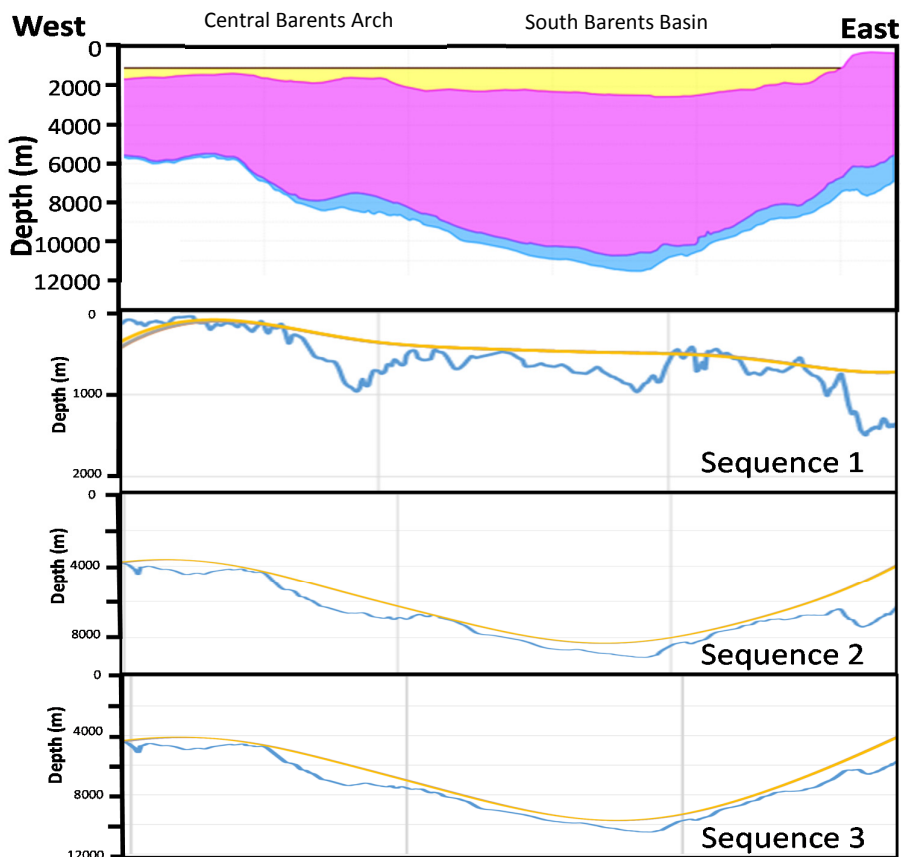


Figure 47: The Eastern Barents Sea evolution for each sequence.

Southwestern Barents Basin

The creation of the southwestern Barents Sea had a major rifting event in the first sequence, most likely related to the latest stages of the Caledonian Orogeny. The second sequence had a high amount of sediments creating subsidence and high sedimentary deflections, but also with some minor increase in tectonic deflections. For the third sequence there was a major increase of tectonic loads related to the opening of the Norwegian-Greenland Sea, causing the rifting to change from the Hammerfest Basin and Nordkapp Basin to the south western Basins as seen in figure 49. The increase of rifting in the third sequence created new structures and uplift in the northwestern parts due to igneous intrusions (HALIP).

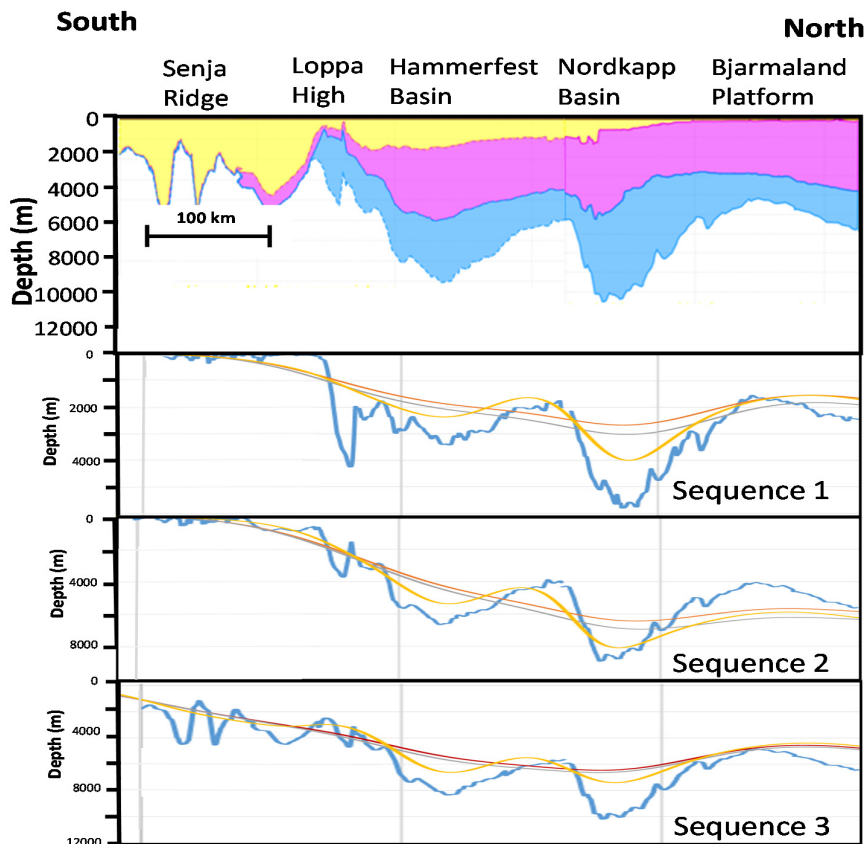


Figure 48: The south western Barents Sea evolution for each sequence.

Northern Barents Basin

Major rifting events in the Devonian and mid-Carboniferous caused locally high tectonic deflections as seen in figure 50, but generally, the northern Barents Sea is characterized by a low wavelength amplitude. The stable platform areas with thick sediment have made the northern Barents Sea resistance to large deflections. Since the first sequence, there is no sign of any tectonic events, resulting in similar flexural features in sequence 2 and 3.

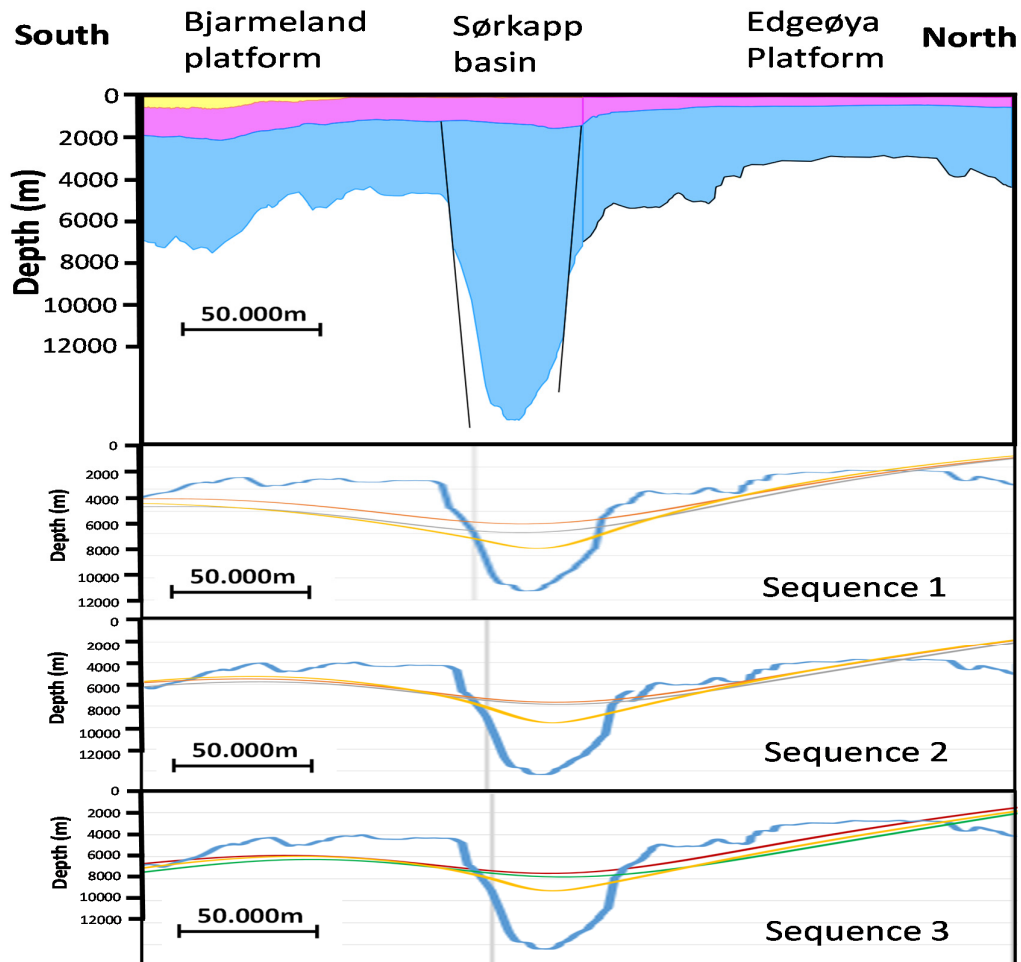


Figure 49: The Eastern Barents Sea evolution for each sequence.

The effect of erosional events on the flexural models

The change in magnitude of erosion for the different sequences throughout the Barents Sea is related to the major erosional phases. Due to limited data, there is not very abrupt changes in the erosion since the local erosional events are poorly mapped and discussed on a regional scale. The change in the flexural response due to the different amounts of loads are therefore mostly close to or the same as the amount of loads since the erosion is calculated within an interval of five kilometers. Sequence 2 (with the base Cretaceous unconformity (BCU) on top) has the highest amount erosion, with a maximum around 2000 meters.

The overall addition of sedimentary loads due to erosion from sequence 1 increases from 0% in the deep basins to 25 % of the total loads in the highs and an average of ~9% in the entire region. From sequence 2, there is an increase of erosion, which increases the sedimentary loads from this sequence to a maximum of ~45%, with an average of approximately 30%. Due to the high erosion and non-deposition of sequence 3, the maximum amount of eroded sediment is hard to quantify, but with an average of about 30% in the Finnmark Platform and Hammerfest Basin area, where the main accumulation of sediments are located. These values represent the percentage increase of sedimentary deflections created in the flexural model due to erosion.

Uncertainty in the results

Due to the large amount of estimated and unknown parameters, there is a large amount of uncertainty in certain areas. Since the wells with time-depth relationship were located in the southern part of the Barents Sea, the depth-converted lines in the northern parts have an increased uncertainty. This could be seen in the northern parts of the transects, where some basins are very deep, which results in a larger flexural response, deeper basin and a higher elastic thickness estimation than what may be real. The only way to reduce this uncertainty is to gain more data about the density and/or time-depth relationship.

These large basins could also be caused by major rifting events creating large tectonic deflections.

The major uncertain factors in the models are related to (1) the density and (2) the velocity (for depth conversion), which has a spread of data as seen in chapter 4.4, (3) the elastic thickness that is represented by the different flexural models and (4) the erosion, which is represented by the maximum and minimum erosion applied. Generally the uncertainty due to different elastic thicknesses varies from 0-500 meters but in some areas the elastic thickness increases to a maximum of ~1500 meters (in the Nordkapp Basin) between the constant elastic thickness of 30 km and the zones with variable elastic thickness of 10 km. Other parameters as the Poisson ratio, Young modulus, interval of flexural calculation for the sediments and the density of the mantle are set to standard values would have less effect on the model. This thesis does also not cover the salt structures found in the Barents Sea (e.g. in the Nordkapp and Tromsø Basin), which could have some local influence on the structures created.

CONCLUSIONS

- 1) 27 flexural models from sequence 1 to 3 representing changes in erosion and elastic thickness has been created to describe the evolution and impact of sedimentary loads.
- 2) Based on the flexural models, there are clearly a change in flexural response due to a change in the elastic plate in the southwestern, northern and eastern Barents Sea.
- 3) The sediments in the larger basins (e.g. Hammerfest Basin, Nordkapp Basin and the South Barents Basin) creates enough flexural response to create deflections (highs) next to the Basins.
- 4) In the western Barents Sea, there is a need for more tectonic deflections in the models to recreate the topography compared to the eastern Barents Sea. This indicates a brittle area
- 5) The eastern Barents Sea seems to have some tectonic deflections most likely related to the latest stages of Caledonian orogeny in the Devonian, but the major deflections are created by the large accumulations of sediments. Since these sediments subside with a low amount of tectonic loads, it is indicating a flexural zone.
- 6) The northern Barents Sea seems to have a low amount of tectonic deflections and low amplitude deflections due to the sedimentary load, which could represent a stable platform area.

- 7) The current time-depth data available for the northern part of the Barents Sea creates a high uncertainty related to the depth conversion and therefore the flexural models.

- 8) Restored sections, shows that most basins in the Barents Sea was finished developed before Cretaceous (Triassic-Jurassic time) with the exception of the most southwestern basins west of the Hammerfest Basin.

FURTHER WORK

Due to the time constrain of this thesis, there is a lot more to look at, regarding the flexural effect of tectonic and sedimentary loads in the Barents Sea. 2D and 3D flexural models can be created in specific areas, to get a detailed view of the sedimentary loads. In addition, an analysis of the flexural loads can be created and combined with the sedimentary loads to create a combined load profile, but this process is very time consuming.

A more reasonable option in regards of time would be to combine the salt structures in for example the Nordkapp and Tromsø basin into the flexural model to see the flexural effect of salt diapirs on the structures.

If time-depth data covering the northern parts of the Barents Sea is provided, the uncertainty of the depth conversion will be reduced, which can confirm or deny the interpretations in the northern parts of this thesis.

REFERENCES

- Anell, I., A. Braathen, and S. Olaussen, 2014, Regional constraints of the Sørkapp Basin: A Carboniferous relic or a Cretaceous depression?: *Marine and Petroleum Geology*, v. 54, p. 123-138.
- Anell, I., A. Braathen, S. Olaussen, and P. Osmundsen, 2013, Evidence of faulting contradicts a quiescent northern Barents Shelf during the Triassic: first break, v. 31, p. 67-76.
- Audet, P., and J.-C. Mareschal, 2004, Variations in elastic thickness in the Canadian Shield: *Earth and Planetary Science Letters* p. 17-31.
- Braitenberg, C., and J. Ebbing, 2007, The gravity potential derivatives as a means to classify the Barents sea basin in the context of cratonic basins: EGM 2007 International Workshop.
- Corfu, F., S. Polteau, S. Planke, J. I. Faleide, H. Svensen, A. Zayoncheck, and N. Stolbov, 2013, U–Pb geochronology of Cretaceous magmatism on Svalbard and Franz Josef Land, Barents Sea Large Igneous Province: *Geological Magazine*, v. 150, p. 1127-1135.
- Faleide, J. I., F. Tsikalas, A. J. Breivik, R. Mjelde, O. Ritzmann, Ø. Engen, J. Wilson, and O. Eldholm, 2009, Structure and evolution of the continental margin off Norway and the Barents Sea, v. 31, p. 82-91.
- Faleide, J. I., E. Vdgnes, and S. T. Gudlaugsson, 1993, Late Mesozoic-Cenozoic evolution of the south-western Barents Sea in a regional rift-shear tectonic setting: *Department of Geology, University of Oslo*, v. 10, p. 186-214.
- Gabrielsen, R. H., 2013, Long-lived fault zones and their influence on the tectonic development of the southwestern Barents Sea: *Journal of the Geological Society*, v. 141, p. 651-662.
- Gac, S., R. S. Huisman, Y. Y. Podladchikov, and J. I. Faleide, 2012, On the origin of the ultradeep East Barents Sea basin: *American Geophysical Union.*, v. 117, p. 1-16.
- Gac, S., R. S. Huisman, N. S. C. Simon, Y. Y. Podladchikov, and J. I. Faleide, 2013, Formation of intracratonic basins by lithospheric shortening and phase changes: a case study from the ultra-deep East Barents Sea basin: *Terra Nova*, v. 25, p. 459-464.
- Gustavsen, F. B., H. Dypvik, and A. Solheim, 1996, Shallow Geology of the Northern Barents Sea: Implications for Petroleum Potential: *The American Association of Petroleum Geologists*, v. 81, p. 1827-1842.
- Hassan, S. Y., 2012, Development of the late Paleozoic, Mesozoic and Cenozoic sedimentary succession in SW Barents Sea and their role in fluid leakage process., *University of Tromsø, Tromsø*, 137 p.
- Henriksen, E., A. Ryseth, G. Larssen, T. Heide, K. Rønning, K. Sollid, and A. Stoupakova, 2011, Tectonostratigraphy of the greater Barents Sea: implications for petroleum systems: *Geological Society, London, Memoirs*, v. 35, p. 163-195.

- Høy, T., and B. A. Lundschieen, 2011, Triassic deltaic sequences in the northern Barents Sea: *Artic Petroleum Geosciences*, v. 35, p. 249-260.
- Kearey, P., M. Brooks, and I. Hill, 2013, *An introduction to geophysical exploration*, John Wiley & Sons.
- Marello, L., 2012, Basin architecture and lithospheric structure of the Barents Sea region from geophysical modelling, Norwegian University of Science and Technology, Trondheim, 191 p.
- Marello, L., J. Ebbing, and L. Gernigon, 2010, Magnetic basement study in the Barents Sea from inversion and forward modelling: *Tectonophysics*, v. 493, p. 153-171.
- Nazarova, I., 2009, Cretaceous-Cenozoic tectonostratigraphic evolution of the Loppa High: Master Thesis thesis, University in Stavanger, Stavanger, 1-67 p.
- Nilsen, K. T., B. C. Vendeville, and J.-T. Johansen, 1995, Influence of Regional Tectonics on Halokinesis in the Nordkapp Basin, Barents Sea: *The American Association of Petroleum Geologists*, v. 65, p. 413-436.
- Nyland, B., L. N. Jensen, J. Skagen, O. Skarpnes, and T. O. Vorren, 1992, Tertiary uplift and erosion in the Barents Sea: Magnitude, timing and consequences: Structural and tectonic modelling and its application to petroleum geology; proceedings, v. 1, Norwegian Petroleum Society Special Publication, 10 p.
- Ostanin, I., Z. Anka, R. di Primio, and A. Bernal, 2012, Identification of a large Upper Cretaceous polygonal fault network in the Hammerfest basin: Implications on the reactivation of regional faulting and gas leakage dynamics, SW Barents Sea: *Marine Geology*, v. 332-334, p. 109-125.
- Ramberg, I. B., I. Bryhni, A. Nøttvedt, and K. Ragnes, 2008, The Making of Land - Geology of Norway, *Norsk Geologisk Forening*, 307-328, 348-355, 378-381, 412-415, 438-439, 472-473 p.
- Richardson, G., T. O. Vorren, and B. O. Tøruðbakken, 1993, Post-Early Cretaceous uplift and erosion on the southern Barents Sea: a discussion based on analysis of seismic interval velocities: *Norsk Geologisk Tidsskrift*, v. 73, p. 3-20.
- Riis, F., and W. Fjeldskaar, 1992, On the magnitude of the Late Tertiary and Quaternary erosion and its significance for the uplift of Scandinavia and the Barents Sea: *Norwegian Petroleum Society*, v. 1, p. 163-185.
- Sclater, J. G., and P. A. F. Christie, 1980, Continental Stretching - an explanation of the Post-Mid-Cretaceous subsidence of the central North-Sea Basin: *Journal of Geophysical Research*, v. 85, p. 3711-3739.
- Sobolev, P., 2012, Cenozoic uplift and erosion of the Eastern Barents Sea – constraints from offshore well data and the implication for petroleum system modelling: *Russian Geological Research Institute*, v. 74, p. 323-338.
- Torsvik, T. H., and S. J. H. Buitert, 2007, Horizontal movements in the eastern Barents Sea constrained by numerical models and plate reconstructions: *Geophys. J. Int.*, v. 171, p. 1376-1389.
- Turcotte, D. L., and G. Schubert, 2002, *Geodynamics*, Second Edition: Cambridge University Press, p. 456.

- Watts, A. B., 1994, Crustal Structure, Gravity anomalies and flexure of the Lithosphere in the vicinity of the Canary Islands: *Geophys. J. Intern.*, v. 119, p. 648-666.
- Watts, A. B., 2001, *Isostasy and Flexure of the Lithosphere*, Cambridge University Press.
- Worsley, D., 2008, The post-Caledonian development of Svalbard and the western Barents Sea: *Polar Research*, v. 27, p. 298-317.

Appendix

A)

top	Top Cretaceous-present	BCU-top Cretaceous	Base Tertiary-BCU	Devonian-Permian
Edgøya plattform		550-700	1500-2000	14-21%
Sørkapp basin	0	550-700	0	5-14%
Gardarbanken high		400-650	500-700	1500-2000
Bjarmeland plattform	1500+500	550-700	1000-1500	7-22%
Maud Basin	1500-2000	0	1500-2000	0-2%
Svalis Dome	2000-2500	300-500	1500-2000	5-30%
Loppa High	900-1500	300-500	1000-1500	5-30%
Hammerfest Basin	800-1500	50-300	1000-1500	2-10%
Sørvest Basin	0-500	0	0	0 %
Senja Ridge	300-400	0	0-500	0-4%
Nordkapp Basin	1500-1700	550-700	1000-1500	2-12%
Finnmark Plattform		550-700	1500-2000	5-25%
Sentral banken high		550-700	667-1500	300-800
Olga Basin	2000-2200	0-250	1000-1500	5-14%
Kong Karl plattform		550-700	1000-1500	14-21%
Central Barents high	0	550-700	500-1000	5-15%
South Barents Basin	0-500	0	0-500	0 %
Eastern Barents Slope		0-300	0-500	0-5%
Tromsø Basin	500/600	0	0-500	2-10%

Figure 50: Erosion at the different structures in meters /percentage of total thickness. The green sections are the platform areas, yellow are the highs and blue is the basin areas. (Nyland et al., 1992; Riis and Fjeldskaar, 1992; Gustavsen et al., 1996; Torsvik and Buiter, 2007; Worsley, 2008; Nazarova, 2009; Hassan, 2012)

B)

Erosion	xmin(km)	xmax(km)	x	z		$\rho3$ (g/cm ³)	z		$\rho2$ (g/cm ³)	z		$\rho1$ (g/cm ³)	h(m)	ρ (g/cm ³)	Normalized:	h4(m)	h3(m)	h2(m)	h1(m)
300	884.5808	884.5808	884.5808	-8899.78	400.2247	2124.991238	-5894.97	3004.807	2641.624141	-4139.31	1755.657	2777.416205	5160.689	2647.754147		0	0.077553	0.582249	0.340198
300	884.5808	1084.581	884.5808	-8899.78	400.2247	2124.991238	-5894.97	3004.807	2641.624141	-4139.31	1755.657	2777.416205	5160.689	2647.754147		0	0.077553	0.582249	0.340198
300	1084.581	1284.581	1084.581	-8895.81	404.1901	2126.36449	-5895.59	3000.222	2641.551237	-4130.38	1765.209	2778.251412	5169.621	2647.948407		0	0.078186	0.580356	0.341458
300	1284.581	1484.581	1284.581	-8890.28	409.7222	2128.280302	-5896.07	2994.207	2641.49446	-4124.79	1771.283	2778.774313	5175.213	2647.849032		0	0.07917	0.578567	0.342263
300	1484.581	1684.581	1484.581	-8884.75	415.2541	2130.196045	-5896.77	2987.976	2641.412181	-4129.53	1767.24	2778.330802	5170.47	2647.153138		0	0.080313	0.577893	0.341795
300	1684.581	1884.581	1684.581	-8879.21	420.7869	2132.1121	-5898.14	2981.077	2641.25147	-4140.62	1757.517	2777.293856	5159.381	2646.069419		0	0.081558	0.577797	0.340645
300	1884.581	2084.581	1884.581	-8879.43	420.5688	2132.03657	-5900.15	2979.283	2641.014868	-4151.41	1748.74	2776.285048	5148.592	2645.383445		0	0.081686	0.57866	0.339654
300	2084.581	2284.581	2084.581	-8882.53	417.4742	2130.964884	-5902.34	2980.186	2640.756999	-4161.88	1740.459	2775.30562	5138.118	2644.91246		0	0.08125	0.580015	0.338735
300	2284.581	2484.581	2284.581	-8885.59	414.4136	2129.904973	-5904.51	2981.073	2640.501341	-4171.44	1733.076	2774.412053	5128.563	2644.494546		0	0.080805	0.581269	0.337926
300	2484.581	2684.581	2484.581	-8888.56	411.4406	2128.875398	-5905.7	2982.862	2640.36212	-4179.04	1726.657	2773.701094	5120.96	2644.225509		0	0.080344	0.582481	0.337174
300	2684.581	2884.581	2684.581	-8890.1	409.8956	2128.340352	-5904.25	2985.856	2640.532559	-4183.92	1720.331	2773.245091	5116.083	2644.122063		0	0.080119	0.583621	0.336259
300	2884.581	3084.581	2884.581	-8893.27	406.7317	2127.244667	-5901.67	2991.594	2640.835337	-4187.41	1714.263	2772.918309	5112.588	2644.264384		0	0.079555	0.585143	0.335302
300	3084.581	3284.581	3084.581	-8899.23	400.7724	2125.180911	-5899.78	2999.451	2641.058507	-4190.04	1709.738	2772.672611	5109.961	2644.635074		0	0.07843	0.586981	0.334589
300	3284.581	3484.581	3284.581	-8905.19	394.8131	2123.117156	-5897.84	3007.343	2641.285899	-4191.99	1705.854	2772.490219	5108.01	2645.051677		0	0.077293	0.58875	0.333957
300	3484.581	3684.581	3484.581	-8908.9	391.099	2121.830932	-5896.69	3012.207	2641.421109	-4195.48	1701.217	2772.164101	5104.523	2645.18464		0	0.076618	0.590105	0.333276
300	3684.581	3884.581	3684.581	-8911.22	388.7781	2121.027185	-5894.35	3016.877	2641.697445	-4198.55	1695.799	2771.877118	5101.454	2645.291196		0	0.076209	0.591376	0.332415
300	3884.581	4084.581	3884.581	-8909.34	390.6576	2121.678072	-5888.72	3020.618	2642.358521	-4199.1	1689.628	2771.825622	5100.903	2645.36651		0	0.076586	0.592173	0.331241
300	4084.581	4284.581	4084.581	-8907.42	392.5823	2122.344611	-5882.12	3025.297	2643.135339	-4195.38	1686.739	2772.173032	5104.618	2645.721171		0	0.076907	0.592659	0.330434
300	4284.581	4484.581	4284.581	-8905.45	394.5491	2123.025731	-5875.47	3029.981	2643.917592	-4191.4	1684.069	2772.545231	5108.599	2646.090476		0	0.077232	0.593114	0.329654
300	4484.581	4684.581	4484.581	-8903.44	396.5575	2123.721256	-5868.77	3034.67	2644.705361	-4189.55	1679.221	2772.718178	5110.448	2646.341552		0	0.077597	0.593817	0.328586
300	4684.581	4884.581	4684.581	-8895.74	404.2637	2126.389978	-5862.03	3033.708	2645.498741	-4187.9	1674.126	2772.872461	5112.098	2646.160471		0	0.07908	0.593437	0.327483
300	4884.581	5084.581	4884.581	-8886.03	413.9659	2129.749931	-5855.24	3030.799	2646.29772	-4186.82	1668.42	2772.974079	5113.185	2645.811959		0	0.08096	0.592742	0.326298
300	5084.581	5284.581	5084.581	-8876.16	423.8397	2133.16931	-5848.42	3027.741	2647.099499	-4180.25	1668.173	2773.588377	5119.754	2645.76766		0	0.082785	0.591384	0.325831
300	5284.581	5484.581	5284.581	-8863.07	436.9266	2137.701413	-5842.42	3020.652	2647.804907	-4165.67	1676.751	2774.951281	5134.329	2645.918585		0	0.085099	0.588325	0.326576
300	5484.581	5684.581	5484.581	-8843.27	456.7271	2144.558491	-5838.75	3004.524	2648.236908	-4148.39	1690.356	2776.566897	5151.606	2645.690076		0	0.088657	0.583221	0.328122
300	5684.581	5884.581	5684.581	-8823.09	476.9144	2151.549522	-5836.66	2986.426	2648.482674	-4131.12	1705.542	2778.182327	5168.882	2645.428544		0	0.092266	0.57777	0.329963
300	5884.581	6084.581	5884.581	-8802.51	497.4891	2158.674713	-5834.56	2967.955	2648.730168	-4113.81	1720.745	2779.80072	5186.189	2645.209603		0	0.095926	0.572281	0.331794

Figure 51: Example of how the different thicknesses in the different seismic lines were calculated. The white areas are the inputs of thickness (z) and location (x), the yellow parts are calculations for the densities ($\rho1$ =sequence 1, $\rho2$ =sequence 2 and $\rho3$ =sequence 3) and the green parts are the calculation needed for the flexural modelling. The normalized section is used for the calculation of densities to weight the densities of the thickest sequences correctly. The maximum and minimum erosion was added in different files to calculate the response.